Spring 3-1-2017

MECHANISMS OF THYMIC TOXICITY INDUCED BY ENVIRONMENTALLY RELEVANT CONCENTRATIONS OF ARSENIC

Huan Xu
University of New Mexico

HUAN XU

Candidate

BIOMEDICAL SCIENCES GRADUATE PROGRAM

Department

This dissertation is approved, and it is acceptable in quality and form for publication:

Approved by the Dissertation Committee:

Dr. Scott W Burchiel , Chairperson

Dr. Ke Jian Liu

Dr. Laurie G Hudson

Dr. Xuexian Yang

MECHANISMS OF THYMIC TOXICITY INDUCED BY ENVIRONMENTALLY RELEVANT CONCENTRATIONS OF ARSENIC

by

HUAN XU

B.S. - Clinical Laboratory Sciences
Shanghai Jiao Tong University, China, 2011
M.S. - Medical Biology
LIU Post, USA, 2013

DISSERTATION

Submitted in Partial Fulfillment of the
Requirements for the Degree of

Doctor of Philosophy
Biomedical Sciences

The University of New Mexico
Albuquerque, New Mexico

May, 2017

DEDICATION

This work is dedicated to my parents, Huanshu Wu and Congbao Xu, and my grandmother, Wenshu Liu, for their continuous support during my graduate studies. This work is also dedicated to my late grandfather Chenghuang Wu, who taught me the importance of focus and dedication, and inspired my interest in science early in my life.

ACKNOWLEDGEMENT

I would like to express the deepest appreciation to my mentor and dissertation committee chairperson, Dr. Scott W. Burchiel, for his help and support. Dr. Burchiel provided me with necessary trainings, useful instructions and invaluable academic advices that I needed to complete the study. His guidance helped me all the time during the research and writing of this dissertation.

I would like to thank the rest of my committee members, Dr. Ke Jian Liu, Dr. Laurie G. Hudson and Dr. Xuexian Yang for their time, patience and insightful comments.

My sincere thanks also goes to Fredine T. Lauer, our lab manager. She provided me with technical support and advice which helped me a lot in the past four years. I would like to thank my fellow labmates, Sebastian Medina, Jamie Stevens and Brian Frederick, for their support and cooperation. I would also like to thank the previous members of the Burchiel lab, Dr. Debra Mackenzie, Dr. Jesse Denson and Shea McClain, for their help for my graduate research.

Last but not least, I would like to thank the University of New Mexico, the Biomedical Sciences Graduate Program, the College of Pharmacy and the Department of Pharmaceutical Sciences, for providing me the opportunity and the financial support for my graduate study.

MECHANISMS OF THYMIC TOXICITY INDUCED BY ENVIRONMENTALLY RELEVANT CONCENTRATIONS OF ARSENIC

By

Huan Xu

B.S. - Clinical Laboratory Sciences
Shanghai Jiao Tong University, China, 2011
M.S. - Medical Biology
LIU Post, USA, 2013

Ph.D. - Biomedical Sciences, University of New Mexico, 2017

ABSTRACT

Arsenic, a ubiquitous environmental contaminant, is known to cause immunotoxicity. However, the mechanisms of arsenic induced immunotoxicity are still not clear. Arsenite (As^{+3}), the trivalent inorganic form of arsenic, was found to increase DNA damage and inhibit PARP activity in thymus cells at 50 nM *in vitro*. Oxidative stress and double strand breaks (DSBs) formation occurred in thymus cells exposed to As^{+3} at 500 nM. The genotoxicity was found to be related to As^{+3} exporter expressions and reversed by zinc supplement. IL-7 signaling, the critical cytokine signal for the early DN thymic T cell proliferation, was found to be suppressed by As^{+3} at 500 nM and MMA^{+3} at 50 nM *in vitro*. The suppressive effects reduced the cell cycle gene expression.

After 30 d *in vivo* exposure of up to 500 parts per billion (ppb) As^{+3}, thymus cells were found to contain the higher levels of arsenic than bone marrow and spleen cells. Correlations between intracellular arsenic concentrations and the increase of DNA damage were found in both the bone marrow and thymus, but not the spleen.

Monomethylarsonous acid (MMA^{+3}) was also found to be more genotoxic than As^{+3} *in vitro* in bone marrow, spleen and thymus, and was demonstrated to be the most prevalent form of arsenic in bone marrow and thymus after *in vivo* exposures.

Benzo(a) pyrene-7,8-dihydrodiol (BP-diol), the metabolite of benzo(a) pyrene (BaP) was found to interact with As^{+3} synergistically at low concentrations to increase the DNA damage and inhibit PARP activity in primary thymus cells. The interactive effects were also demonstrated to increase the expression of CYP1A1 and CYP1B1, two critical enzymes for the metabolism of BP-diol to the DNA adduct forming compound, benzo(a) pyrene-7,8-dihydrodiol-9,10-epoxide (BPDE).

The differential sensitivity to As^{+3} of double negative (DN) and double positive (DP) thymus cell subsets was also evaluated and compared. Higher intracellular accumulation of As^{+3} was found in DN cells, with the higher DNA damage than DP cells after *in vitro* As^{+3} treatments. The expressions of two As^{+3} exporters, Mdr1 and Mrp1, were shown to be inversely correlated with the selective genotoxicity in DN cells.

These studies contributed to our understanding of the mechanisms associated with the toxicity induced by environmentally relevant concentrations of arsenic and its potential interactions with other environmental contaminants.

TABLE OF CONTENTS

LIST OF FIGURES

LIST OF TABLES

CHAPTER 1

GENERAL INTRODUCTION

GENERAL INTRODUCTION

T cell development in thymus

T cells originate from hematopoietic stem cells in the bone marrow and are transported into the thymus for development. The thymus is a pink-colored, two lobed organ located between the heart and the sternum. The size of the thymus grows bigger until adolescent periods. Thymus atrophy occurs physiologically and the stromal tissue of the thymus starts to be replaced by fat after adolescence. Although T cell lymphopoiesis lasts throughout adult life, it becomes less and less active with aging (Palmer, 2013).

The earliest T cells in thymus are double negative for both CD4 and CD8 cell surface markers, which are classified as double negative (DN) cells. Once the functional T cell receptor (TCR) β chain is formed, the cells are advanced to a double positive (CD4+, CD8+, DP) stage. DP cells are presented with self-antigens by the major histocompatibility complexes (MHCs) of the thymic cortical epithelial cells. Only those DP cells that can interact well (not too strongly or too weakly) with MHC molecules can receive a survival signal. All the other DP cells will undergo apoptosis. The process is called positive selection, which ensures that only the functional early T cells can survive and advance to CD4 or CD8 single positive (SP) stage. CD4SP and CD8SP cells are then moved to the thymic medulla. Medullary thymic epithelial cells and thymic dendritic cells present self-antigens on MHC class I (for CD8SP cells) and MHC class II (for CD4SP cells) molecules. SP cells that overreact with the self-antigens receive apoptotic signals. The process is called negative selection, which prevents autoimmunity. These

selection processes together make sure that only the functional and self-tolerant T cells are produced and released from the thymus (Klein et al., 2014).

Based on the specific cell surface marker expressions of developing T cells at different stages, we can easily differentiate DN, DP and SP thymic T cell populations by cell surface marker staining and flow cytometry (Fig 1.1). CD3 is an important part of TCR signaling complex, which is expressed on the cell surface from late stage DN cells to mature T cells (). CD4 and CD8 can be used to separate DN, DP, CD4SP and CD8SP cell populations. The DN cell population can also be further differentiated in to DN1, DN2, DN3 and DN4 subsets, using cell surface markers CD25 and CD44.

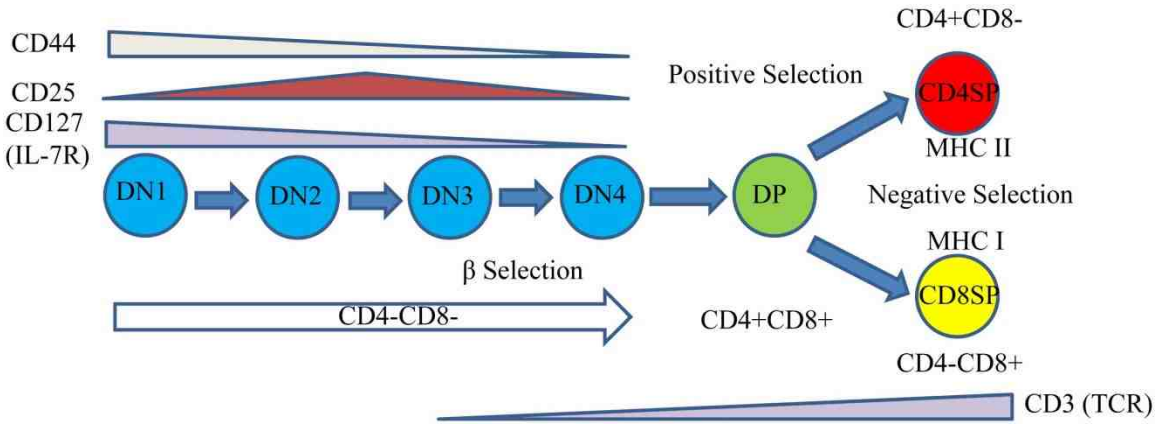

Figure 1.1. Specific cell surface markers on developing thymic T cells. T cells are originated from bone marrow and transferred in to the thymus at DN1 stage. DN1, DN2, DN3 and DN4 cells can be differentiated by CD25 and CD44/CD127 (IL-7 receptor). DN, DP, CD4SP and CD8SP cells can be differentiated by CD4 and CD8. CD3 starts to be expressed on the thymic T cell surfaces from the DN3 stage.

Arsenic metabolism and distribution *in vivo*

Millions of people around the world are exposed to arsenic, a ubiquitous food and drinking water contaminant. The trivalent inorganic form of arsenic, arsenite (As^{+3}), and the pentavalent inorganic form of arsenic, arsenate (As^{+5}), are the common contaminants in groundwater. These inorganic forms of arsenic is classified as group I carcinogens by The International Agency for Research on Cancer (IARC). The metabolism pathway of inorganic arsenical species has been studied and revealed by many research groups (Drobna et al., 2009; Vahter and Concha, 2001). As shown in Fig 1.2, arsenite methyltransferase (AS3MT) is a critical enzyme for the metabolism and detoxification of arsenic *in vivo*. Variations in the AS3MT gene between individuals play an important role in the differential sensitivity of cells and tissues to arsenic-induced toxicity (Douillet et al., 2016). Previous studies have also demonstrated that the intermediate monomethylated form of arsenite, monomethylarsonous acid (MMA^{+3}), is more toxic than the inorganic form, As^{+3}. The dimethylated forms of arsenic have relatively limited toxicities compared to other forms of arsenic (Gusman et al., 2013; Sun et al, 2014).

Studies on arsenic *in vivo* distribution revealed that the amounts of arsenic in different organs varied after acute and chronic exposures in humans and animals. Early literature from legal investigations showed that the arsenic accumulates in the liver after acute high-dose exposures (Underhill, 1914). Another more recent case revealed that most of the arsenic was distributed in the liver after acute exposure, followed by the kidney, heart and spleen (Benramdane et al., 1999). A 90 d *in vivo* study with 10-60 ppm arsenite in drinking water on Wistar Albino rats demonstrated that more arsenic accumulated in the spleen than kidney and heart, and there was no significant increase of

arsenic accumulations in the spleen with increasing doses (Al-Forkan et al., 2016). Knockout of AS3MT was showed to increase arsenic accumulation and toxicity in mice (Hughes et al., 2010). More studies need to be done on the arsenic distribution and speciation in the immune organs after *in vivo* exposure to understand mechanisms of toxicity and differential sensitivity of tissues.

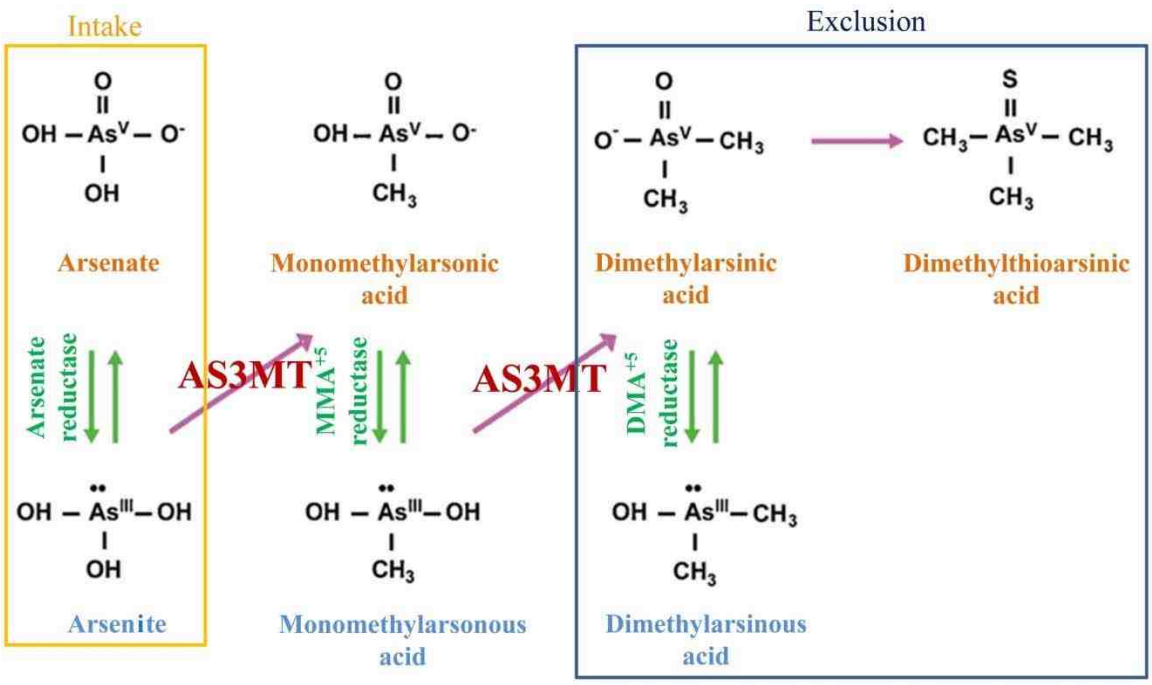

Figure 1.2. Biotransformation of inorganic arsenical species in mammals. AS3MT, arsenite methyltranserase, is the critical enzyme in the metabolism of inorganic and mono-methylated arsenical species. The inorganic forms of arsenic, arsenate (As^{+5}) and arsenite (As^{+3}) are metabolized into dimethylated forms and excluded from the body.

Arsenic immunotoxicity and thymic toxicity

Arsenic is known to cause deleterious effects on the immune system. *In vivo* studies have demonstrated that arsenic exposure can induce oxidative stress and inflammation (Dutta et al., 2015; Flora et al., 2007). The functions of T cells, B cells, NK cells and macrophages were also showed to be suppressed by arsenic both *in vivo* and *in vitro* (Dangleben et al., 2013). A simplified scheme of the general arsenic effects on the immune system is demonstrated in Fig 1.3. Reduced immune surveillance may contribute to the carcinogenesis and other arsenic-related diseases.

Many previous arsenic immunotoxicity studies focused on high concentrations (Ahmed et al., 2014; Patra et al., 2013; Sakurai et al., 2004). It is uncommon that people can be exposed to arsenic at ppm levels. Our previous studies have demonstrated that arsenic can cause immunosuppression at extremely low concentrations. 500 nM As^{+3} was showed to suppress the functions of immune cells from mouse spleen (Li et al., 2010). The proliferation of the early B cells in bone marrow was also showed to be suppressed by As^{+3} at 50 nM (Ezeh et al., 2014). Dose-dependent suppression was also observed at ~0.1–10 ppb As^{+3} concentrations in human peripheral blood T cells in some individuals (Burchiel et al., 2014). These findings not only identified the immunotoxicity of arsenic at low concentrations, but also support the idea that more immunotoxicity studies on arsenic should be conducted at low concentrations within the nanomolar range.

Since the early T cells mature in the thymus, the alterations on T cells caused by arsenic may take place on the developing T cells in the thymus. Epidemiology and animal studies have revealed that arsenic can cause thymic atrophy, induce oxidative stress in thymus cells and alter cell cycle related gene expression (Table 1.1). These studies

revealed the toxic effects of arsenic to the thymus cells. However, the doses of arsenic applied in most of these animal studies were higher than environmentally relevant concentrations.

Many studies revealed that thymic dysfunction could result in T cell-based immunodeficiencies (Amariglio et al., 2010; Jeong et al., 2015; Nunes-Alves et al., 2013). The toxicity induced by arsenic in the early developing thymic T cells may affect the matured T cells at later stages. Studies have demonstrated that arsenic suppressed the proliferation and function of human T cells (Burchiel et al., 2014; Hernández-Castroet al., 2009; Morzadec et al., 2012). A study on a New Hampshire pregnancy cohort revealed that *in utero* arsenic exposure could alter the cytokine secretion of the T cells from the neonates' cord blood (Nadeau et al., 2014). Another study compared the T cell proliferation and cytokine secretion between 20 arsenic exposed individuals and 18 arsenic unexposed individuals indicated that 200 ppb arsenic exposure from drinking water significantly suppressed the T cell secretion of IFN-γ, IL2, IL10, IL5, and IL4 (Biswas et al., 2008). These studies provided evidence that the arsenic induced suppression on the matured peripheral T cells may result from the arsenic toxicity on the early developing thymic T cells.

The current known mechanisms of arsenic toxicity include the suppression of DNA repair, induction of oxidative stress, alteration of cellular signaling, and epigenetic modifications (Dangleben et al., 2013). These mechanisms, except the epigenetic modifications, will be explored in this project.

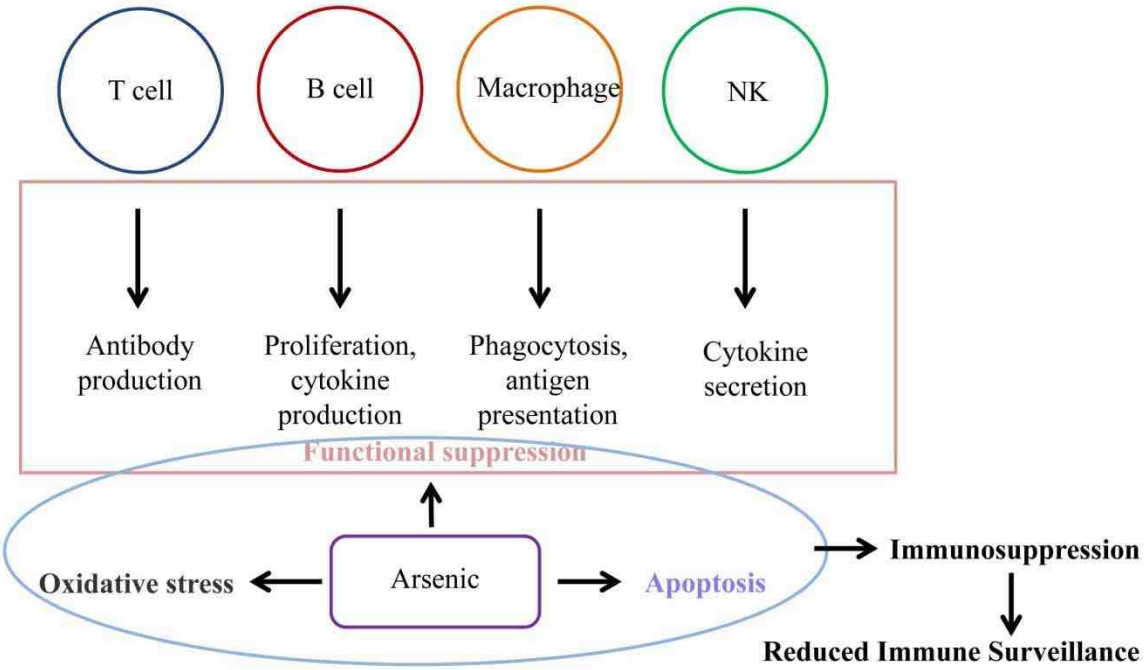

Figure 1.3. Arsenic induced immunotoxicity. Arsenic can cause oxidative stress and induce apoptosis in multiple types of immune cells. Arsenic exposure is also known to suppress the functions of T cells, B cells macrophages and NK cells. These effects together contribute to reduced immune surveillance.

Table 1.1. Epidemiology and animal studies conducted by other groups on arsenic induced thymic toxicity.

Human *in utero* exposures				
Exposure	Country	Cohort	Effects	Reference
Urinary arsenic 4–1126 ppb	Bangladesh	130 women and their kids	Thymus atrophy	Raqib et al, 2009
Placenta arsenic 17–598 ppb	Bangladesh	286 women and their kids	Decreased sjTRECs[1] levels	Ahmed et al, 2012
Animal *in vivo* studies				
Exposure	Length	Species	Effects	Reference
6.66 mg/kg	4 wks, 5 d/wk	4 wk old Male Wistar rats	Thymus atrophy	Schulz et al, 2002
10 mg/kg	7 d	5 wk old male C57BL/6J mice	Cell cycle gene expression decrease	Nohara et al, 2008
5 mg/kg	6, 12, 24, 48 and 72 h	7 wk old female C57/BL6 and KM mice	Thymus atrophy, oxidative stress	Duan et al., 2015

1. sjTREC are the index to measure the developing T cell function in thymus

Poly(ADP-Ribose) polymerase (PARP) inhibition by arsenic

The PARP family comprises 17 members, and play important roles in DNA repair and cell survival regulation (Jubin et al., 2016). PARP1 is the most important member in the PARP family for DNA repair, since the activation of some other PARP family proteins, like PARP2, is dependent on PARP1 activation (Beck et al., 2014). PARP1 is a zinc finger protein and the initiator of the base excision repair (BER) for single strand breaks (SSBs). PARP1 is also known to participate in the repair of double strand breaks (DSBs) caused by oxidative damage. The DNA binding domain of PARP1 contains two C3H1 zinc fingers. Besides its role in DNA repair, PARP1 is also involved in caspase-independent programed cell death (Los et al., 2002). Studies also revealed that PARP1 activation plays a role in the induction of asthma and autoimmune conditions (Virág, 2005). Some PARP1 inhibitors have been found in clinical trials to induce apoptosis in cancer cells (Cepeda et al., 2006).

PARP1 is known to be inhibited by As^{+3}, which can disrupt the coordination sphere in the zinc finger environment of the PARP1 DNA binding domain, and replace the zinc in the zinc finger (Zhou et al., 2011). As^{+3} can interact with C3H1 and C4 zinc fingers and MMA^{+3} is known to interact with C2H2, C3H1 and C4 zinc fingers (Zhou et al., 2014). In addition to its ability to replace zinc in the zinc fingers of PARP1, both As^{+3} and MMA^{+3} can induce oxidative stress in cells at high concentrations (Qin et al., 2008). Reactive oxygen species (ROS) and reactive nitrogen species (RNS) can also inhibit PARP1 activity (Zhou et al., 2011; 2016). Therefore, the dual actions of arsenic at low and high concentrations are considered to be the major mechanisms of PARP1 inhibition (Fig 1.4). There is evidence that DNA damage caused by spontaneous base loss and ROS

are repaired by BER (Carrozza et al., 2009). Inhibition of the PARP1, one of the key factors in BER, will leave the damaged DNA damage unrepaired, leading to DSBs with DNA replication (Zharkov, 2008). There is also evidence showing that PARP1 contributes to the activity other DNA repair protein such as XPA, which is an important factor for the repair of DSBs (King et al., 2012).

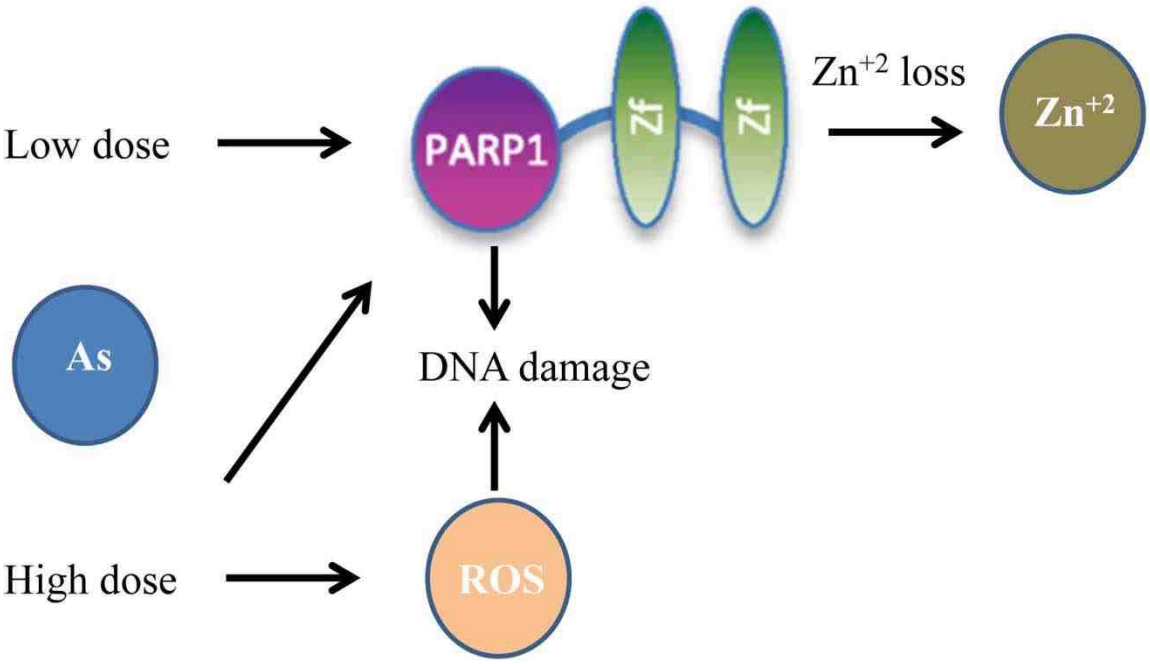

Figure 1.4. Dual actions of arsenic in the inhibition of PARP1. Arsenic at low doses replaces the zinc (Zn^{+2}) on the zinc fingers of the PARP1 DNA binding domain. Arsenic at high doses can also generate ROS, in addition to the direct replacement of Zn^{+2}. Both Zn^{+2} loss and ROS production causes DNA damage increase in cells.

Suppression of common γ chain receptor signaling by arsenic: IL-7 signaling in thymus cell development

The common γ chain, also known as IL-2 receptor subunit gamma, is a cytokine receptor subunit that is found to be associated with IL-2, IL-4, IL-7, IL-9, IL-15 and IL-21 receptors (Asao et al., 2001; Noguchi et al., 1993; Russell et al., 1993; Takeshita et al., 1992). The signaling of these cytokine receptors is known to involve janus kinases (JAKs) and signal transducer and activator of transcriptions (STATs). Many studies have demonstrated that the common γ chain receptors can be suppressed by arsenic. In patients with adult T-cell leukemia, arsenic treatments were found to decrease IL-4 signaling (Kchour et al., 2013). IL-2 and IL-4 signaling was also demonstrated to be suppressed by As^{+3} at high concentrations (Cheng et al., 2004; Choudhury et al., 2016). Although the mechanism of the common γ chain receptor signaling suppression by arsenic is still not clear, studies revealed that As^{+3} and MMA^{+3} inhibited the phosphorylation of JAKs and STATs, the important downstream factors in the signal transduction (Cheng et al., 2004; Ezeh et al., 2016).

IL-7 is secreted by stromal cells in bone marrow and thymus cortex. IL-7 signaling is required for the development of the early thymic T cells (Namen et al., 1988). The conversion of the DN cells to DP cells is showed to be controlled by the IL-7 signaling (Boudil et al., 2015). In the IL-7 signaling pathway, the binding of IL-7 to IL-7 receptor leads to a cascade of signals involving JAK1, JAK3 and STAT5 (Fig 1.5). STAT5 is phosphorylated by phospho-JAK1 (pJAK1), and phospho-STAT5 (pSTAT5) is stabilized by phospho-JAK3 (pJAK3) (Haan et al., 2011). Previous studies in our lab revealed that trivalent forms of arsenic can decrease pSTAT5 in pre-B cells in bone

marrow, inhibiting the transcriptions of cell proliferation genes like PAX5 (Ezeh et al., 2016). Since IL-7 signaling is critical for DN T cell development, the suppression of IL-7 signaling by arsenic may be a mechanism of arsenic-induced immunotoxicity to the early T cells. Therefore, the non-genotoxicity study will be focused on whether arsenic can suppress the IL-7 signaling on DN cells in thymus.

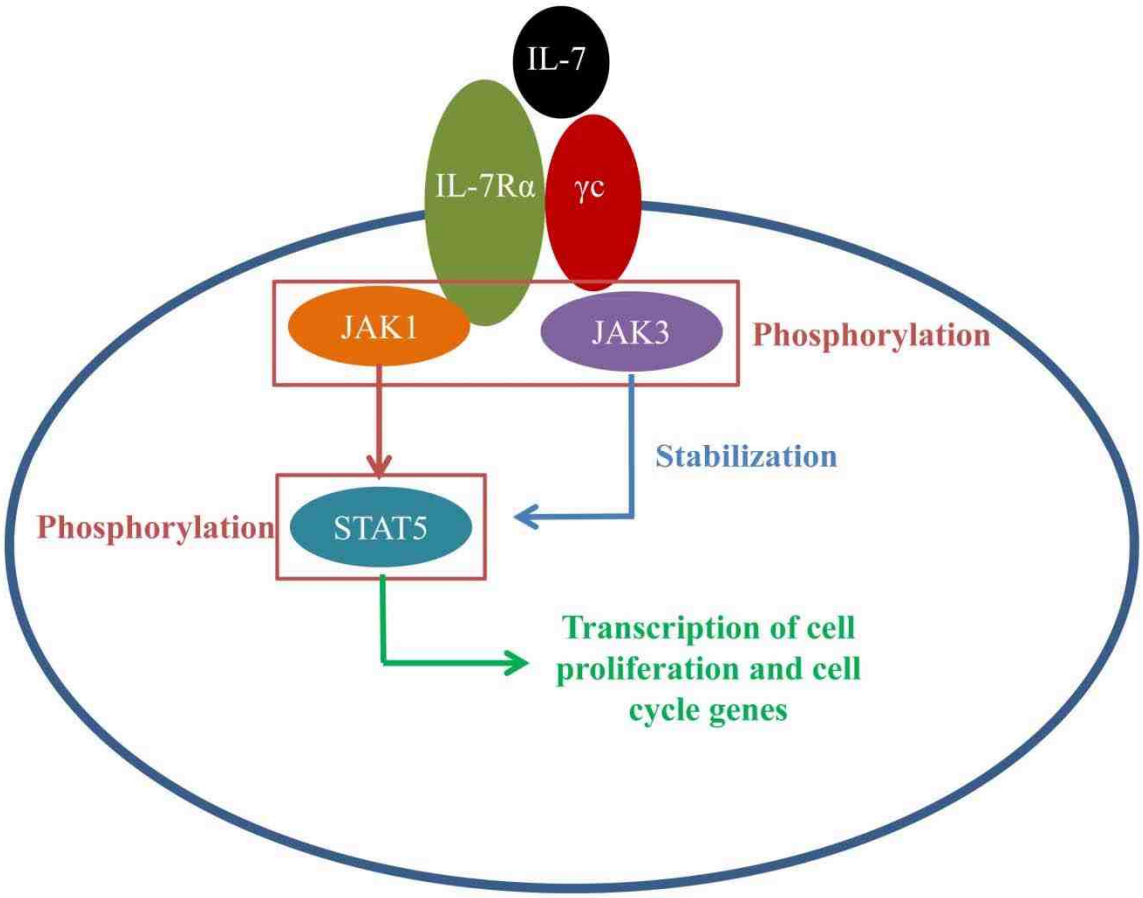

Figure 1.5. The IL-7 receptor signaling pathway. The IL-7 receptor has an α chain and a common γ chain (γc). JAK1 and JAK3 are phosphorylated by the IL-7 receptor after the binding of IL-7 cytokine to the receptor. STAT5 is phosphorylated by pJAK1 and the phosphorylation is stabilized by pJAK3. Phosphorylated STAT5 is the transcriptional factor for many cell proliferation and cell cycle genes.

Arsenic efflux transporters in eukaryotic cells

There are many studies on arsenic toxicity in different organs and cells. However, few studies have addressed one fundamental question- when cells are exposed to arsenic, how much arsenic can really get into the cells? Aquaglyceroporins (AQPs) play a central role in the uptake or As^{+3} into cells. Phosphate transporters are the major importers of As^{+5} (DiTusa et al., 2016). The organic anion transporting polypeptides (OATP1B1, OATP1B2) and the glucose permeases (GLUT1, GLUT2, GLUT5) are also important importers of As^{+3} (Calatayud et al., 2012; Jiang et al., 2010; Leung et al., 2007; Liu et al., 2004). While the multidrug resistance transporters and the multidrug resistance-associated transporters, Mdr1 (Abcb1, P-gp1) and Mrps (ABCCs) are known exporters of inorganic As^{+3}, the AQP9 and GLUT2 transporters are also demonstrated to be responsible for the transportation of MMA^{+3} and DMA^{+3} out of the cells (Drobná et al., 2020; Liu et al., 2006). There is also evidence showing that the exportation of As^{+3} by Mrps requires the conjugation with glutathione (GSH), and the exportation by Mdr1 is GSH –independent (Maciaszczyk-Dziubinska et al., 2012). An overview of the current understanding of arsenic transporters (importers and exporters) is presented in Fig 1.6.

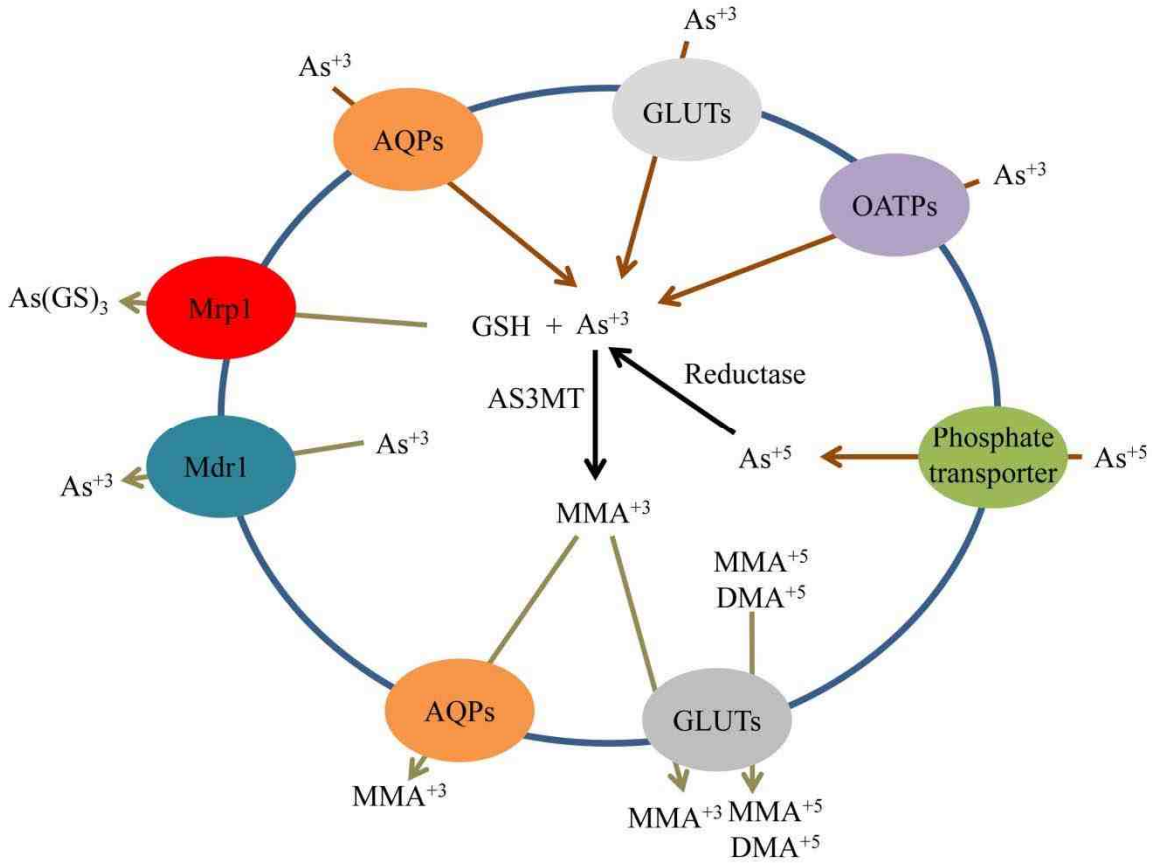

Figure 1.6. Arsenic transporters in immune cells. Uptake of As^{+5} is mediated by phosphate transporter(s). AQPs, GLUTs and OATPs are the known importers of As^{+3}. Mrp1 is expressed by immune cells and exports GSH conjugated As^{+3}. Mdr1 is a GSH independent exporter of As^{+3}. MMA^{+3} is exported by certain AQPs and GLUTs. MMA^{+5} and DMA^{+5} are transported out of the cell by GLUTs.

Benzo(a) pyrene (BaP) metabolism and immunotoxicity

BaP, a well-studied polycyclic aromatic hydrocarbon (PAH), is a group I carcinogen, as classified by International Agency for Research on Cancer (IARC). BaP is known to cause colon and other cancers in humans (Le Marchand et al., 2002). BaP is a pro-carcinogen that requires metabolism by three enzymes, CYP1A1, CYP1B1 and epoxide hydrolase (Jones et al., 1995; Shimada and Fujii-Kuriyama, 2004). When BaP gets into the human body, it is first transformed into benzo(a) pyrene-7,8-dihydrodiol (BP-Diol), which is then converted into benzo(a) pyrene-7,8-dihydrodiol-9,10-epoxide (BPDE) (Fig 1.7). BPDE can covalently bind to DNA, forming DNA adducts which induce single and double strand DNA breaks (Kim et al., 1998; Schwarz et al., 2001).

Many studies have demonstrated that BaP exposure can cause immunotoxicity (Li et al., 2010; Rodríguez-Fragoso et al., 2009). BaP *in vivo* exposure at 3 mg/kg for 35 d was found to cause thymus atrophy and decrease in lymphocyte numbers and antibody secretions (De Jong et al., 1999). Similar suppressive effects on immune functions were also found in mice and fish after exposures to BaP or its metabolites (Carlson et al., 2004; Schellenberger et al., 2009). An *in vitro* study on BaP toxicity using primary mouse immune cells revealed that the BaP adduct formation and cytotoxicity are correlated with the suppressive effects on spleen cell functions (Ginsberg et al., 2009). These immunotoxic effects of BaP may be strengthened when combined with arsenic at certain concentrations.

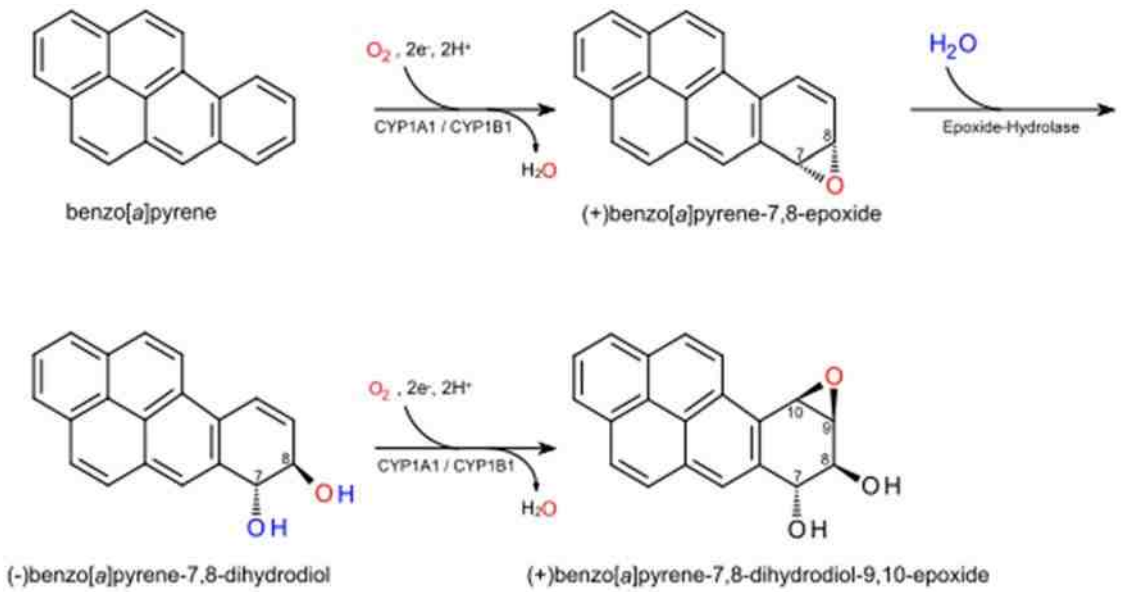

(https://en.wikipedia.org/wiki/Benzo(a)pyrene)

Figure 1.7. Metabolism of BaP *in vivo*. BaP is metabolized to the epoxide form by CYP1A1 and CYP1B1. Epoxide hydrolase is required to form BP-Diol. BP-Diol is also metabolized to BPDE by CYP1A1 and CYP1B1.

Arsenic and polycyclic aromatic hydrocarbon (PAH) interactions

Previous studies have demonstrated that arsenic can interact with many other environmental agents, such as UV light (Cooper et al., 2009, 2013; Evans et al., 2004; Zhou et al., 2011). Since polycyclic aromatic hydrocarbons (PAHs) are ubiquitous pollutants in the environment, it is common that arsenic and PAH co-exposure can occur. Many studies have addressed the concerns about arsenic and PAH interactions. A study on smokers from arsenic polluted areas showed that As^{+3} exposure in drinking water was related to the increased risk of lung cancer (Hertz-Piccioto et al., 1992). Increased adduct formation was also found in the lung and skin tissues from As^{+3} and BaP co-exposed mice (Evans et al., 2004). A study using mouse hepatocytes indicated that As^{+3} potentiated the genotoxicity induced by BaP (Maier et al., 2002). Previous studies in our laboratory demonstrated that combined exposures of low doses of As^{+3} and PAHs suppressed the T-dependent antibody responses in mouse splenocytes (Li et al., 2010). A more recent study also showed that low doses of As^{+3} and MMA^{+3} interacted with extremely low doses of Dibenzo[def, p]chrysene (DBC) synergistically to suppress mouse bone marrow lymphoid progenitor cells (Ezeh et al., 2015). These studies indicated that arsenic and certain PAHs may be interactive at low concentrations and induce synergistic genotoxicity to suppress the target organs or cells.

HYPOTHESIS AND SPECIFIC AIMS

The overall hypothesis is that arsenic at environmentally relevant concentrations disrupts the development of thymocytes through both genotoxic and non-genotoxic mechanisms, and interacts with other environmental agents such as PAHs to enhance the genotoxic effects.

Specific Aims

Specific Aim 1: To examine both the genotoxic and non-genotoxic effects of environmentally relevant concentrations of arsenic (As) in mouse thymus cells, and compare the arsenic induced genotoxicity in three important immune organs (bone marrow, spleen and thymus).The hypothesis to be tested is that arsenic can induce both genotoxicity and non-genotoxicity in mouse thymus cells. The study will not only examine the potential toxic effects of arsnic at very low concentrations, but also provide the mechanistic insights to the thymic toxicity and immunosuppression previously observed by other groups in population studies. The As^{+3} induced genotoxicity *in vivo* will be examined in bone marrow, spleen and thymus. Aim 1 is separated into the genotoxic effects (Chapter 2), the non-genotoxic effects (Chapter 3), and the comparison of the sensitivities to As^{+3} of the three immune organs (Chapter 4).

Specific Aim 2: To investigate the interaction between polycyclic aromatic hydrocarbons (PAHs) and the trivalent inorganic form of arsenic, As^{+3}, on genotoxic pathways in primary mouse thymocytes. The hypothesis to be tested is that certain PAHs such as BaP

can increase DNA damage in thymus cells, and As^{+3} at low concentrations inhibits the DNA repair system by suppressing PARP activity without causing a significant increase in oxidative stress, leading to a synergistic genotoxic effect that increase the DNA damage induced by the PAHs or As^{+3} alone. The study (Chapter 5) will reveal the possible synergistic genotoxic effects induced by the combined exposures of PAHs and arsenic and identify the potential mechanisms.

Specific Aim 3: To determine the differences in sensitivity of mouse thymocyte subsets to inorganic arsenic and associated mechanisms. Based on our observations from Specific Aim 1 and Aim 2, the hypothesis to be tested is that the differences in sensitivity of the DN cells and DP cells are due to their differences in transporter expressions and high intracellular As^{+3} accumulations. The study (Chapter 6) will not only provide a mechanistic view of differential sensitivity to arsenic in the same type of cells at different developmental stages, but also answer a fundamental question in As^{+3} toxicity studies: when exposed to As^{+3}, how much As^{+3} really gets inside the cells?

Aim 1 will provide the possible mechanisms of how arsenic induces the suppression of early developing T cells in thymus, which may potentially cause the suppression of immune function. Since the combination exposures are common in real environmental conditions, the mechanism of the interactive effects between PAH and arsenic revealed in Aim 2 will be a good example and reference for environmental exposure studies and safety assessment. Results from Aim 3 will provide a potential mechanism that why certain malignant cells are resistant to arsenic induced toxicity.

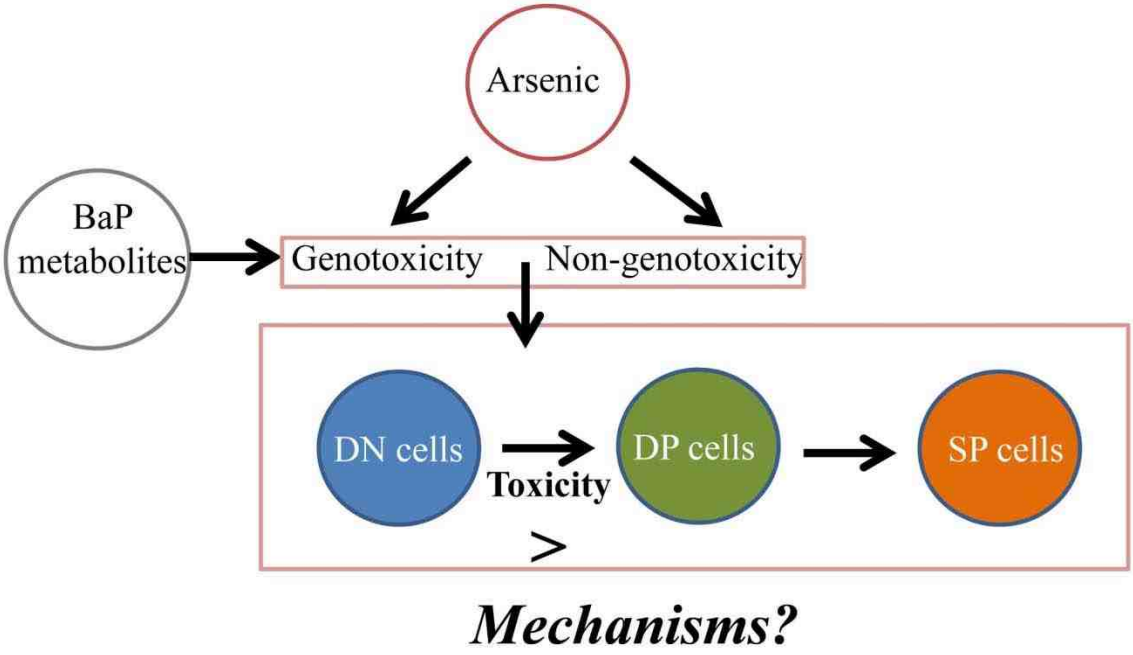

Figure 1.8. The premise for current study.

Hypothesis: arsenic induces both genotoxicity and non-genotoxicity in thymus cells. BaP and its metabolites can interact with arsenic to exert the genotoxicity. DN and DP cells have differential sensitivity to arsenic induced genotoxicity regulated by the transportation of arsenic.

?1. Do low doses of arsenic cause genotoxicity and non-genotoxicity in thymus cells?

?2. Could BaP and its metabolites interact with arsenic in genotoxicity?

?3. Are there any differences in sensitivity of DN and DP cells to arsenic? Mechanisms?

Animal and cell models; Rationale for arsenic concentrations

Based on the previous studies in our lab, male C57BL/6J mice were purchased from Jackson Laboratory at 8 weeks old. After 1 week of accommodation to our animal facility, mice were exposed to 0 to 500 ppb As^{+3} for 30 d via drinking water to mimic the long-term environmental arsenic exposures. Epidemiology studies indicated that people can environmentally expose to arsenic up to 700 ppb concentrations (Chowdhury et al., 2000). The dose range in the study was lower than many other arsenic *in vivo* studies.

Both isolated primary mouse thymus cells and a DN mouse thymic T cell line, D1, were used in the *in vitro* studies. D1 cells were generated from the thymus cells of male p53 knockout mice (Kim et al., 2003). The cells are highly IL-7 dependent and negative for both CD4 and CD8 cell surface markers. Most of the genotoxicity studies were performed on primary thymus cells first. The D1 cells were used in gentoxicity studies after experimental confirmation that arsenic induced genotoxic effects in D1 cells were comparable to primary thymus cells. D1 cells were also used in IL-7 signaling studies as DN thymus cells, since primary DN cells are a small population among thymus cells (~5%). Therefore, the use of the D1 cell line in our study helped to save the time and cost, and reduced the use of animals. For the *in vitro* arsenic treatments, concentrations were kept within nanomolar range (10 ppb ≈ 130 nM).

CHAPTER 2

Environmentally-Relevant Concentrations of Arsenite Induce Dose-Dependent Differential Genotoxicity Through Poly(ADP-ribose) Polymerase (PARP) Inhibition and Oxidative Stress in Mouse Thymus Cells

Huan Xu[*], Xixi Zhou[*], Xia Wen[†], Fredine T. Lauer[*], Ke Jian Liu[*], Laurie G. Hudson[*], Lauren M. Aleksunes[†], and Scott W. Burchiel[* §]

*The University of New Mexico College of Pharmacy, Department of Pharmaceutical Sciences, Albuquerque, NM 87131

†Rutgers, the State University of New Jersey, Ernest Mario School of Pharmacy, Department of Pharmacology and Toxicology, Piscataway, NJ 08854

§To whom correspondence should be addressed. Fax: (505) 272-6749. Email: sburchiel@salud.unm.edu

Toxicological Sciences, 149(1): 31-41. DOI: 10.1093/toxsci/kfv211.

Received July 17, 2015; Revision received August 25, 2015; Accepted September 9, 2015; Published online October 5, 2015.

ABSTRACT

Inhibition of DNA repair and oxidative stress are two common mechanisms associated with arsenic-induced genotoxicity. The purpose of this study was to examine mechanisms of genotoxicity induced by environmentally-relevant doses of arsenite (As^{+3}) in mouse thymus cells. An increase in DNA damage and a decrease in PARP activity were seen *in vitro* following exposure to 50 nM As^{+3} in primary mouse thymus cells and a murine thymus pre-T cell line, D1. 3,4-Dihydro-5[4-(1-piperindinyl) butoxyl]-1(2H)-isoquinoline (DPQ), a well-characterized PARP inhibitor, also produced DNA damage in D1 cells, confirming the correlation between PARP inhibition and DNA damage increase. As^{+3} at 500 nM induced double strand breaks (DSBs) in DNA and oxidative stress at 4 h in D1 cells, which was reversed at 18 h. No apoptosis or decrease of viability was observed in these exposures. 4-hydroxy-2,2,6,6-tetramethylpiperidin-1-oxyl (TEMPOL), a widely-used antioxidant, was utilized to confirm that oxidative stress is partially responsible for the increase of strand breaks in 500 nM As^{+3} exposure at 4 h. Expression of As^{+3} exporters, Mdr1 and Mrp1, were found to be induced by 500 nM As^{+3} in D1 cells, suggesting a possible mechanism for reversal of oxidative stress and DSBs at the 18h timepoint. Finally, we showed that DNA damage and PARP inhibition by As^{+3} were reversed by zinc (Zn^{+2}) at approximate equimolar doses. Collectively, these results demonstrate that As^{+3} at doses within the nanomolar range induce genotoxicity by inhibiting PARP, and produces oxidative stress at higher concentrations, which can be reversed by a Zn^{+2} treatment.

INTRODUCTION

Two primary forms of inorganic arsenic (As), trivalent arsenite (As^{+3}) and pentavalent arsenate (As^{+5}), are found in air, food and drinking water in many countries around the world. As^{+3} exposure is associated with diseases such as skin lesions, diabetes, cardiovascular diseases, and different types of cancers (Argos et al., 2010; Schuhmacher-Wolz et al., 2009; Vahter et al., 2008). Although growing evidence indicates that As^{+3} affects the immune system in multiple aspects, the exact mechanisms are still poorly understood (Dangleben et al., 2013). Oxidative stress due to formation of reactive oxygen species (ROS) and inhibition of DNA repair are the two most common mechanisms proposed for As-induced genotoxicity (Faita et al., 2013). An increase in ROS has been observed in multiple models after As^{+3} treatment such as keratinocytes, lymphoid cells, and many types of cancer cells (Cooper et al., 2009; Li et al., 2001; Zhang et al., 2011). ROS production leads to multiple effects in different types of cells, including apoptosis or necrosis, cell cycle arrest, generation of both single (SSB) and double strand breaks (DSB), and gene mutation (Bauer et al., 2011; Shi et al., 2004; Wiseman et al., 1996).

Poly(ADP-ribose) polymerase (PARP), the 'nick sensor' in base excision repair (BER) for SSBs and direct participant in the repair of oxidative DNA damage, is directly inhibited by As^{+3} (Qin et al., 2012; Zhou et al., 2011). PARP is a protein with a DNA binding domain containing two C3H1 zinc (Zn) finger motifs, and replacement of Zn with As^{+3} is believed to be the mechanism that disrupts the coordination sphere in the Zn finger environment, impairing function of the protein (Zhou et al., 2014). There is also evidence that DNA damage caused by spontaneous base loss or genotoxic agents are

repaired by BER (Zharkov, 2008), and inhibition of PARP may leave damaged DNA unrepaired, leading to the formation of DSBs in a replication-dependent manner (Carrozza et al., 2009). DSBs are repaired through non-homologous end joining, microhomology-mediated end joining, or homologous recombination, which are detrimental to cells and may lead to mutation or apoptosis (Kaina, 2003; Lieber, 2010).

Previous studies in our laboratory reported that *in vivo* drinking water exposure to As^{+3} suppresses mouse bone marrow and spleen cell function (Ezeh et al., 2014). Exposure of spleen cells *in vitro* suppressed T cell dependent humoral immunity at concentrations as low as 500 nM (Li et al., 2010). Studies in human peripheral blood mononuclear cells (HPBMC) showed a dose-dependent suppression of T cell proliferation at extremely low concentrations of As^{+3} (0.1-10 nM) in some individuals (Burchiel et al., 2014). These studies demonstrate that human and mouse lymphocytes are extremely sensitive to low concentrations of As^{+3} that likely reflect environmental exposures. Because our previous studies showed the bone marrow cells are sensitive to low doses of As^{+3} exposure (Ezeh et al., 2014), the purpose of the present studies was to examine whether thymus cells are also sensitive to As^{+3} and to determine potential mechanisms of genotoxicity.

METHODS

Isolation of primary mouse thymus cells

C57BL/6J male mice were purchased at 8 to 10 weeks of age from Jackson Laboratory (Bar Harbor, ME). All animal experiments were performed following the protocols approved by the Institutional Animal Use and Care Committee at the University of New Mexico Health Sciences Center. Mouse thymuses were harvested and transferred to the laboratory in Hanks Balance Salt Solution (HBSS, Lonza, Walersville, MD). Cells from each thymus were prepared as single cell suspensions by placing the organ between the frosted ends of two microscope slides (Fisher Scientific, Pittsburgh, PA) and squeezed into a dish containing 5 mL of the mouse medium [RPMI-1640 (Sigma-Aldrich, St.Louis, MO) with 10% FBS (HyClone Laboratories, Logan, UT), 2 mM L-glutamine (Life Technologies, Grand Island, NY), 100 mg/ml streptomycin, 100 units/ml penicillin (Life Technologies)]. Cells from 3 mice were pooled, centrifuged at 200 x*g* for 10 min and resuspended in the mouse medium. Cell viability was determined by acridine orange/propidium iodide (AO/PI) staining and counting using the Nexcelom Cellometer 2000.

Culture and treatment of D1 cell

The D1 cell line is a CD3+CD4-CD8-, IL-7 dependent pre-T cell line established from p53−/− mouse thymocytes (Kim et al., 2003). It was a generous gift from Dr. Scott K. Durum (Center for Cancer Research, National Institute of Health, Frederick, MD). It is one of the few mouse pre-T cell lines that can be used to examine effects of xenobiotics on early thymic T cells. Cells were maintained in RPMI 1640 with 10% FBS (Atlanta

Biologicals, Flowery Branch, GA), 2 mM L-glutamine, 100 mg/ml streptomycin, 100 units/ml penicillin, and 50 ng/ml recombinant mouse IL-7 (PeproTech, Rocky Hill, NJ). Cells were seeded at $5x10^4$ cells/ml and subcultured every 3-4 days. Cell numbers and viabilities were determined by Trypan Blue and Nexcelom Cellometer 2000. For different experiments, cells were treated with sodium arsenite (Sigma-Aldrich), 4-hydroxy-2,2,6,6-tetramethylpiperidin-1-oxyl (TEMPOL) (Sigma-Aldrich), or 3,4-Dihydro-5[4-(1-piperindinyl) butoxyl]-1(2H)-isoquinoline (DPQ) (Santa Cruz Biotechnology, Dallas, TX).

The Single Cell Gel Electrophoresis assay (Comet assay)

All reagents for the Comet assay were purchased from Trevigen (Gaithersburg, MD) unless otherwise noted. After treatments, cells were washed with Dulbecco's phosphate-buffered saline without Ca^{+2} and Mg^{+2} ($DPBS^-$, Mediatech, Manassas, VA) and immobilized in a bed of low melting point agarose on a Trevigen CometSlide™. Cells were lysed with Lysis Solution + 10% DMSO (Sigma-Aldrich), and electrophoresed in basic buffer (pH>13) with 21 volts in 30 minutes. Slides were dried, stained with Sybr Green and imaged by epifluorescence microscopy. From the image, 50 cells from each well on each of the slides were scored using CometScore (TriTek Corp., Sumerduck, VA). DNA damage was reported by percentage of DNA in tail (Collins AR, 2004).

PARP activity assay

A PARP/Apoptosis Kit from Trevigen was used to detect PARP activity in As^{+3} treated cells. Experiments were performed following the protocol described by Sun et al., 2012. After harvest, cells were lysed with Cell Extraction Buffer and total protein

concentrations in cell extracts were determined by BCA Protein Assay (Thermo Scientific, Rockford, IL). 200 ng of total proteins was combined with activated DNA and nicotinamide adenine dinucleotide (NAD) and loaded into a histone-coated strip well to form PAR and be fixed on the well bottom. After 30 min incubation at room temperature (RT), anti-PAR monoclonal antibody was added to the well to bind to PAR followed by an HRP conjugated secondary antibody. TACS- Sapphire™ was used to generate the chemiluminescence signal, then stopped by adding 0.2 M HCl. The signal was detected using SpectraMax® 340PC microplate reader (Molecular Devices).

Phospho-H2AX (Gamma H2AX) Flow Cytometry Assays

Alexa Fluor® 647 mouse anti-H2AX (pS139) was purchased from BD Biosciences (San Jose, CA). Antibody was diluted with $DPBS^-$ 1:9 before use. Harvested cells were washed with cold $DPBS^-$. 3.7% freshly prepared formaldehyde was added to fix the cells for 10 min at RT. After another wash, cells were permeablized with -20°C 90% methanol at RT for 5 min. Cells were washed again and then stained with 50 µl per sample of diluted antibody at RT for 1 h in dark. Stained cells were washed rinsed and resuspended with $DPBS^-$ and analyzed on BD Accuri™ C6 flow cytometer.

Gamma H2AX Western Blot

Total protein lysate (10 µg) was resolved on a 10% Criterion® Tris-HCl gels (Bio-Rad, Hercules, CA) and transferred onto a nitrocellulose membrane (Bio-Rad). After blocking for 1h at RT in TBST [50 mM Tris + 150 mM NaCl + 0.05% Tween 20] containing 5% blotting-grade blocker (Bio-Rad), the membrane was then incubated with a phospho-H2AX (Ser139) antibody (Rabbit, 1:1000, Cell Signaling Technology, Danvers, MA) overnight at 4 °C. After washing with TBST, the membrane was incubated

for 1 h at RT with anti-rabbit IgG, HRP-linked antibody (1:1000, Cell Signaling Technology). Following incubation, the membrane was washed and the resulting signal was detected with the SuperSignal West Femto Chemiluminescent Substrate (Thermo Scientific).

Dihydroethidium (DHE) staining

DHE was purchased from Life Technologies, resuspended with 158 µl DMSO and diluted with 20 ml $DPBS^-$ to a final concentration of 5 µM. D1 cells were treated with 0, 50 or 500 nM As^{+3} for 2, 4 or 18 h. After treatment, cells were washed twice with cold wash buffer [$DPBS^-$ +1% FBS +0.9% sodium azide (Sigma-Aldrich)]. Each sample was stained using 5 µM DHE in DPBS- with 37 °C incubation for 30 min. Cells were then washed with cold wash buffer, resuspended in 500 µl DPBS- and analyzed on BD Accuri™ C6 flow cytometer.

Annexin V/Propidium Iodide staining

FITC Annexin V Apoptosis Detection Kit II (Cat. No. 556570) was purchased from BD Biosciences. D1 cells exposed to 50 and 500 nM As^{+3} *in vitro* were washed twice with $DPBS^-$. 1 x 10^5 cells were resuspended in 100 µl 1X Annexin V Binding Buffer, 5 µl of FITC Annexin V and 5 µl of Propidium Iodide Staining Solution were added to each sample for 15 min at RT in dark. 400 µl of 1X Annexin V Binding Buffer was added and the samples were analyzed by BD Accuri™ C6 flow cytometer. D1 cells treated with 10 µM Etoposide for 4 h were used as positive control. D1 cells blocked with 5 µg of purified recombinant Annexin V and unstained D1 cells were used for gating.

RNA isolation and HO-1 qPCR

RNeasy Mini Kit ™ and QIAshredder™ (Qiagen, Valencia, CA) were used according to manufacturer's instructions to isolate RNA from As^{+3} treated D1 cells. RNA was then quantified on an Agilent Nanodrop spectrophotometer. All samples were stored at -20 °C until assayed. For each reverse transcriptase (RT) reaction, 60 µl containing a minimum of 1080 ng RNA was run on PTC-200 Thermal Cycler (MJ Research, Reno, NV) using the High Capacity cDNA Reverse Transcription Kit (Applied Biosystems, Foster City, CA) under the following conditions: 25 °C for 10 min, 37 °C for 2 h. Samples were then diluted to ~9 ng/ µl with RNase, DNase free water and stored at -20 °C. Real time PCR (qPCR) reactions utilizing Mm_Hmox1_1_SG QuantiTect® Primer Assay and QuantiTect® SYBR® Green PCR Kit (Qiagen) were carried out on Applied Biosystem's 7900HT system in a 384 well plate at 10 µl per reaction and 1 µL cDNA (~9 ng total RNA) was added to each well. qPCR thermal cycling parameters used were polymerase activation 15 min 95 °C, denature 15 s at 94 °C, anneal 30 s at 55 °C, and extend 30 s at 72 °C (denature-anneal-extend for 40 cycles). Comparative C_T (first amplification cycle exceeding threshold) method was applied for relative quantification, using GADPH gene as the endogenous reference. To calculate the comparative C_T, briefly, the difference in C_T (ΔC_T) values between target and endogenous control were determined. Then the fold differences in gene expression ($\Delta\Delta C_T$) and the ΔC_T of the control was subtracted from the ΔC_T of the target (ΔC_T target-ΔC_T calibrator). This calculation is described in detail in the manual from Applied Biosystems.

As^{+3} Exporter Assays

RNA samples of 500 nM As^{+3} treated D1 cells harvested at 2, 4 and 18 h were prepared as above. The concentration of total RNA was quantified by UV spectrophotometry at 260/280 nm using a Nanodrop spectrophotometer 2000 (Thermo Scientific). Complementary DNA was generated from 1 μg RNA using the High Capacity cDNA Reverse Transcription Kit (Life Technologies). The mRNA expression of mouse transporters was quantified by qPCR using SYBR® Green to detect amplified products in the Applied Biosystem's 7900HT PCR system. Primers used in the analysis are listed below. Ct values were converted to ΔΔCt values by comparing to a reference gene, ribosomal protein 13a (Rpl13a). For Mrp1 and Mdr1 protein expressions, Cell lysates (10-13 μg protein/well) were separated by SDS-PAGE electrophoresis and transferred to a nitrocellulose membrane at 4°C overnight. After blocking with 5% nonfat dry milk in 0.5% phosphate buffered saline with 0.5% of Tween 20 (PBS/T), membranes were incubated with primary antibodies against Mdr1 (C219) (Novus Biologicals, Littleton, CO) and Mrp1 (Alexis, Farmingdale, NY) followed by incubations with species-appropriate secondary antibodies for 1 to 2 h. The SuperSignal West Dura Chemiluminescent Substrate (Thermo Scientific) was applied to the membranes prior to detection of luminescence using a FluorChem Imager (Alpha Innotech, San Leandro, CA). Target protein band intensities were semi-quantified and normalized to β-actin levels (ab8227 antibody, Abcam).

Table 2.1 Primers used for As^{+3} exporter qPCR analysis

Transporters	Forward (5'-3')	Reverse (5'-3')
Mrp1	GCTGTGGTGGGCGCTGTCTA	CCCAGGCTCAGCCACAGGAA
Mrp2	AGCAGGTGTTCGTTGTGTGT	AGCCAAGTGCATAGGTAGAGAAT
Mdr1a	TGCCCCACCAATTTGACACCCT	ATCCAGTGCGGCCTGAACCA
Mdr1b	GTGTTAAAGGGGCGATGGGCG	AGGCTTGGCCAGACAACAGCTT

Statistics

Data were analyzed using Excel 2010 and Sigma Plot 12.5 software. One-way analysis of variance (ANOVA) and Dunnett's t-test were used to determine differences between control and treatment groups. For *in vivo* As^{+3} treatment, both treatment groups consisted of five animals and each animal was analyzed in triplicates. For the *in vitro* experiments, three replicates were performed and analyzed for each single dose.

RESULTS

As^{+3} exposure increased DNA damage and inhibited PARP in primary mouse thymus cells *in vitro*

Primary thymus cells from C57BL/6J male mice were isolated and treated with 5 and 50 nM As^{+3} and harvested at 4 and 18 h. An increase in DNA damage and a decrease in PARP activity were seen in cells treated with 50 nM As^{+3} at both time points (Fig. 2.1A and 2.1B), indicating the genotoxic effects of As^{+3} on mouse thymus cells *in vitro*. These results not only demonstrate that environmentally-relevant doses of As^{+3} induce genotoxic events in mouse thymus cells, but also suggest that inhibition of PARP activity by As^{+3} is involved in, and may be the mechanism responsible for the increase in DNA damage.

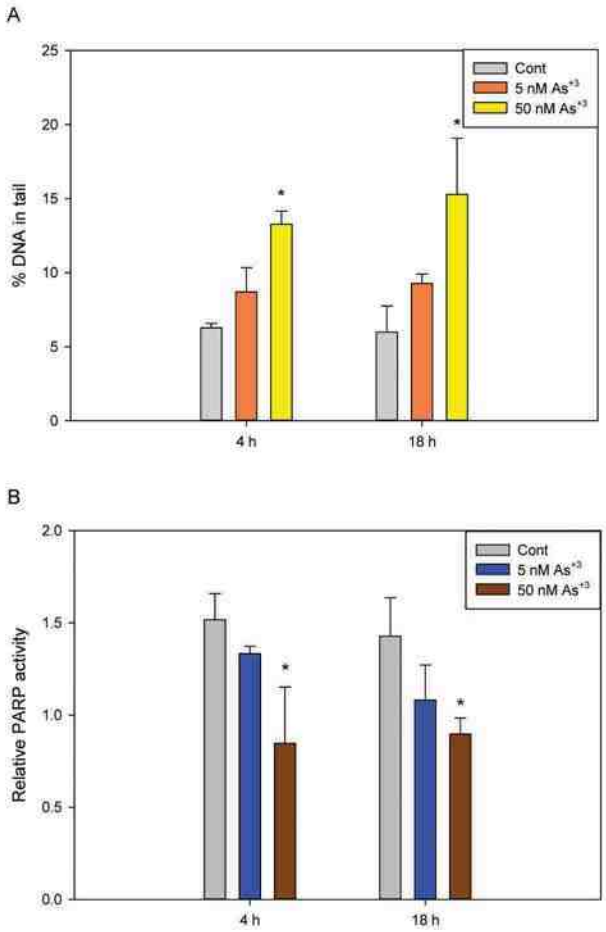

Figure 2.1. Genotoxicity in primary mouse thymus cells exposed to As^{+3} *in vitro*. Naïve primary thymus cells from C57BL/6J male mice were exposed to 5 and 50 nM for As^{+3} for 4 and 18 h *in vitro*. A, DNA damage was measured by percentage of DNA in tail using the alkaline Comet assay. B, PARP activity was measured with Trevigen ELISA kits represented by absorbance at 450 nm. *Significantly different compared to control ($p<0.05$, n=5). Results are Means ± SD.

Increased DNA damage after As^{+3} exposure is directly related to PARP inhibition in pre-T cells

We utilized an IL-7 dependent, CD3+CD4-CD8- pre-T cell line, D1, to further examine the genotoxicity induced by As^{+3} in mouse thymus cells. D1 cells were treated with As^{+3} at 5, 50 and 500 nM *in vitro* for 4 and 18 h. A significant increase of DNA damage was observed in 50 and 500 nM As^{+3} treated cells for 4 and 18 h (Fig. 2.2A). A significant decrease in PARP activity was also seen at 4 and 18 h in 50 and 500 nM As^{+3} treated cells (Fig. 2.2B). Therefore, As^{+3} induced similar genotoxic events in D1 cells as compared to primary thymus cells.

To determine if DNA damage increased by As^{+3} is related to PARP inhibition, we treated the D1 cells with a potent PARP inhibitor, DPQ. A significant increase in DNA damage was observed with 1 μM DPQ at 4 h (Fig. 2.2C) and 0.1μM DPQ at 18 h (Fig. 2.2D), indicating that the DNA damage observed with As^{+3} treatments was likely to be the result of PARP inhibition, which leaves damaged DNA unrepaired. However, because the DNA damage in the DPQ treatments seemed to have a limitation at around 15% of DNA in tail, while As^{+3} induced DNA damage easily exceeded this amount, it was thought that As^{+3} may act through additional mechanisms than inhibiting PARP alone, such as oxidative stress at higher concentrations (Fig. 2.2C and 2.2D).

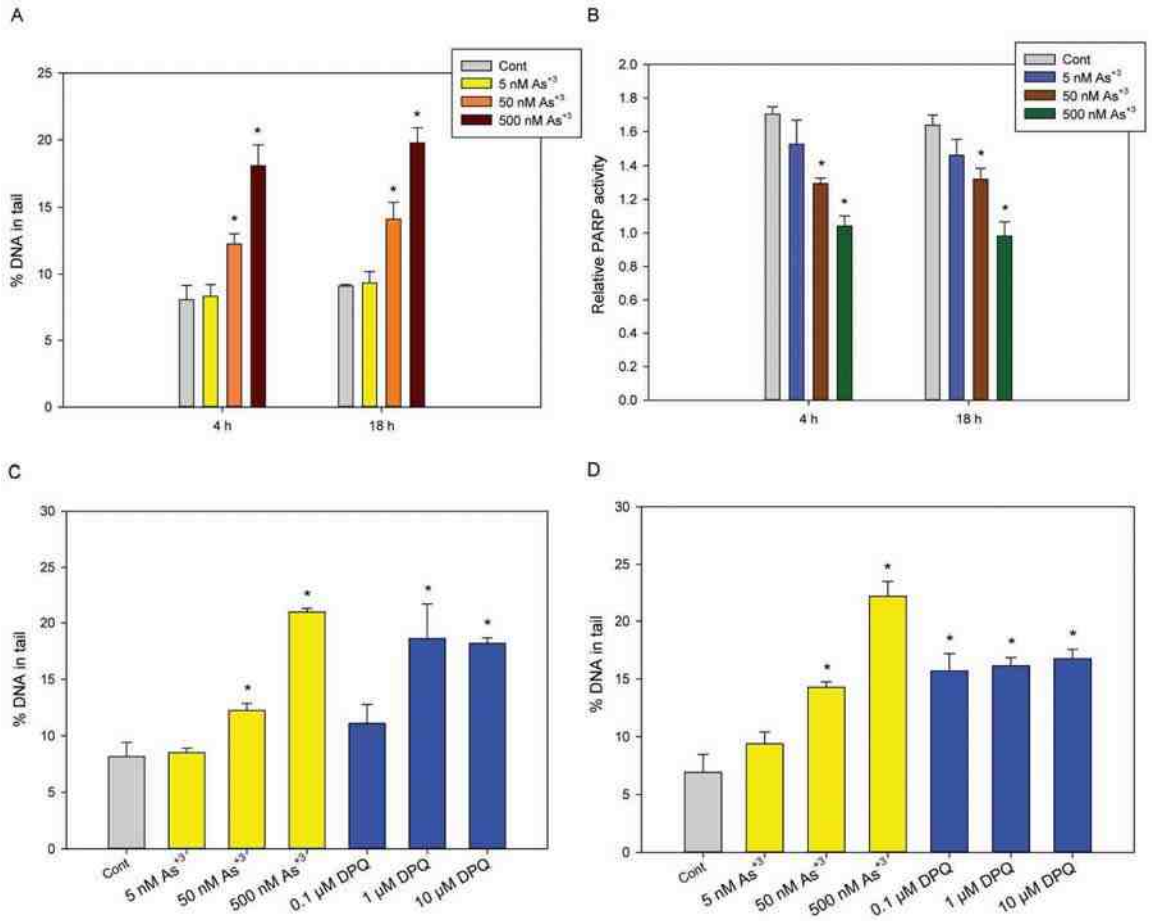

Figure 2.2. Genotoxicity in D1 cells exposed to As^{+3} or PARP inhibitor (DPQ). D1 cells were treated with 5, 50 or 500 nM As^{+3} for 4 and 18 h. A, DNA damage was measured by percentage of DNA in tail using alkaline Comet assay. B, PARP activities were measured with Trevigen ELISA kit represented by absorbance at 450 nm. C and D, DNA damage were measured by alkaline Comet assay in D1 cells treated with 5, 50 and 500 nM As^{+3} and 0.1, 1 and 10 µM PARP inhibitor, DPQ for 4 h (C) and 18 h (D). *Significantly different compared to control ($p<0.05$). Results are Means ± SD.

As^{+3} exposure at 50 and 500 nM induces double strand breaks in D1 cells at early time points

The DNA damage observed in alkaline Comet assay represents the total strand breaks including both single and double strand breaks (Collins, 2004). We have already shown that 500 nM As^{+3} caused significant genotoxicity which exceeded the effects of PARP inhibitor, so it was hypothesized that besides the inhibition of DNA repair, oxidative stress may also be involved higher levels of As^{+3} exposure (e.g., 500 nM). When DSBs occur, H2AX is phosphorylated on serine 139, also known as gamma H2AX and is often used as a marker for DSBs (Mah et al., 2010). Therefore, we treated D1 cells with 0, 50 and 500 nM of As^{+3} and harvested cells at 2, 4 and 18 h. Phospho-H2AX antibody was used to stain the cells in order to measure the phospho-H2AX level using flow cytometry. An increase in phospho-H2AX mean channel fluorescence was observed in cells exposed to 500 nM As^{+3} at both 2 and 4 h time points, but not at 18 h (Fig. 2.3A), indicating that double strand breaks were generated by As^{+3} treatment in D1 cells in early stages at high concentration (500 nM). We also confirmed the observation by Western Blot (Fig. 2.3B).

Time-dependent oxidative stress in D1 cells exposed to As^{+3}

Oxidative stress is commonly associated with the induction of DSBs. We used DHE staining to examine the superoxide level and Heme Oxygenase-1 (HO-1) expression by qPCR to see if oxidative stress is involved in the genotoxicity induced by As^{+3}. As determined by DHE fluorescence, a significant increase in superoxide level was observed at 500 nM following 2-4 h of treatment (Fig. 2.3C), but not at the 18 h time

point, indicating that it is an early stage event occurring at high exposure levels. HO-1 is known to be induced by oxidative stress and considered to be protective to cells (Vile et al., 1994). An approximate 8-fold increase in HO-1 expression was observed at 2 h and a more significant 20-fold increase was seen at 4 h in 500 nM As^{+3} treatment, but dropped to control levels at 18 h (Fig. 2.3D). These results suggested a time-dependent oxidative stress and DSBs occurrence in D1 cells treated with a high dose of As^{+3} (500 nM).

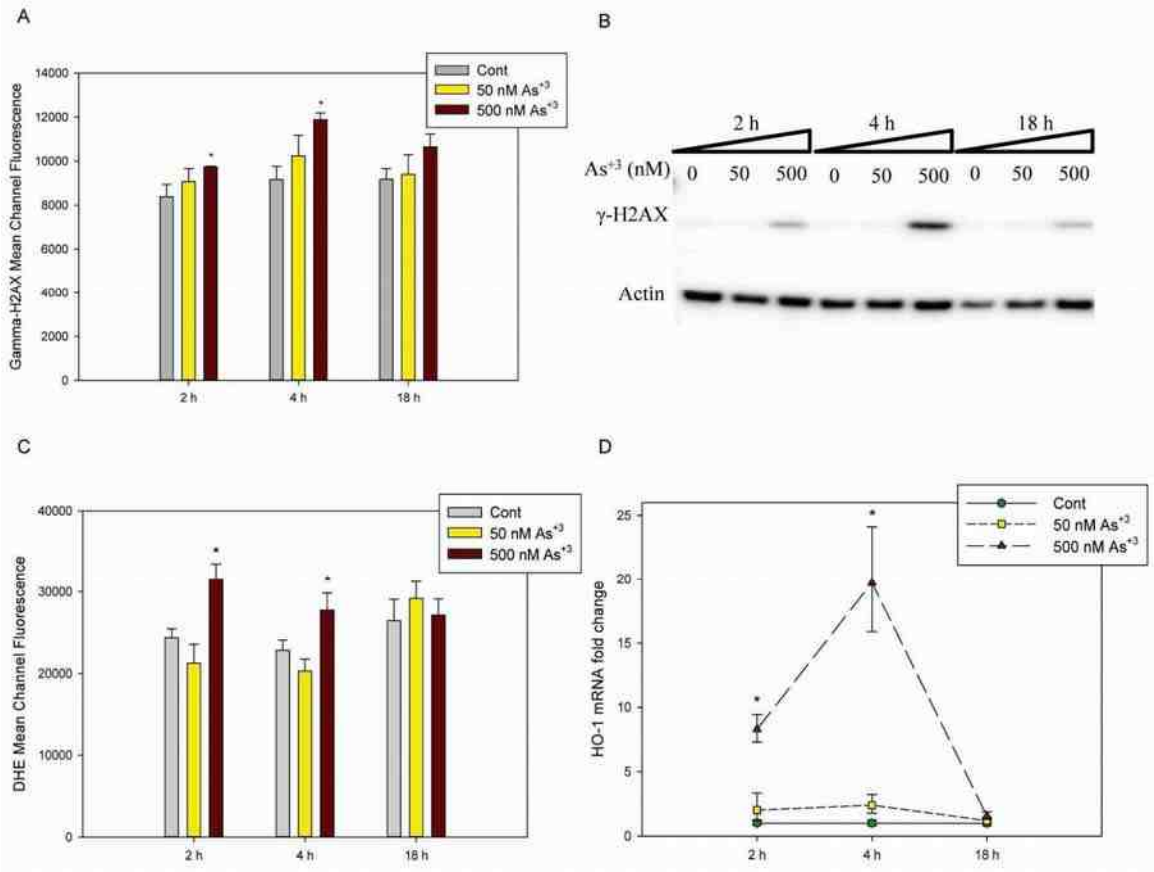

Figure 2.3. Phospho-H2AX (γ-H2AX) expression and oxidative stress in D1 cells exposed to As^{+3}. D1 cells were treated with 50 or 500 nM As^{+3}. Phospho-H2AX expression levels were measured by flow cytometry (A), represented by Mean Channel Fluorescence or Western Blot (B). C, Mean Channel Fluorescence of DHE. D, HO-1 RNA levels were measured by qPCR on cDNA samples from As^{+3} treated D1 cells. *Significantly different compared to control ($p<0.05$). Results are Means ± SD.

Exposure to As^{+3} did not induce apoptosis in D1 cells

Since DNA strand breaks and oxidative stress apoptosis may lead to cell death and the loss of PARP activity through caspase catalyzed PARP cleavage (Los et al., 2002), Annexin V and Propidium Iodide (PI) were used to check if D1 cells were apoptotic after As^{+3} exposure. No significant changes were found in both viability (% of Annexin V-, PI- cells, Fig. 2.4A and 2.4B) and % of apoptotic cells (% of Annexin V+ cells, Fig. 2.4A and 2.4C) in D1 cells exposed to 50 and 500 nM As^{+3} at 2, 4 and 18 h. The results excluded the possibility that decrease of PARP activity observed in low concentrations of As^{+3} exposure was induced by increase of apoptosis.

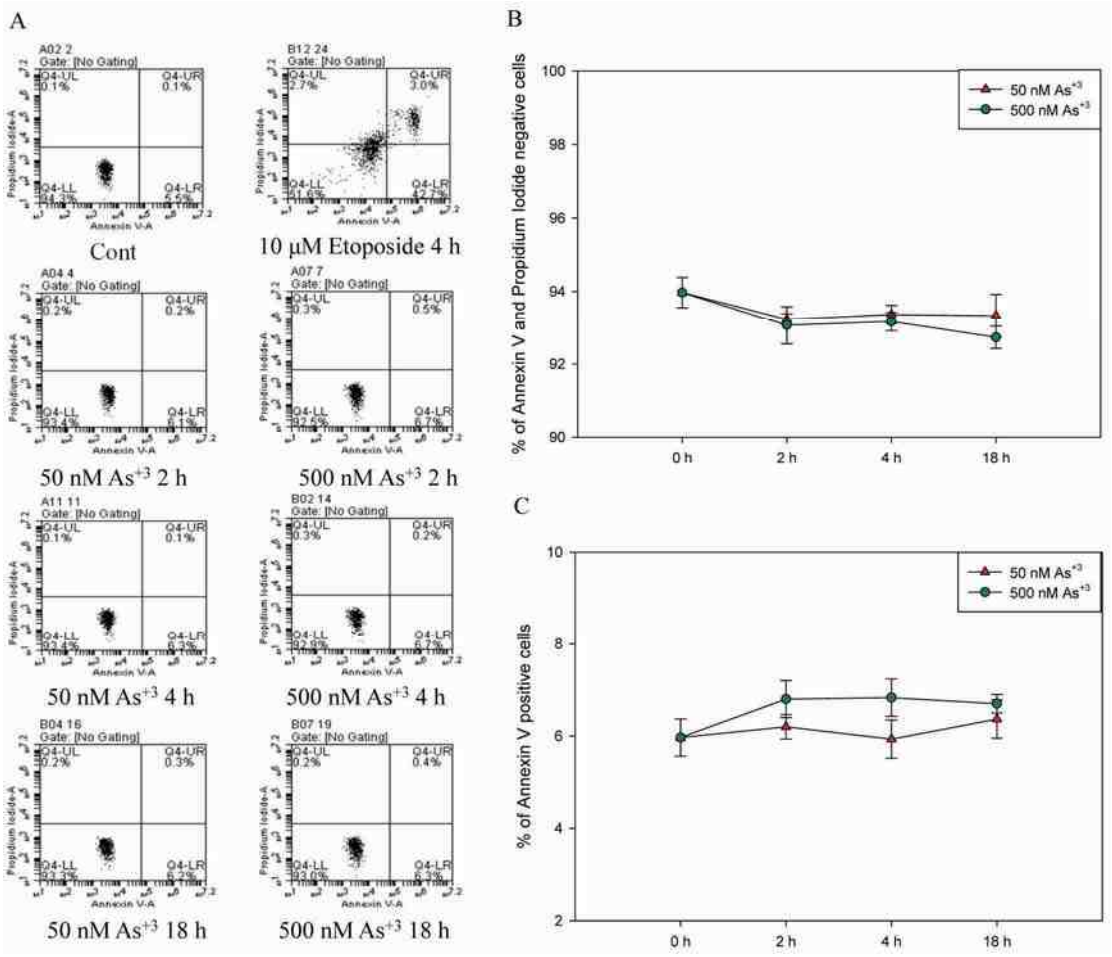

Figure 2.4. Annexin V and Propidium Iodide Staining in D1 cells exposed to As^{+3}. D1 cells were treated with 50 or 500 nM As^{+3} for 2, 4 and 18 h, or 10 µM Etoposide as positive control. A. Flow cytometry results showing D1 cells which are Annexin V-PI- (LL), Annexin V+PI- (LR), Annexin V-PI+ (UL), or Annexin V+PI+ (UR). B, viability (% of Annexin V-PI- cells). C. % of apoptotic cells (% of Annexin V+ cells).

Oxidative stress was partially responsible for the increase of DNA damage in 500 nM As^{+3} exposure at 4 h

In order to confirm that oxidative stress and superoxide production is directly related to the increase of DNA damage at 500 nM As^{+3}, we utilized a superoxide scavenger, TEMPOL, to perform co-exposure studies with As^{+3} for 4 h, at which time point oxidative stress was observed (Fig. 2.3C and 2.3D). A significant decrease of superoxide levels was observed in 500 nM As^{+3} and 100 μM TEMPOL co-exposure comparing to 500 nM As^{+3} only (Fig. 2.5A), indicating that TEMPOL inhibited the production of superoxide induced by 500 nM As^{+3}. At the same time, DNA damage was also decreased by a small amount (~2%) in As^{+3} and TEMPOL co-exposure (Fig. 2.5B), suggesting that oxidative stress and superoxide production was directly related to the DNA damage in 500 nM As^{+3} exposure at 4 h, but that oxidative stress and DSBs represent only a small percentage of total DNA strand breaks. PARP activity was not affected by adding TEMPOL in As^{+3} exposure (Fig. 2.5C). Collectively, these results indicate that oxidative stress contributes to DNA damage in D1 cells exposed to 500 nM As^{+3} at 4 h.

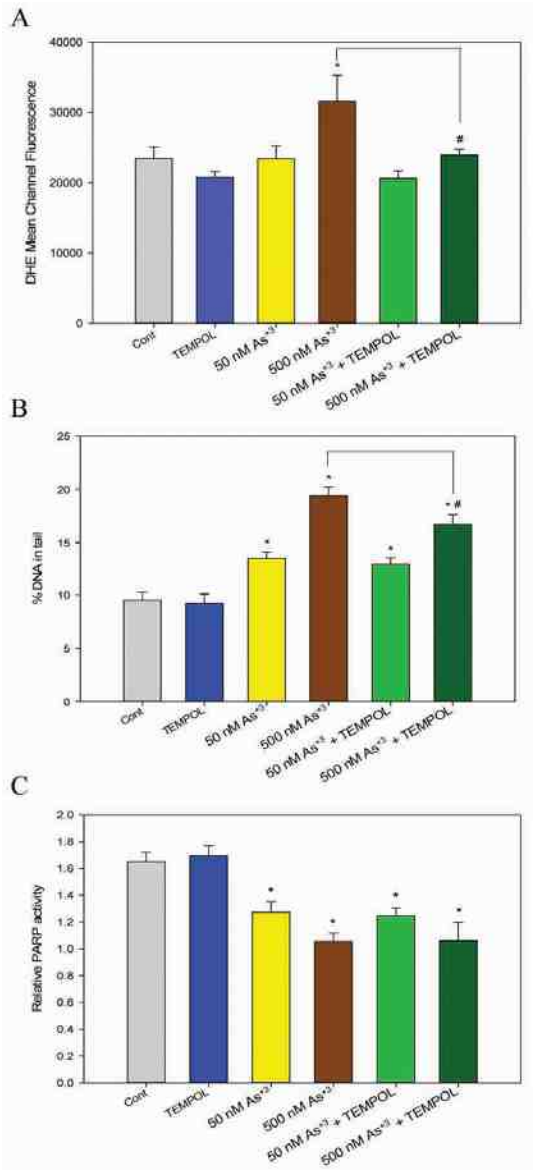

Figure 2.5. Superoxide level and genotoxicity in D1 cells exposed to As^{+3} and TEMPOL for 4 h. D1 cells were exposed with 50 or 500 nM As^{+3}, with or without co-exposure to 100 µM TEMPOL. A. Mean Channel Fluorescence of DHE represents superoxide level. B. DNA damage was measured by percentage of DNA in tail using alkaline Comet assay. C. PARP activity was measured with Trevigen ELISA kits represented by absorbance at 450 nm. *Significantly different compared to control ($p<0.05$). # Significantly different compared to 500 nM As^{+3} ($p<0.05$).Results are Means ± SD.

Induction of As^{+3} exporters by 500 nM As^{+3}

Because 500 nM As^{+3} induced DSBs and oxidative stress in D1 cells at early time points (2 and 4 h) but not at 18 h, we examined potential mechanisms responsible for this reversal . One possible mechanism is that 500 nM As^{+3} induces the expression of As^{+3} exporters such as the multidrug resistance-associated proteins 1 and 2 (Mrp1, Mrp2) or the multidrug resistance protein 1 (Mdr1) (Liu et al., 2001; Liu et al., 2002). Enhancement of efflux transporter expression could reduce intracellular levels of As^{+3} thereby reducing the toxic effects. Therefore, we examined the mRNA expression of Mrp1, Mrp2, Mdr1a and Mdr1b in D1 cells treated with 500 nM As^{+3} at 2, 4 and 18 h. An increase of Mrp2 (and to some extent Mrp1) expression was observed in D1 cells treated with 500 nM As^{+3} at 18 h (Fig. 2.6B). Interestingly, Mdr1a and Mdr1b were up-regulated at 2 h and down-regulated by 18 h (Fig. 2.6C and 2.6D), which was different from the expression of Mrp1 and 2 (Fig. 2.6A and 2.6B). Western Blots confirmed that the protein level of Mrp1 was up-regulated at 18 h (Fig. 2.7A and 2.7B). However, Mdr1 protein levels were not decreased at 18 h, which was different from the mRNA expression (Fig. 2.7C and 2.7D). Mrp2 protein was not detectable in D1 cell lysates. Collectively, these results suggest that the induction of As^{+3} exporters may play a role in regulating As^{+3} induced genotoxicity at high concentrations (500 nM).

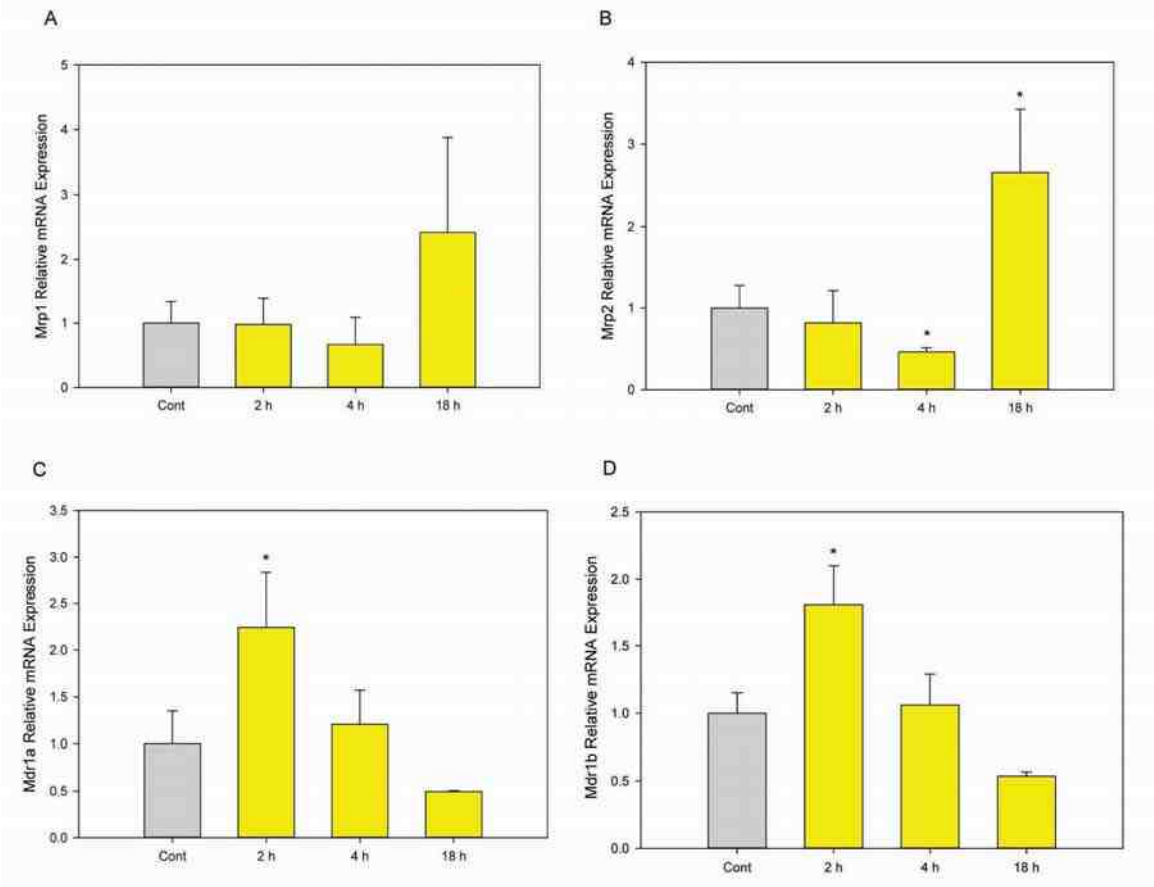

Figure 2.6. mRNA expression of As^{+3} exporters in D1 cells treated with 500 nM As^{+3}. D1 cells were treated 500 nM As^{+3}, expression of Mrp1, Mrp2, Mdr1a and Mdr1b at 2, 4 and 18 h was examined by RT-PCR. A, Mrp1. B, Mrp2. C, Mdr1a. D, Mdr1b. *Significantly different compared to control ($p<0.05$). Results are Means ± SD.

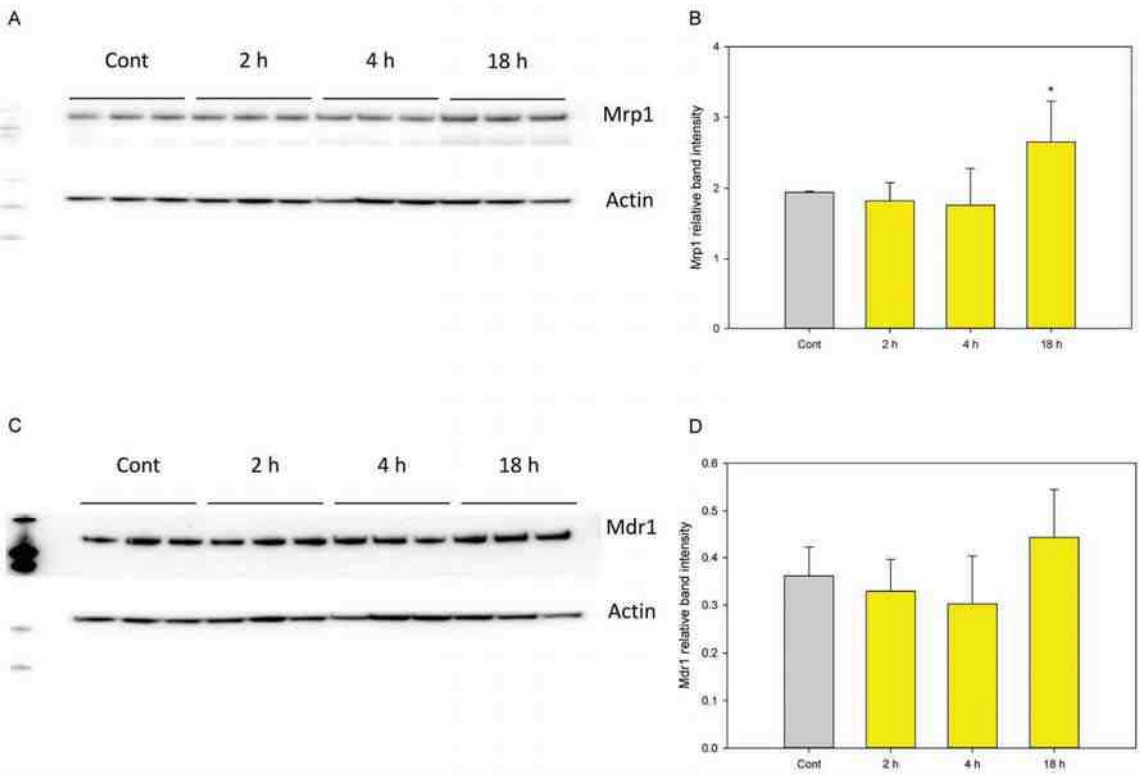

Figure 2.7. Protein levels of Mrp1 and Mdr1 in D1 cells treated with 500 nM As^{+3}. D1 cells were treated 500 nM As^{+3}, expression of Mrp1and Mdr1 at 2, 4 and 18 h was examined by Western Blot. A, Mrp1 Western Blot. B, Mrp1 band intensity normalized to Actin. C, Mdr1 Western Blot. D, Mdr1 band intensity normalized to Actin. *Significantly different compared to control ($p<0.05$). Results are Means ± SD.

1 μM Zn^{+2} reversed the DNA damage and PARP inhibition induced by As^{+3}

Since PARP is a zinc finger protein and Zn^{+2} was found to reverse the PARP inhibition induced by As^{+3} in HaCat cells (Sun et al., 2012), we wanted to know if Zn^{+2} would reverse the DNA damage induced by As^{+3} in mouse pre-T cells. D1 cells were treated with 50 or 500 nM As^{+3}, 1 μM Zn^{+2} and the combinations as Zn^{+2} + As^{+3}. 1 μM Zn^{+2} reversed the DNA damage induced by 50 and 500 nM As^{+3} at both 4 and 18 h (Fig. 2.8A). In addition, PARP inhibition induced by 50 and 500 nM As^{+3} at both 4 and 18 h was also reversed by 1 μM Zn^{+2} (Fig. 2.8B). Therefore, the genotoxic effects induced by As^{+3} in thymus cells can be reversed by Zn^{+2}, suggesting that Zn may be involved in the mechanism of action of As^{+3}.

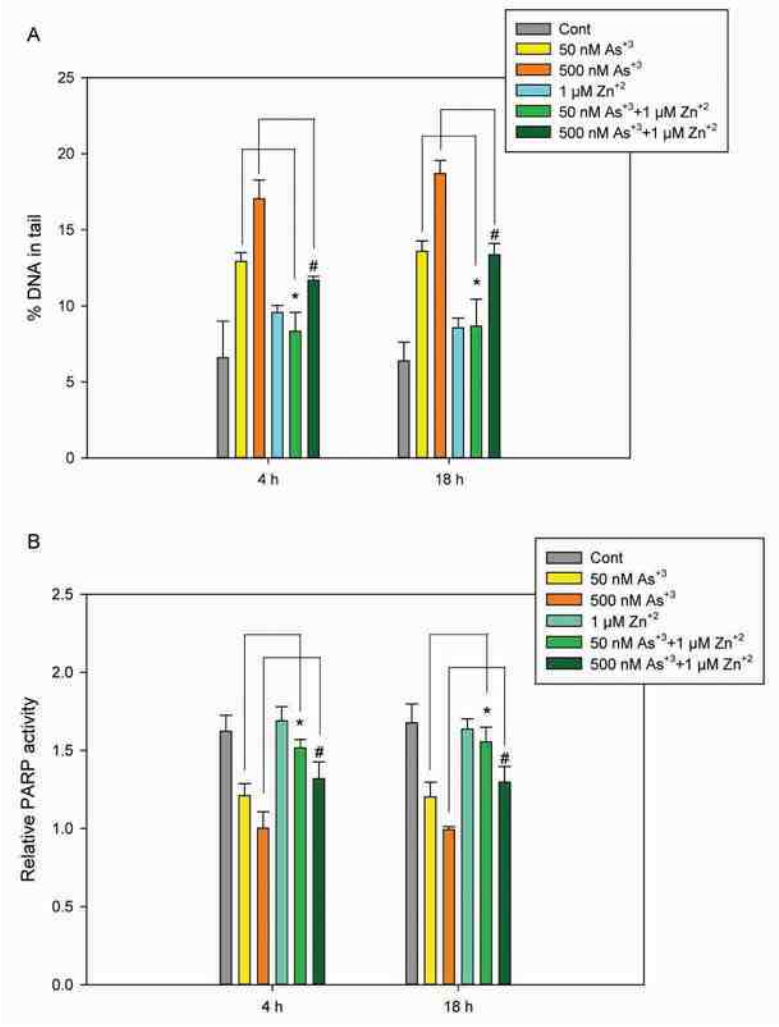

Figure 2.8. Protective effect of Zn^{+2} supplement in As^{+3} induced DNA damage and PARP activity in D1 cells. D1 cells were treated with 50 and 500 nM As^{+3}, 10 µM Zn^{+2}, or the combinations. A, DNA damages were measured by percentage of DNA in tail using alkaline Comet assay. B, PARP activities were measured with Trevigen ELISA kit represented by absorbance at 450 nm. *Significantly different compared to 50nM As^{+3} ($p<0.05$), # Significantly different compared to 500 nM As^{+3} ($p<0.05$). Results are Means ± SD.

DISCUSSION

Suppression of immune function by As has been observed *in vivo* and *in vitro* by several groups (Burchiel, et al., 2014; Ezeh et al, 2014; Gonsebatt et al., 1994; Nadeau et al., 2014; Vahter et al., 2008; Ahmed et al., 2014; Biswas et al., 2008; Soto-Peña et al., 2006), and may potentially contribute to unregulated cancer cell growth. As^{+3} is considered to be a co-carcinogen in keratinocytes, as it does not induce detectable DNA damage at low concentrations without the co-existence of other carcinogens such as UV light (Qin et al., 2012). As^{+3} inhibits DNA repair enzymes such as PARP and XPA (Zhou et al., 2011), which may decrease the ability of cells to repair spontaneous endogenous strand breaks (Swenberg et al., 2011), leading to an increase in DNA damage. Our results showed that As^{+3} alone induced a significant increase in DNA damage in mouse thymus cells (Fig. 2.1A, 2.1C and 2.2A) by inhibiting PARP. Also, thymus cells required less As^{+3} to induce DNA damage than keratinocytes, indicating there is a difference between their sensitivities to As^{+3}. The difference may be due to the exposure relating to passive and active transporters of As^{+3} (Jiang et al., 2006), the ability to metabolize As^{+3}, or differences in other intra/extracellular pathways affected by As^{+3}. It is important to further identify the mechanisms underlying these differences in sensitivity.

PARP is the initiator of BER, which has a critical role in DNA repair. Recent studies have also revealed the relationship between PARP inhibition and immunosuppression. PARP-1 was found to regulate TGF-β receptor expression in immune cells, and inhibition of PARP-1 up-regulated Foxp3, a primary marker for Tregs, and an increase in Th17 cell number (Zhang et al., 2013). In our experiment, there was a

significant decrease in PARP activity and increased DNA damage in both primary thymus cells and the D1 cell line treated with very low concentrations of As^{+3} (50 nM). PARP inhibition induced by As^{+3} may not only affect T cell development in the thymus, but may also cause immunosuppression in peripheral T cells.

PARP is also known to affect other DNA repair pathways, including non-homologous end-joining and homologous recombination (Yelamos et al., 2011). We found that As^{+3} at 500 nM induced DSBs at 4 h, which may be the result of ROS production (Qin et al., 2008). However, these DSBs decreased at 18 h, which correlated with the decrease in oxidative stress markers. Therefore, it is likely that the DBSs were induced by oxidative stress. In addition, since neither oxidative stress nor DSBs were induced by 50 nM As^{+3}, we conclude that As^{+3} induces DNA damage mainly through the inhibition of PARP at these lower concentrations leading to the increase of spontaneous strand breaks in thymus cells, while oxidative stress only occurs in cells treated with a higher dose (500 nM) of As^{+3}.

Because of the transient nature of oxidative stress and DSB induced by 500 nM treatment with As^{+3} in D1 cells, we examined the expression of different As^{+3} efflux proteins, hypothesizing that the induction of arsenic exporters would limit exposure and protect cells. Mrp1 and Mrp2 are well-characterized exporters of As^{+3} and key players in As^{+3} detoxification (Maciaszczyk-Dziubinska et al., 2012). Induction of Mrp1 and Mrp2 mRNA expression only occurred at the 500 nM exposure concentration of As^{+3} and correlated with the rapid protection of D1 cells from oxidative stress and DSBs (Fig 2.4A and 2.4B). While the mRNA expression of Mdr1a and Mdr1b were differentially induced, with Mrp1 increased at 18 hr and Mdr1a increased at 2 hr, but returning to

control levels at 18h (Fig 2.4C and 2.4D). Western Blots also revealed that Mrp1 was up-regulated at 18 h by 500 nM As^{+3}(Fig. 2.5A and 2.5B). One major difference between these exporters is that Mdr1 exporters do not transport glutathione (GSH) conjugates (Maciaszczyk-Dziubinska et al., 2012), while Mrp1 and Mrp2 are GSH-dependent (Leslie et al., 2004; Kala et al., 2000). Therefore, it is possible that the efflux of As^{+3} at 18 h requires the conjugation with GSH. Besides the adaptive regulation of exporters, further studies are needed to reveal if there are changes in the expression of As^{+3} importers. Studies on the relationship between As^{+3} transporter expressions and intracellular As^{+3} level may further clarify the role of these proteins in regulating As^{+3} toxicity by cells.

Zn^{+2} has been demonstrated to counteract PARP inhibition following As^{+3} exposure (Cooper et al., 2013; Kumar et al., 2010). In our experiment, we found that Zn^{+2} reversed the DNA damage and PARP inhibition at 1 μM in D1 cells. However, when we increased Zn^{+2} concentration to 10 μM, Zn^{+2} itself induced DNA damage (data not shown). Therefore, Zn^{+2} exposure can reverse the As^{+3} genotoxic effects at appropriate concentrations, while excess amounts of Zn^{+2} are harmful to cells.

In summary, As^{+3} induces significant genotoxic effects in mouse thymus cells at environmentally-relevant concentrations and within the nanomolar range *in vitro*. At low concentrations (50 nM), inhibition of DNA repair caused by PARP inhibition is mainly responsible for SSB genotoxicity in the absence of oxidative stress. At higher concentrations (500 nM), As^{+3} induces transient oxidative stress and DSBs that are limited by the induction of exporters that reduce concentrations of intracellular arsenic.

The dose-dependent differential genotoxicity of As^{+3} at environmentally-relevant levels can be reversed by Zn^{+2} supplement.

FUNDING

This work was funded by National Institute of Environmental Health Sciences at the National Institutes of Health [grant number R01 ES019968, P30 ES005022].

CHAPTER 3

Environmentally Relevant Concentrations of Arsenite and Monomethylarsonous Acid Inhibit IL-7/STAT5 Cytokine Signaling Pathways in Mouse CD3+CD4-CD8- Double Negative Thymus Cells

Huan Xu[a], Fredine T. Lauer[a], Ke Jian Liu[a], Laurie G. Hudson[a] and Scott W. Burchiel[a, b]

[a]The University of New Mexico College of Pharmacy, Department of Pharmaceutical Sciences, Albuquerque, NM 87131

[b]To whom correspondence should be addressed. Fax: (505) 272-6749. Email: sburchiel@salud.unm.edu

Toxicology Letters, 247: 62-68. DOI: 10.1016/j.toxlet.2016.02.014.

Received 6 November, 2015; Revised 4 February, 2016; Accepted 22 February, 2016; Available online 24 February, 2016.

ABSTRACT

Environmental arsenic exposure is a public health issue. Immunotoxicity induced by arsenic has been reported in humans and animal models. The purpose of this study was to evaluate mechanisms of As^{+3} and MMA^{+3} toxicity in mouse thymus cells. Because we know that MMA^{+3} inhibits IL-7 signaling in mouse bone marrow pre-B cells, we studied the influence of As^{+3} and MMA^{+3} on T cell development in the thymus at the earliest stage of T cell development (CD4-CD8-, double negative, DN) which requires IL-7 dependent signaling. We found in a DN thymus cell line (D1) that a low concentration of MMA^{+3} (50 nM) suppressed IL-7 dependent JAK1,3 and STAT5 signaling. As^{+3} suppressed STAT5 and Jak3 activations at higher concentration (500 nM). Cell surface expression of the IL-7 receptor (CD127) was also suppressed by 50 nM $MMA^{+}3$, but was increased by 500 nM As^{+3}, indicating possible differences in the mechanisms of action of these agents. A decrease in cyclin D1 protein expression was observed in D1 cells exposed to As^{+3} at 500 nM and MMA^{+3} starting at 50 nM, suggesting that arsenic at these environmentally-relevant doses suppresses early T cell development through the inhibition of IL-7 signaling pathway.

HIGHLIGHTS

- As^{+3} and MMA^{+3} suppress IL-7 signaling as measured by pSTAT5 in DN thymocytes.
- JAK1 was inhibited by MMA^{+3}, while JAK3 was inhibited by MMA^{+3} and As^{+3}.
- MMA^{+3} decreased but As^{+3} increased cell surface expression of the IL-7 receptors.
- MMA^{+3} and As^{+3} exposures selectively decreased the DN cell population *in vitro*.
- In DN cells, MMA^{+3} (50 nM) and As^{+3} (500 nM) inhibited cyclin D1 expression.

INTRODUCTION

Arsenic exposure in food and drinking water is a worldwide public health issue. Arsenic is known to cause suppression of the immune system in multiple systems (Ahmed et al., 2014; Biswas et al., 2008; Nadeau et al., 2014; Soto-Peña et al., 2006; Vahter et al., 2008). However, the mechanism of arsenic induced immunosuppression is still poorly understood. Previous studies in our laboratory found that environmentally-relevant doses of arsenite (As^{+3}) and its metabolite, monomethylarsonous acid (MMA^{+3}) suppressed T cell function and early B cell proliferation at extremely low concentrations (Burchiel et al., 2014; Ezeh et al., 2014), indicating that immune cells are very sensitive to As^{+3} and MMA^{+3} exposure.

Early T cells are originally produced in bone marrow and transported into the thymus for development and selection. T cells in thymus go through double negative (CD4-CD8-, DN), double positive (CD4+CD8+, DP) and single positive (CD4+/CD8+, SP) stages, committing to either CD4+ T helper cells or CD8+ cytotoxic T cells (Germain, 2002). The conversion of early pre-T DN cells to DP cells is controlled by IL-7 signaling (Boudil et al., 2015). Suppression of DN T cells has been documented to have detrimental effects on immune functions (Ohm et al., 2003; Seinen and Penninks, 1979). IL-7 is secreted by stromal cells in bone marrow and thymus and is a critical cytokine for the proliferation of T cells during DN stage (Namen et al., 1988). The IL-7 receptor (IL-7R) is a heterodimer consisting both an α chain and a common γ chain (γc). The binding of IL-7 to IL-7R leads to a cascade of signals of Janus Kinases (JAKs) and Signal Transducers and Activators of Transcription (STATs), inducing the transcription of

multiple genes such as Pim1 and Cyclin D1 (de Groot et al., 2000; Linowes et al., 2013). STAT5 is phosphorylated by phospho-JAK1 (pJAK1) and phospho-STAT5 (pSTAT5) is stabilized by phospho-JAK3 (pJAK3) (Haan et al., 2011). Once pSTAT5 is dimerized and translocated into the nucleus, it binds to STAT5 response elements on genes that control proliferation and differentiation (Nosaka et al., 1999).

Arsenic-induced alterations in cell signaling, including the inhibition of tyrosine kinase activation or ROS production, can have potent non-genotoxic effects on cells (Qian et al., 2003). The inhibitions on STATs and JAKs in γc receptor signaling by arsenic were observed by different groups (Cheng et al., 2004; Hayashi et al., 2002). However, all these existing studies were conducted with high doses of arsenic. Since there is evidence showing that low concentrations of As^{+3} and MMA^{+3} inhibit the proliferation of IL-7 dependent lymphoid progenitors (Ezeh et al., 2014), the present study was focused on the effects of environmentally-relevant non-cytotoxic doses of As^{+3} and MMA^{+3} within nanomolar ranges on IL-7 signaling pathway of DN mouse thymus cells, the early developing T cell population which affects the whole immune system.

MATERIAL AND METHODS

Chemicals and reagents

Sodium arsenite (CAS 774-46-5, $NaAsO_2$) was purchased from Sigma-Aldrich (St. Louis, MO). MMA^{+3} was a gift from Dr. Terry Monks at Southwest Environmental Health Science Center of the University of Arizona. Hanks Balanced Salt Solution (HBSS) was purchased from Lonza (Walkersville, MD). Penicillin/Streptomycin 10,000 (mg/ml)/10,000 (U/ml) (Pen/Strep) and 200 mM L-Glutamine were purchased from Life Technologies (Grand Island, NY). β-Mecaptoethanol (2-ME), Dulbecco's phosphate buffered saline w/o Ca^{+2} or Mg^{+2} ($DPBS^-$), and base medium RPMI 1640 were purchased from Sigma Aldrich. Mouse IL-7 was purchased from Peprotech (Rocky Hill, NJ). Fetal Bovine Serum (FBS) was purchased from Atlanta Biologicals (Flowery Branch, GA.), Alexa Fluor® 488 Rat Anti-Mouse CD127 (Cat. No. 561533), Alexa Fluor® 488 Rat IgG2b, κ Isotype Control (Cat. No. 557726), FITC Rat Anti-Mouse CD8a (Cat. No. 553031), APC Rat Anti-Mouse CD4 (Cat. No. 553051), PE-Cy™7 Hamster Anti-Mouse CD3e (Cat. No. 552774), purified mouse anti-JAK1 monoclonal antibody (Cat. No. 610231) and purified mouse anti-STAT5 (Cat. No. 610191) were purchased from BD Biosciences (San Jose, CA). PE Anti-Hu/Mo pSTAT5 (Y694) (Cat. No. 12-9010-42), PE Mouse IgG1 κ Isotype Control (Cat. No. 12-4714-42) and IC fixation buffer (Cat. No. 00-8222-49) were purchased from eBioscience (San Diego, CA). Cyclin D1 (DCS-6) PE (Cat. No. sc-20044 PE) was purchased from Santa Cruz Biotechnology (Santa Cruz, CA). Anti-phospho-STAT5 (Tyr694) (Cat. No. 9359), anti-phospho-JAK1 (Tyr1022/1023) (Cat. No.3331), anti-phospho-JAK3 (Tyr980/981) (Cat No. 5031), anti-JAK3 (Cat. No.

3775), anti-rabbit IgG –HRP secondary antibody (Cat. No. 7074) and anti-mouse IgG-HRP secondary antibody (Cat. No. 7076) were purchased from Cell Signaling Technology (Danvers, MA).

Thymus cells *in vitro* treatments and intracellular flow cytometry assays

Thymus were harvested from three C57BL/6J male mice purchased at 8 weeks of age from Jackson Laboratory (Bar Harbor, ME), cells were isolated and pooled. Mice were handled in accordance with protocols approved by the Institutional Animal Use and Care Committee at the University of New Mexico Health Sciences Center in our AAALAC-approved animal facility. One million cells were treated with different doses of As^{+3} or MMA^{+3} in the medium consisting of RPMI-1640, 10% FBS, 1% Pen/Strep, and 2mM L-Glutamine at 37 ºC for 18 h. For pSTAT5 intracellular staining, cells were washed and resuspended in 100 µl of $DPBS^{-}$ and incubated with 5 ul cocktail consisting of 0.5 µg of CD8, CD4 and CD3 antibodies or DPBS- (unstained) for 30 min at RT in dark and fixed by adding 100 µl of IC fixation buffer and incubated for 30 min at RT in dark. Following incubation, cells were washed twice with DPBS- and then incubated in 100 µl of 90% -20 ºC methanol for 30 min 4 ºC in dark. Washed cells were resuspended in 100 µl of $DPBS^{-}$ and stained with 5 µl of intracellular staining antibody (pSTAT5, cyclin D1) or isotype control and incubated for 30 min at RT in dark. Cells were washed twice with $DPBS^{-}$ before being analyzed on an AccuriC6 Flow Analyzer (BD Biosciences).

D1 cells pSTAT5 and pJAKs Western Blot assays

The D1 cell line was a gift from Dr. Scott K. Durum (Center for Cancer Research, National Institute of Health, Frederick, MD). It is a CD3+CD4-CD8-, IL-7 dependent

pre-T cell line established from p53−/− mouse thymocytes (Kim et al., 2003). Cells were maintained in RPMI 1640 with 2 mM L-glutamine, 1% Pen/Strep, 55 μM 2-ME and 50 ng/mL IL-7. Cells were arrested in G1 phase by 18 h of IL-7 deprivation and treated with As^{+3} or MMA^{+3} at the same time. 50 ng/mL of IL-7 was added to induce IL-7 signaling for 30 min before harvesting. Cell lysates (20 μg protein/well) were separated by SDS-PAGE electrophoresis and transferred onto nitrocellulose membranes for 15 min using semi-dry transferring system (Bio-Rad, Hercules, CA). Membranes were blocked with 5% Blotting Grade Blocker (Bio-Rad) in TBST (50 mM Tris, 150 mM NaCl and 0.05% Tween 20), and incubated with antibodies for pSTAT5, pJAK1 or pJAK3, followed by HRP conjugated antibodies. The membranes were stripped with pH 2.2 glycine stripping buffer (15 g glycine, 1 g SDS and 10 ml Tween 20 in a total of 1 L) and probed for total STAT5, JAK1 and JAK3. Signals were detected using SuperSignal West Femto Chemiluminescent Substrate (Thermo Scientific, Rockford, IL) and FluorChem™ M System (ProteinSimple, San Jose, CA).

D1 cells CD127 staining

After treatments with As^{+3} or MMA^{+3}, D1 cells were washed, resuspended in 100 μl DPBS- and stained with 0.5 μg of anti-CD127 or IgG2b κ Isotype Control for 30 min at RT in the dark. Cells were washed twice with $DPBS^{-}$ before analyzed on an AccuriC6 Flow Analyzer

Statistics and Data Analysis

All data were analyzed with Excel 2010 or SigmaPlot version 12.5, one way analyses of variance (ANOVA) and Dunnetts t-test were used to determine the differences between control and treatment groups. For flow cytometry experiments, each

single dose was done in triplicate. For Western Blot experiments, three independent experiments were performed for each assay. Image J (1.48v) software (NIH, downloaded from website: http://rsb.info.nih.gov/ij/) was used to obtain band intensities for treatments and control samples.

RESULTS

As^{+3} and MMA^{+3} suppressed STAT5 phosphorylation in mouse DN T cells *in vitro*

Mouse thymus cells were isolated and exposed to 5, 50 and 500 nM As^{+3} and MMA^{+3} *in vitro* for 18 h. The DN T cell population was defined as negative for both CD4 and CD8 markers in CD3+ thymocytes (Fig. 3.1A) using flow cytometry. STAT5 phosphorylation was measured by intracellular staining and found to be inhibited by As^{+3} at 500 nM and MMA^{+3} from 50 nM (Fig. 3.2B), indicating a suppression of the IL-7 signaling pathway at these doses *in vitro*.

A DN, IL-7 dependent mouse thymic cell line, D1, was utilized to confirm our observations in the primary mouse DN T cells. STAT5 activation is IL-7 responsive in D1 cells, and neither As^{+3} or MMA^{+3} induced STAT5 phosphorylation without IL-7 (Fig. 3.1C and 3.1D). A significant decrease in STAT5 phosphorylation was seen in 500 nM As^{+3} and 50 nM MMA^{+3} treatments (Fig. 3.1C and 3.1D), confirming the observations in primary mouse DN T cells.

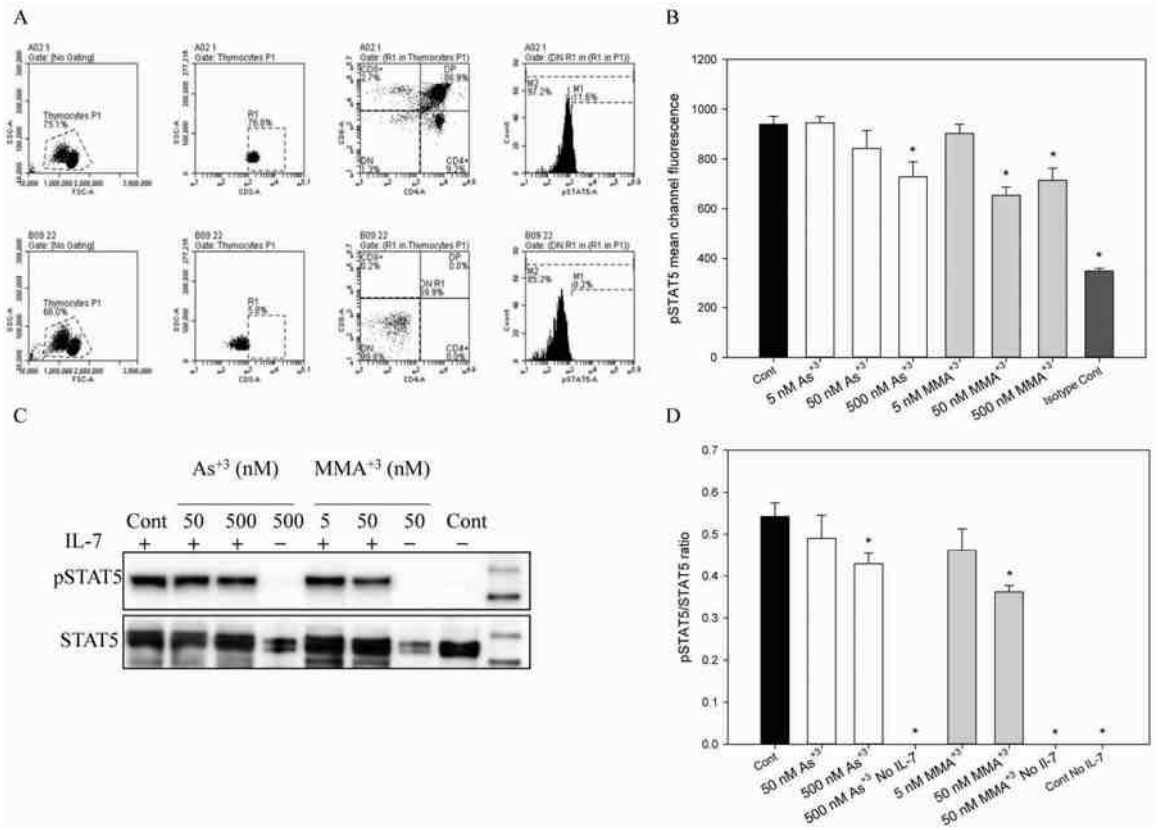

Figure. 3.1. Suppression of STAT5 phosphorylation in DN primary thymus T cells exposed to As^{+3} and MMA^{+3} *in vitro*. Primary mouse thymus cells were treated with 5, 50 and 500 nM As^{+3} and MMA^{+3}. A, DN T cell population defined by CD3, CD4 and CD8 cell surface markers and isotype control for pSTAT5 intracellular staining. B, intracellular pSTAT5 levels were measured by multiparameter flow cytometry. In panels 1C and 1D, D1 cells were starved 18 h for IL-7 with As^{+3} and MMA^{+3} treatments. pSTAT5 levels were measured 30 min after re-adding IL-7, three independent experiments were performed. C, one representative pSTAT5 and STAT5 blot. D, pSTAT5 to STAT5 band intensities from three independent experiments. *Significantly different compared to control ($p<0.05$). Results are Means ± SD.

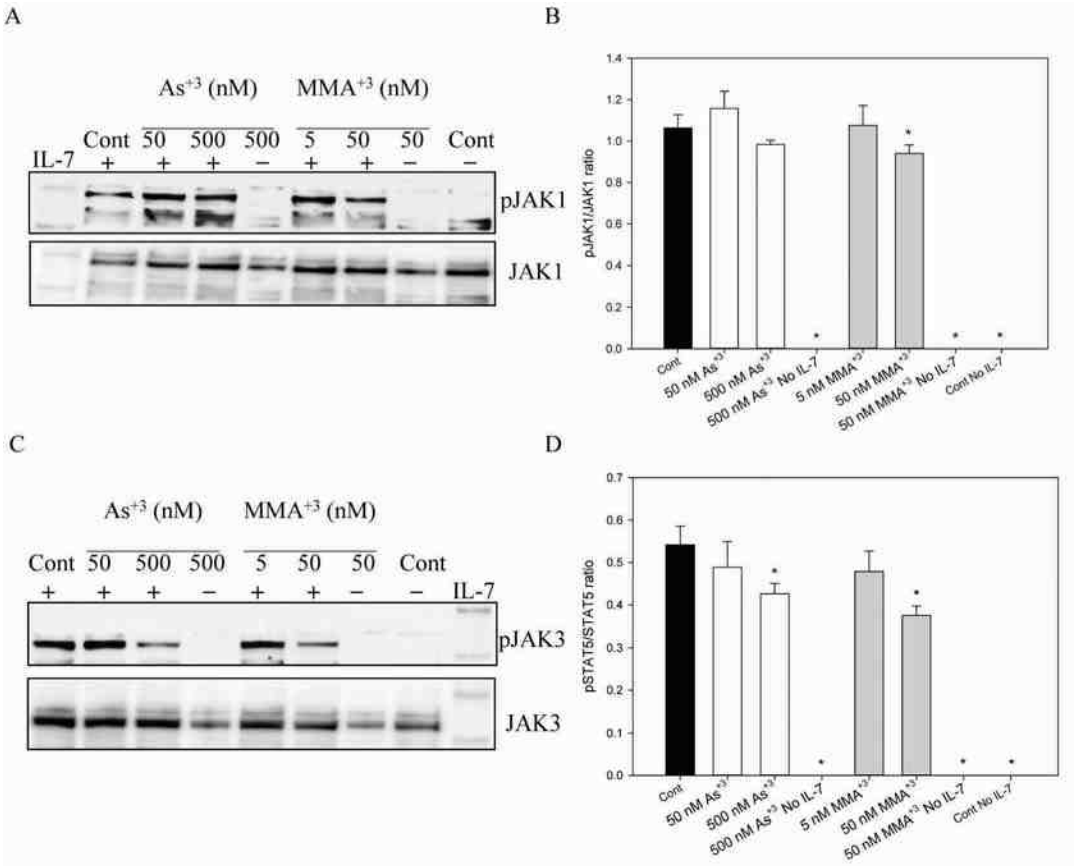

Figure. 3.2. Suppression of JAK1 and JAK3 phosphorylation in a mouse DN cell line (D1) exposed to As^{+3} and MMA^{+3} *in vitro*. D1 cells were starved 18 h for IL-7 with As^{+3} and MMA^{+3} treatments. pJAK1 and JAK3 levels were measured 30 min after re-adding IL-7, three independent experiments were performed. A, one representative pJAK1 and JAK1 blot is shown. B, pJAK1 to JAK1 band intensities from three independent experiments are shown. C, one representative pJAK3 and JAK3 blot is shown. D, pJAK3 to JAK3 band intensities from three independent experiments are shown. *Significantly different compared to control ($p<0.05$). Results are Means ± SD.

As^{+3} and MMA^{+3} suppressed JAK1 and JAK3 phosphorylation in D1 cells *in vitro*

Since the suppression of STAT5 phosphorylation was observed in DN T cells, phosphorylation of JAK1 and JAK3, upstream tyrosine kinases which phosphorylate STAT5 in the IL-7 signaling pathway, was examined by Western Blot after IL-7 stimulation in D1 cells. As we can see in Fig. 3.2, the absence of IL-7 also depleted JAK1 and JAK3 phosphorylation. 50 nM MMA^{+3} exposure suppressed JAK1 phosphorylation (Fig. 3.2A and 3.2B) and 500 nM As^{+3} or 50 nM MMA^{+3} exposures inhibited JAK3 phosphorylation (Fig. 3.2C and 3.2D) in IL-7 stimulated D1 cells. These results indicate that suppression of STAT5 phosphorylation by As^{+3} and MMA^{+3} exposures may be due to JAK1 and JAK3 inhibition.

MMA^{+3} suppressed IL-7R (CD127) expression on cell surface

In order to see if IL-7R expression is affected by As^{+3} and MMA^{+3} treatments, D1 cells exposed to 50 and 500 nM As^{+3} or 5 and 50 nM MMA^{+3} for 18 h *in vitro* were stained with CD127 antibody. A decrease in cell surface expression of IL-7R was observed in D1 cells exposed to 50 nM MMA^{+3} (Fig. 3.3). Interestingly, 500 nM As^{+3} increased the expression of IL-7R, indicating that As^{+3} and MMA^{+3} may have differential mechanisms in IL-7 signaling suppression.

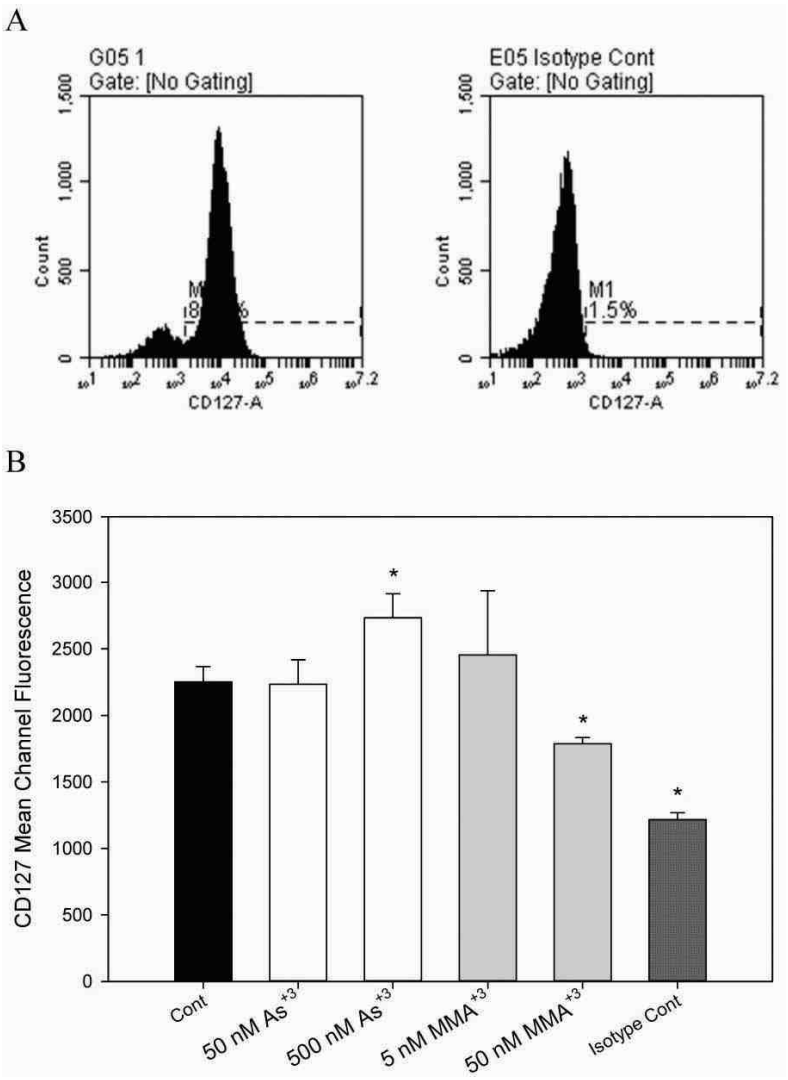

Figure. 3.3. IL-7R (CD127) cell surface expression in D1 cells exposed to As^{+3} and MMA^{+3} *in vitro*. D1 cells were exposed to As^{+3} and MMA^{+3} for 18 h and stained with anti-CD127 antibody. A, isotype and staining control. B, surface IL-7R expression measured by CD127 mean channel fluorescence.*Significantly different compared to control ($p<0.05$). Results are Means ± SD.

As^{+3} and MMA^{+3} selectively targeted DN T cells and decreased cell cycle protein expression

Since the suppression of IL-7 signaling pathways in mouse DN T cells by As^{+3} and MMA^{+3} was confirmed, we wanted to determine whether the DN subset is selectively affected and evaluate a potential mechanism. We performed intracellular staining for cyclin D1, an indicator of cell cycle progression which is transcriptionally regulated by STAT5 activation (Matsumura et al., 1999). These studies were performed in primary mouse DN thymus cells exposed to As^{+3} and MMA^{+3} for 18 h *in vitro*. For MMA^{+3} exposures, we also applied doses between 50 nM and 500 nM to get more information on dose response within the nanomolar range. MMA^{+3} significantly decreased the number of DN cells, but had no effect on the DP cell populations (Fig 4A, 4B). We have previously shown that these concentrations did not affect cell viability, therefore the fact that fewer cells were being recovered suggested that MMA and As^{+3} might affect the entry of cells into this compartment by blocking IL-7 dependent proliferation and differentiation. We therefore examined cyclin D1 expression in the DN cells treated with MMA^{+3} (50-200 nM) and As^{+3} (500 nM). A statistically significant inhibition of cyclin D1 was seen at 100 nM MMA^{+3} and 500 nM As^{+3} indicating that these STAT5-depdent proteins was affected by these treatments (Fig. 4C, D).

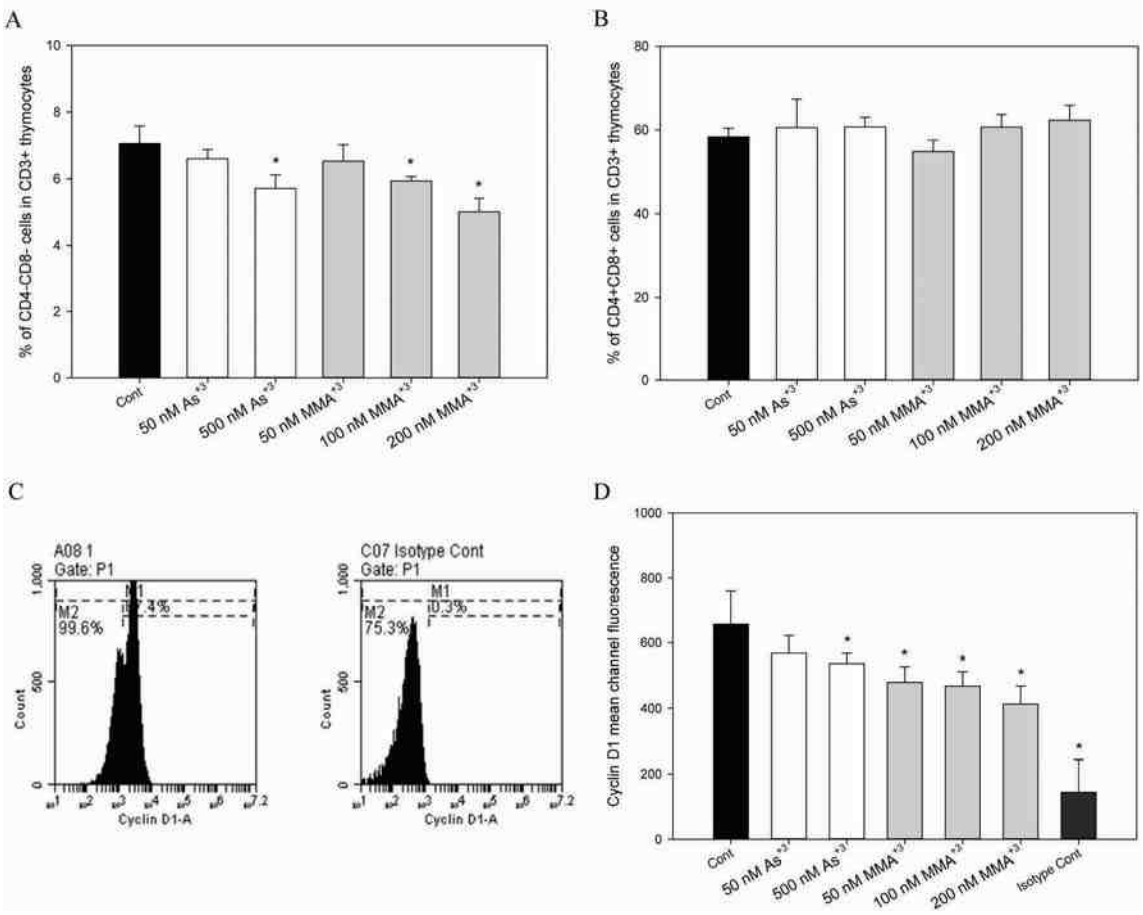

Figure. 3.4. As^{+3} and MMA^{+3} selectively affected DN cells and suppressed cyclin D1 expression. A, Decrease in the percentage of CD3+ DN (CD4-, CD8-) cells recovered from primary thymus cells treated for 18 h with MMA^{+3} or As^{+3}. B, lack of effect of MMA^{+3} and As^{+3} on the CD3+ DP (CD4+,CD8+) population of thymus cells. C, cyclin D1 fluorescence detected by flow cytometry is shown for a specific antibody (left) and an isotype control (right) for primary mouse thymus cells. D, cyclin D1 expression measured by multiparameter flow cytometry in CD3+ DN primary mouse thymocytes treated with 50 and 500 nM As^{+3} or 50, 100 and 200 nM MMA^{+3} for 18 h *in vitro*. *Significantly different compared to control ($p<0.05$). Results are Means ± SD.

DISCUSSION

Environmental exposures to arsenic via drinking water and food are known to be associated with vascular diseases, lung diseases, and different types of cancers (Argos et al., 2010; Chen, et al., 2011; Navas-Acien et al., 2005). Immunological suppression caused by arsenic has been related to the occurrence of several diseases and has been addressed by many research groups (Dangleben et al., 2013). However, most of the studies on arsenic immunotoxicity used high concentrations within low to high micromolar. Since the accessible doses of arsenic in the environment are usually low (Josyula et al., 2006), studying the immunotoxic effects of nanomolar doses of arsenic are important for environmentally-relevant exposures. Previously, we demonstrated that As^{+3} had differential genotoxic effects in mouse DN thymus cells at low concentrations that did not induce apoptosis (Xu et al., 2015). Therefore, the present study shows that As^{+3} and MMA^{+3} inhibits a critical signaling pathway in the same cell population via nongenotoxic mechanism resulting in inhibition of pre-T cell differentiation.

IL-7 signaling is critical for early T cell development in thymus. It has been showed that high concentrations of As^{+3} significantly inhibited γc receptor signaling such as IL-2 and IL-6 (Cheng et al., 2004). Previously, we showed that MMA^{+3} had a strong inhibitory effect on IL-7 signaling in pre-B cells within nanomolar range (Ezeh et al, 2015). The observation of a similar pattern of suppression by low concentrations of As^{+3} and MMA^{+3} in bone marrow Pre-B and thymic DN T cells suggests a common mechanism of arsenic induced immunosuppression in lymphoid progenitor cells. Because IL-7R (CD127) expression was decreased by MMA^{+3} in both systems, it is possible that

receptor modulation, in addition to actions on downstream targets is responsible for inhibition of STA5 signaling. Because 500 nM As^{+3} increased the receptor expression in D1 cells, and did not affect CD127 expression in a pre-B cell model (Ezeh et al., 2015), it is likely that As^{+3} suppression of IL-7 signaling occurs downstream of the receptor by actions on JAK or STAT by modulating protein phosphorylation (Xue et al., 2011; Paul et al., 2007). Therefore, the possibility that inorganic and organic forms of arsenic act by different mechanisms in γc receptor signaling should be further explored.

As^{+3} is the prevalent form in nature. After the intake if As^{+3}, MMA^{+3} is formed *in vivo* through the action of arsenite-3-methyltransferase, which is highly expressed in the liver (Aposhian et al., 2000). Previous studies have indicated that MMA^{+3} is more toxic than As^{+3} (Orihuela et al., 2013; Petrick et al., 2000). In this study, MMA^{+3} was found to be 10 times more effective in suppressing STAT5 and JAK1, 3 phosphorylations (Fig. 3.1 and 3.2). Trivalent arsenicals are known to induce toxicity by binding to thiol-containing molecules (Styblo et al., 1995). The differences between As^{+3} and MMA^{+3} in protein binding is that As^{+3} requires a structure with 3 cysteines, while MMA^{+3} needs only 2, which significantly increases the numbers of its binding targets (Shen et al, 2013). Therefore, it is possible that MMA^{+3} reacts directly on the IL-7R, resulting a suppression of the downstream factor activations. As^{+3} is documented to inhibit zinc finger proteins such as PARP (Zhou et al., 2011).

Since DN thymus cells are sensitive to As^{+3} and MMA^{+3} at low doses, the immunosuppression induced by arsenic exposure may occur at very early stages of T cell differentiation in the thymus. There are reports showing that prenatal arsenic exposures are related to the altered lymphoid cell development and thymic atrophy (Ahmed et al.,

2012; Raqib et al., 2009). It is very possible that these early life developmental suppressions are associated with the high sensitivity of the DN T cell population. Therefore, studies addressing the differences between the DN population and other populations such as the DP T cells or mature T cells are also important for understanding the mechanisms of arsenic induced immunosuppression in environmental exposures.

Collectively, As^{+3} and MMA^{+3} inhibit IL-7 signaling in mouse DN thymus cells at environmentally relevant concentrations. The two forms of arsenic have differential effective doses and may act through distinct mechanisms. The suppression of the IL-7 signaling result in the decrease of cyclin D1, a STAT5 transcriptionally-regulated cell cycle protein, suggesting a mechanistic explanation of the reduction of the DN T cell population, which exhibits high sensitivity to arsenic exposures.

ACKNOWLEDGEMENTS

This work was funded by a grant from the National Institute of Environmental Health Sciences (R01-ES019968). Monomethylarsonous acid (MMA^{+3}) was obtained from Drs. Terry Monks and Todd Caminesch at the Southwest Environmental Health Sciences Center (P30-ES006694, Synthetic Core, which was funded by the University of Arizona Superfund Program (P50-ES04940).

CHAPTER 4

Differential Sensitivities of Bone Marrow, Spleen and Thymus to Genotoxicity Induced By Environmentally Relevant Concentrations of Arsenite

Huan Xu[a], Shea McClain[a], Sebastian Medina[a], Fredine T. Lauer[a], Christelle Douillet[b], Ke Jian Liu[a], Laurie G. Hudson[a], Miroslav Stýblo[b], and Scott W. Burchiel[a c]

[a]The University of New Mexico College of Pharmacy, Department of Pharmaceutical Sciences, Albuquerque, NM 87131

[b]Department of Nutrition, Gillings School of Global Public Health, University of North Carolina at Chapel Hill, Chapel Hill, NC 27516

[c]To whom correspondence should be addressed. Fax: (505) 272-6749. Email: sburchiel@salud.unm.edu

Toxicology Letters, 262: 55-61. DOI: 10.1016/j.toxlet.2016.09.008.

Received 11 July, 2016; Revised 8 September, 2016; Accepted 17 September, 2016; Available online 19 September, 2016.

ABSTRACT

It is known in humans and mouse models, that drinking water exposures to arsenite (As^{+3}) leads to immunotoxicity. Previously, our group showed that certain types of immune cells are extremely sensitive to arsenic induced genotoxicity. In order to see if cells from different immune organs have differential sensitivities to As^{+3}, and if the sensitivities correlate with the intracellular concentrations of arsenic species, male C57BL/6J mice were dosed with 0, 100 and 500 ppb As^{+3} via drinking water for 30 d. Oxidation State Specific Hydride Generation- Cryotrapping- Inductively Coupled Plasma- Mass Spectrometry (HG- CT- ICP- MS) was applied to analyze the intracellular arsenic species and concentrations in bone marrow, spleen and thymus cells isolated from the exposed mice. A dose-dependent increase in intracellular monomethylarsonous acid (MMA^{+3}) was observed in both bone marrow and thymus cells, but not spleen cells. The total arsenic and MMA^{+3} levels were correlated with an increase in DNA damage in bone marrow and thymus cells. An *in vitro* treatment of 5, 50 and 500 nM As^{+3} and MMA^{+3} revealed that bone marrow cells are most sensitive to As^{+3} treatment, and MMA^{+3} is more genotoxic than As^{+3}. These results suggest that the differential sensitivities of the three immune organs to As^{+3} exposure are due to the different intracellular arsenic species and concentrations, and that MMA^{+3} may play a critical role in immunotoxicity.

HIGHLIGHTS

- MMA^{+3} is the main species presented in bone marrow and thymus in As^{+3} exposed mice.
- Bone marrow is the most sensitive lymphoid tissue to arsenic-induced genotoxicity.
- Increase in DNA damage is correlated with more intracellular MMA^{+3} in bone marrow and thymus.
- An *in vivo* exposure to 100 ppb As^{+3} induced genotoxicity in bone marrow and thymus.
- MMA^{+3} is more genotoxic than As^{+3} *in vitro*.

INTRODUCTION

Arsenic (As) contamination in food and drinking water is a world-wide public health issue. The trivalent inorganic form of As, arsenite (As^{+3}), is the most prevalent form in the environment. Exposure to As is associated with multiple diseases such as skin lesions, diabetes, cardiovascular diseases, and cancers (Argos et al., 2010; Schuhmacher-Wolz et al., 2009; Vahter et al., 2008). Once As^{+3} gets into the body, it is metabolized into monomethyl and dimethyl trivalent and pentavalent species (Aposhian and Aposhian, 2006). Monomethylarsonous acid (MMA^{+3}) has been shown to be more toxic than As^{+3} both *in vivo* and *in vitro* (Petrick et al., 2001; Styblo et al., 2000). MMA^{+3} can be further metabolized to dimethylarsonous acid (DMA^{+3}) or dimethylarsinic acid (DMA^{+5}) and excluded from the body.

Arsenic induced immunotoxicity has been studied by many groups both *in vitro* and *in vivo* (Ahmed et al., 2014; Nadeau et al., 2014; Biswas et al., 2008; Vahter et al., 2008; Soto-Peña et al., 2006; Gonsebatt et al., 1994). However, only a few studies have addressed the toxicity of As exposure to immune cells at environmentally relevant concentrations. Previous studies in our laboratory showed that *in vivo* drinking water exposure to As^{+3} at very low concentrations suppresses mouse bone marrow and spleen cell functions (Ezeh et al., 2014; Li et al., 2010). Human peripheral blood mononuclear cells (HPBMC) studies also showed a dose-dependent suppression of T cell proliferation at extremely low concentrations of As^{+3} (0.1-10 nM) in some individuals, with virtually all individuals susceptible to T cell immunosuppression by MMA^{+3} (Burchiel et al., 2014). Therefore, lymphocytes are extremely sensitive to As^{+3} exposure at

environmentally relevant levels. However, it is unclear whether immunotoxicity is likely due to As^{+3} or MMA^{+3}.

T cells are generated in bone marrow and transferred to the thymus for development, while B cells develop in bone marrow. The spleen is a critical immune organ for the storage of both T and B cells and for systemic immune responses. In a previous study on the genotoxicity induced by As^{+3} in mouse thymus cells, we showed that mouse thymus cells are extremely sensitive to As^{+3} induced DNA damage, which is correlated with the inhibition of a base excision repair factor, Poly (ADP-ribose) polymerase (PARP) (Xu et al., 2016b). In the present study, the sensitivities of the three immune organs, bone marrow, spleen and thymus to As induced genotoxicity were compared both *in vivo* and *in vitro*. The species and levels of intracellular arsenic contents in the cells from the three immune organs were also determined and compared.

METHODS

Chemicals and Reagents

Sodium arsenite (CAS 774-46-5, $NaAsO_2$, Purity ≥ 90%) was purchased from Sigma-Aldrich (St. Louis, MO). Methylarsine iodide (MMA^{+3}) was obtained from Drs. Terry Monks and Todd Caminesch at the Southwest Environmental Health Sciences Center, University of Arizona. Penicillin/Streptomycin (Pen/Strep) and L-Glutamine were purchased from Life Technologies (Grand Island, NY). Dulbecco's phosphate buffered saline w/o Ca^{+2} or Mg^{+2} ($DPBS^-$) was purchased from Mediatech (Manassas, VA). Dimethyl sulphoxide (DMSO), RPMI 1640 and Iscove's Modified Dulbecco's Medium (IMDM) base medium were purchased from Sigma Aldrich. Fetal Bovine Serum (FBS) was purchased from Atlanta Biologicals (Flowery Branch, GA). Hanks Balanced Salt Solution (HBSS) was purchased from Lonza (Walkersville, MD). Sodium Hydroxide (NaOH) was purchased from EMD Chemicals Inc. (Gibbstown, NJ). 0.5 M EDTA solution was purchased from Promega (Madison, WI). The Comet Assay kit (Cat. No. 4252-040-ESK), hOGG1 FLARE™ Assay kit (Cat. No. 4130-100-FK) and the PARP activity kit (Cat. No. 4685-096-K) were purchased from Trevigen (Gaithersburg, MD). The BCA assay kit (Cat. No. 23225) was purchased from Thermo Scientific (Rockford, IL).

Mouse In Vivo Exposures

C57BL/6J male mice were purchased at 8 weeks of age from Jackson Laboratory (Bar Harbor, ME). All animal experiments were performed following the protocols approved by the Institutional Animal Use and Care Committee at the University of New

Mexico Health Sciences Center. Following one week of acclimation, mice (2–3 per cage) were exposed to As^{+3} at different concentrations via drinking water for 30 d. As^{+3} doses were prepared fresh weekly by weighing each water bag and determining the appropriate amount of stock As^{+3} solution to add to each bag to yield 100 and 500 ppb. No treatment was added to control bags. Water bags were weighed after each week and the change in weight was used to estimate the amount of water consumed by each group. The As^{+3} concentrations in drinking water were verified using Mass Spectrometry by Dr. Abdul-Mehdi S. Ali at Department of Earth and Planetary Sciences, University of New Mexico. Mice were fed 2020X Teklad global soy protein-free extruded rodent diet (Envigo, Indianapolis, IN) throughout the experiment.

Isolation of Bone Marrow Cells

Bone marrow cells were isolated according to the procedures described in Ezeh et al., 2014. Basically, mouse femurs were collected into HBSS medium in our animal facility and transferred to our laboratory to extract cells. Femurs were placed in petri dish containing 5 ml of cold sterile bone marrow medium (500 ml IMDM with 2% FBS, 2 mM L-glutamine, and 100 mg/ml Pen/Strep) and trimmed to expose interior marrow shaft of the femur, the end of the femur were then cut off. one cc syringe and 25 gauge needle were used to flush the bone marrow medium through the femur several times to release cells into the petri dish. The suspension was immediately transferred to a 15 ml centrifuge tube, centrifuged at 200 x*g* for 10 min, aspirated, and washed with bone marrow medium. The cell count and viability were determined by acridine orange/propidium iodide (AO/PI) staining on a Nexcelom Cellometer 2000.

Isolation of Thymus and Spleen Cells

Thymus and spleen were isolated following the sterile procedures described in Xu, et al., 2016. Basically, mouse thymus and spleen were harvested in our animal facility and transferred to the laboratory in HBSS on ice. Single cell suspensions of spleen and thymus cells were prepared by homogenizing the organ between the frosted ends of two sterilzed microscope slides (Fisher Scientific, Pittsburgh, PA) into a dish containing 5 mL of cold mouse medium (500 ml RPMI 1640 with 10% FBS, 2 mM L-glutamine, and 100 mg/ml Pen/Strep). Suspended cells were centrifuged at 200 x*g* for 10 min, aspirated, and washed with mouse medium. The cell count and viability were determined by AO/PI staining on a Nexcelom Cellometer 2000.

Oxidation state specific Hydride Generation- Cryotrapping- Inductively Coupled Plasma- Mass Spectrometry (HG- CT- ICP- MS)

The analysis of tri- and pentavalent As species was performed by HG-CT-ICP-MS as previously described (Currier et al., 2014; Matousek et al., 2013). Briefly, cell pellets were lysed in ice-cold deionized water. The trivalent species, As^{3+}, MMA^{3+}, and dimethylarsinite (DMA^{3+}) were measured in an aliquot of cell lysate directly, without pretreatment. Another aliquot was treated with 2% cysteine and analyzed for total inorganic As ($As^{3+} + As^{5+}$), total methyl-As ($MMA^{3+} + MMA^{5+}$), and total DMAs ($DMA^{3+} + DMA^{5+}$). Calibration curves were generated using cysteine-treated pentavalent As standards, (at least 98% pure) as previously described (Hernández-Zavala et al., 2008). The concentrations of pentavalent As species were determined as a difference between the values obtained for cysteine-treated aliquots and values from untreated

sample aliquots. The instrumental LODs for As species analyzed by HG-CT-ICP-MS ranged from 0.04 pg As for methylated arsenicals to 2.0 pg As for inorganic arsenicals.

In Vitro As^{+3} and MMA^{+3} Treatments

Bone marrow, spleen and thymus cells were isolated as described above from three 13-week old male C57BL/6J mice and pooled. Cells were washed and resuspended at 1 x 10^6 cells/ml in IMDM (for bone marrow cells) or mouse medium (for spleen and thymus cells). As^{+3} or MMA^{+3} were added to each wells to the final concentrations of 0 (control), 5, 50 and 500 nM. Cells were placed into a humidified 37 °C, 5% CO_2 incubator for 4 h. Treated cells were harvested by centrifugation at 200 x*g* for 10 min and resuspended in cold $DPBS^-$. After another wash with cold $DPBS^-$, the cells were ready for Comet assay analysis.

Comet Assay (Single Cell Gel Electrophoresis Assay) and Fragment Length Analysis using Repair Enzymes (FLARE) Assay

Treated cells were immobilized in a bed of low melting point agarose on a Trevigen CometSlide™ following the Comet assay kit instructions. Cells were then lysed with Lysis Solution with 10% DMSO (Sigma-Aldrich) over night. On the next day, DNA in the lysed cells were unwound with basic buffer (8 g NaOH with 500 mM EDTA in 1 L of Milli-Q water, pH>13) at room temperature for 45 min. For FLARE assay, human 8-oxoguanine DNA glycosylase 1 (hOGG1) from the FLARE kit was diluted to 1:5 and applied to the wells. Slides were then incubated at 37 °C for 30 min before adding the unwinding buffer. For both assays, slides were electrophoresed in ice cold basic buffer with 21 volts for 30 min. Slides were washed, dried and stained with Sybr Gold (1:10000 dilution in TE buffer) and imaged using an epifluorescence microscope. Fifty randomly

selected cells from each well were scored using CometScore software (TriTek Corp., Sumerduck, VA). DNA damage was reported by percentage of DNA in tail (Collins, 2004).

PARP activity assay

The PARP activity assay was performed using the Trevigen PARP activity kit. All reagents were supplied by the kit unless otherwise specified. The procedures were previously described by Sun et al., 2012. Basically, cells were lysed with the Cell Extraction Buffer supplied in the kit, and the protein concentration was determined by the BCA Protein Assay. Two hundreds ng of total proteins from each sample was combined with activated DNA and nicotinamide adenine dinucleotide (NAD) supplied by the kit, and then placed into a histone-coated strip well to formed PAR complex which was fixed to the bottom of the well. Anti-PAR monoclonal antibody was then added to the well to bind to PAR complex, followed by a Horseradish peroxidase (HRP) conjugated secondary antibody against the primary antibody. TACS- Sapphire™ was used a substrate to generate the chemiluminescence signal. An equal amount of 0.2 M HCl was added to stop the reaction. The signals were detected using SpectraMax® 340PC microplate reader (Molecular Devices, Sunnyvale, CA) at 450 nm wavelength.

Statistics

Data were analyzed using Excel 2013 and Sigma Plot v12.5 software. One-way analysis of variance (ANOVA) and Dunnett's t-test were used to determine differences between the control and treatment groups. Pearson Correlation and polynomial linear regression were used to analyze the correlations between intracellular As concentrations and DNA damage increases. For *in vivo* As^{+3} treatment, 5 animals (n=5) were assigned to

each treatment group. For the *in vitro* experiments, three replicates were performed and analyzed for each dose.

RESULTS

Intracellular arsenic species in the bone marrow, spleen and thymus cells of drinking water exposed mice

9-week old C57BL/6J male mice were exposed to 0, 100, and 500 ppb As^{+3} through drinking water for 30 d. No change in mouse body weight or water intake was observed during or after the exposure (Table 4.1). As^{+3} intake was calculated from the water intake of each mouse and the As^{+3} concentrations in the drinking water determined by mass spectrometry. Bone marrow, spleen and thymus were harvested from each mouse and the cells were isolated. Although not statistically significant, there was a trend of decrease in thymus weight, as well as the bone marrow and thymus cell recoveries (Table 4.1). The spleen weight and cell recovery were not affected by As^{+3} exposure. In order to measure the intracellular species and amounts of arsenic in these tissues from As^{+3} exposed mice, we used a very sensitive HG- CT- ICP- MS system to analyze the intracellular As levels in 5 x 10^6 cells pelleted from each tissue, as well as 50 µl plasma from each mouse (Table 4.2). A dose-dependent increase in total intracellular As levels was observed in bone marrow, spleen and plasma but not the spleen. Control mice showed detectable levels of As, presumably due to small amounts of As present in food and City of Albuquerque drinking water, which has As levels less than 5 ppb. Interestingly, the major increased As species in bone marrow and thymus was the trivalent methylated form, MMA^{+3}, which was almost undetectable in 500 ppb exposed spleen cells. Therefore, these results not only demonstrated that spleen is the least exposed tissue among the three immune organs, but also indicated that MMA^{+3} may be

the major cause of genotoxicity in As^{+3} *in vivo* exposures. The concentrations of arsenic in plasma were an order of magnitude higher than those in cells from immune tissues; here DMA^{+3} and DMA^{+5} are the major metabolites.

Table 4.1. Mouse body weight, water, arsenic (As) intake, tissue weight, cell recovery and viability of 30 d 0 (Cont), 100 and 500 ppb As^{+3} *in vivo* drinking water exposed male C57/BL6 mice[1].

Treatments		Mouse body weight (g)	Water intake (ml/d)	As intake (ng/d)[2]
Cont		27.71 ± 1.66	3.34 ± 0.11	18.50 ± 0.77
100 ppb		27.53 ± 2.69	3.68 ± 0.27	420. 54± 12.32*
500 ppb		27.50 ± 1.42	3.59 ± 0.34	2111.32 ± 323.19*
		Tissue weight (mg)	Cell recovery (x 10^6 cells)	Viability (%)
Bone Marrow	Cont		51.35 ± 12.75	86.16 ± 2.93
	100 ppb		42.78 ± 4.82	88.64 ± 1.72
	500 ppb		43.14 ± 8.12	87.46 ± 2.10
Spleen	Cont	106 ± 6.60	186.6 ± 13.39	77.72 ± 3.19
	100 ppb	106 ± 6.04	183.4 ± 14.31	74.75 ± 1.71
	500 ppb	103 ± 10.03	180.8 ± 30.96	76.32 ± 2.65
Thymus	Cont	52.32 ± 7.31	71.32 ± 14.50	87.16 ± 1.56
	100 ppb	46.24 ± 5.73	69.62 ± 17.24	87.68 ± 1.20
	500 ppb	40.88 ± 11.69	60.34 ± 16.85	87.98 ± 0.89

[1]Mice were 9-week old when the exposure started. 5 mice (n = 5) were treated for each single dose. Drinking water was changed each week and water intake was calculated from the change in the weight of the water. Cell recovery and viability were obtained using a Cellometer 2000 with AO/PI staining. Results are Means ± SD.
[2]As intake was calculated based on drinking water samples measured by Mass Spectrometry and daily water intake of each mouse.
*Significantly different from Control ($p < 0.5$).

Table 4.2. Arsenic (As) species and amounts in bone marrow, spleen, thymus cells (5 x 10^6 cells), and 50 µl plasma in C57/BL6 male mice exposed to 0 (Cont), 100 and 500 ppb As^{+3} *in vivo* for 30 d. Samples were analyzed by Oxidation State Specific Hydride Generation- Cryotrapping- Inductively Coupled Plasma- Mass Spectrometry (HG- CT-ICP- MS)[1].

Tissues	Exposure doses	As amount by species (pg)						Total As
		As^{+3}	MMA^{+3}	DMA^{+3}	As^{+5}	MMA^{+5}	DMA^{+5}	
Bone Marrow	Cont	ND	ND	0.52 ± 0.10	5.46 ± 0.74	0.03 ± 0.01	0.88 ± 0.13	6.88 ± 0.63
	100 ppb	ND	0.07 ± 0.04	1.77 ± 0.73*	7.60 ± 1.78	0.34 ± 0.15*	2.02 ± 0.21*	11.80 ± 2.49*
	500 ppb	ND	45.70 ± 0.69	4.13 ± 0. 85*	11.70 ± 3.54*	10.35 ± 1.31*	7.52 ± 3.12*	79.44 ± 8.47*
Spleen	Cont	0.29 ± 0.10	ND	0.16 ± 0.12	10.14 ± 1.90	0.43 ± 0.41	0.51 ± 0.07	11.21 ± 2.19
	100 ppb	0.11 ± 0.08	0.12 ± 0.05	0.97 ± 0.71	11.62 ± 2.89	0.29 ± 0.08	0.66 ± 0.33	13.73 ± 2.79
	500 ppb	0.51 ± 0.26	0.22 ± 0.17	1.83 ± 0.42*	11.33 ± 2.86	1.61 ± 2.13	1.15 ± 0.27*	16.45 ± 3.54
Thymus	Cont	2.62 ± 0.91	0.13 ± 0.10	0.44 ± 0.18	11.86 ± 3.01	0.61 ± 0.86	0.22 ± 0.14	15.83 ± 3.06
	100 ppb	5.51 ± 2.49	25.70 ± 4.50*	0.81 ± 0.16	14.34 ± 6.40	8.08 ± 1.86*	0.63 ± 0.07*	54.42 ± 10.10*
	500 ppb	ND	125.43 ± 21.23*	3.17 ± 2.01*	NA	3.47 ± 3.59	NA	146.79 ± 43.34*
Plasma	Cont	ND	3.79 ± 2.561	138.92 ± 13.00	NA	9.72 ± 9.86	226.76 ± 17.11	386.35 ± 21.54
	100 ppb	ND	2.40 ± 0.50	363.87 ± 131.87*	43.36 ± 21.12	28.59 ± 7.57*	639.43 ± 144.39*	1077.66 ± 381.32*
	500 ppb	ND	12.72 ± 4.92*	802.84 ± 66.46*	63.56 ± 25.92	57.07 ± 17.58*	2027.22 ± 358.66*	2963.41 ± 332.48*

[1]5 mice (n = 5) were treated for each single dose. Sample lost happened during collections and injections. Values are in picograms (pg). Results are Means ± SD.
NA, n < 3 due to sample lost.
ND, below detection range.
*Significantly different from Cont ($p < 0.5$).

Differential sensitivities of bone marrow, spleen and thymus in DNA damage and PARP activity to *in vivo* arsenic exposures

To compare the genotoxicity between lymphoid tissues, we performed Comet Assay on the cells obtained from the spleen, thymus, and bone marrow. Results showed a significant increase in DNA damage in both bone marrow and thymus cells starting at 100 ppb (Fig. 4.1A and 4.1C). No increase of DNA damage was observed in spleen cells (Fig. 4.1B). The activity of PARP was also measured as a common endpoint to see if the DNA repair ability was also inhibited. Arsenic is known to cause PARP inhibition, which has been shown to result in increased DNA damage (Qin et al., 2008; Xu et al., 2016b; Zhou et al., 2011). A dose-dependent decrease in PARP activity was seen in bone marrow and thymus cells (Fig. 4.2A and 4.2C). No change in PARP activity was observed in spleen cells (Fig. 4.2B). These results showed that bone marrow and thymus cells are more prone to genotoxicity compared to spleen cells, which may be the result of higher intracellular As and MMA^{+3} concentrations in *in vivo* exposures.

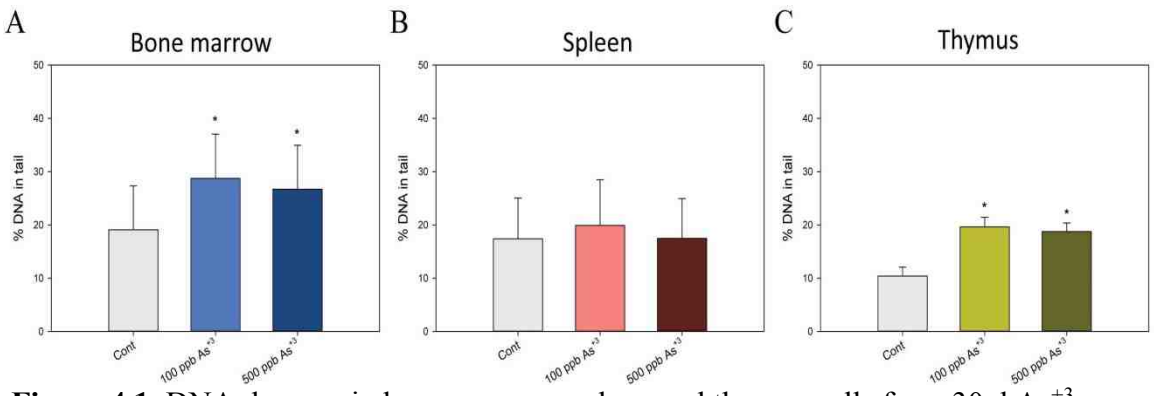

Figure 4.1. DNA damage in bone marrow, spleen and thymus cells from 30 d As^{+3} drinking water exposed mice. 9-week old male C57BL/6J mice were exposed to 0, 100 and 500 ppb As^{+3} through drinking water for 30 d. Bone marrow, spleen and thymus cells were isolated and the DNA damage was measured by Comet assay. A, bone marrow. B, spleen. C, thymus. *Significantly different compared to control ($p<0.05$, n=5). Results are Means ± SD.

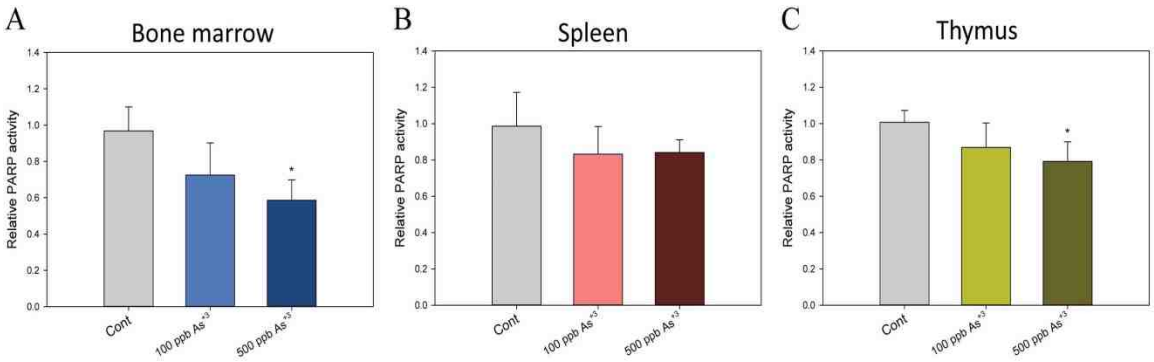

Figure 4.2. PARP activity in bone marrow, spleen and thymus cells from 30 d As^{+3} drinking water exposed mice. 9-week old male C57BL/6J mice were exposed to 0, 100 and 500 ppb As^{+3} through drinking water for 30 d. Bone marrow, spleen and thymus cells were isolated and the PARP activity assay was used to measure the PARP activity in the cell protein lysates. A, bone marrow. B, spleen. C, thymus. *Significantly different compared to control ($p<0.05$, n=5). Results are Means ± SD.

Correlations between DNA damage increase and intracellular arsenic concentrations in bone marrow, spleen and thymus cells

In vivo exposures to As^{+3} resulted a dose-dependent increase in total As and MMA^{+3} intracellular concentrations in bone marrow and thymus cells. We performed a regression analysis to reveal the relationships between total As or MMA^{+3} intracellular levels and the DNA damage in bone marrow, spleen and thymus cells. As shown, the amount of DNA damage correlated with the intracellular total As as well as the MMA^{+3} levels in bone marrow and thymus cells (Fig. 4.3A, 4.3C, 4.3D and 4.3F). There was no correlation between the DNA damage and intracellular As in the spleen cells (Fig. 4.3B and 4.3E). This analysis demonstrated that higher *in vivo* exposure to As^{+3} can increase the intracellular total As and MMA^{+3} in the bone marrow and thymus cells, which may induce or increase DNA damage in these immune tissues.

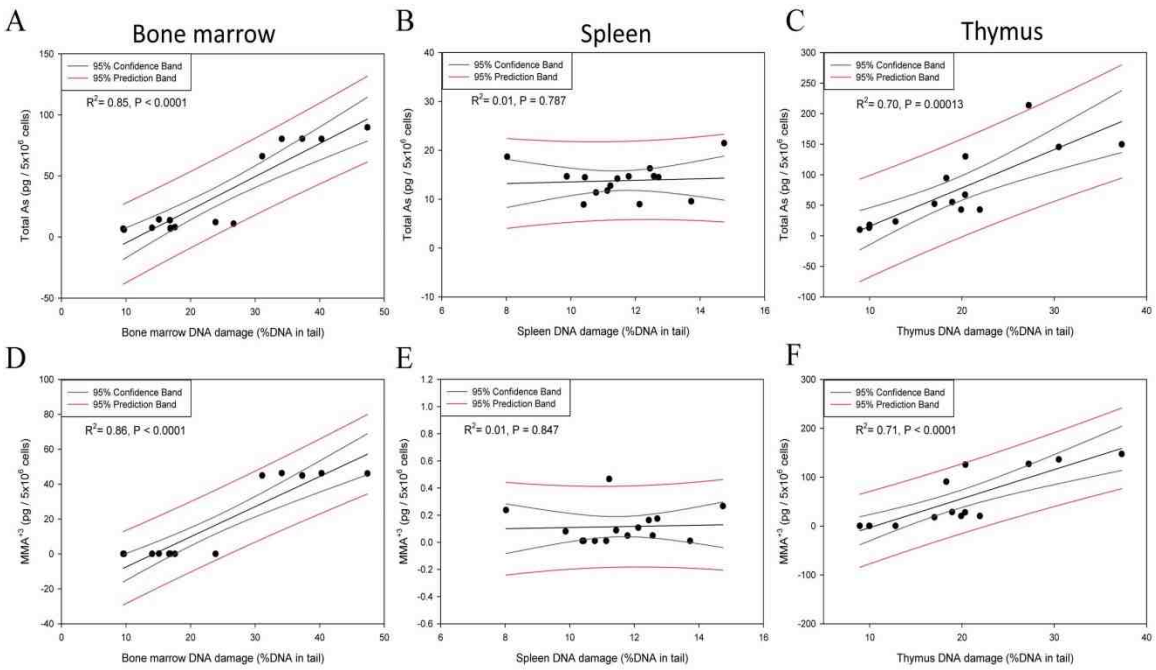

Figure 4.3. Correlations between intracellular total As or MMA^{+3} concentrations and DNA damage in bone marrow, spleen and thymus cells from 30 d As^{+3} drinking water exposed mice. A, total As and DNA damage in bone marrow cells. B, total As and DNA damage in spleen cells. C, total As and DNA damage in thymus cells. D, MMA^{+3} and DNA damage in bone marrow cells. E, MMA^{+3} and DNA damage in spleen cells. F, MMA^{+3} and DNA damage in thymus cells.

Differential sensitivities of bone marrow, spleen and thymus in DNA damage to *in vitro* arsenic exposures

In order to see if the differential sensitivities observed between spleen, thymus and bone marrow were due to different cell type susceptibilities, we directly added As^{+3} and MMA^{+3} to primary cultures of these cells. Cells were isolated and treated with 5, 50 and 500 nM As^{+3} or MMA^{+3} *in vitro* for 4 h and then were assessed for DNA damage using Comet assay. As shown in Fig 4.4A, bone marrow cells were sensitive to As^{+3} at concentrations as low as 5 nM. Spleen and thymus cells were only sensitive to As^{+3} treatment at the high concentration (500 nM, Fig. 4.4B and 4.4C). However, cells from all the three organs were sensitive to MMA^{+3} starting at the 5 nM concentration, indicating that MMA^{+3} is more genotoxic than As^{+3} *in vitro*. It was also observed that bone marrow cells seemed to be the most sensitive among all the three organs. However, the sensitivities of spleen and thymus were comparable *in vitro*, indicating that the lower sensitivity in spleen cells observed in the *in vivo* experiment was due to lower As accumulation. The FLARE assay is a modified type of Comet assay that uses hOGG1 to enhance its sensitivity to detect oxidative DNA damage (Smith et al., 2006). We performed the FLARE assay with same samples used for the Alkaline Comet assay following 4 h incubation with As^{+3} and MMA^{+3}. The results obtained from the FLARE assay were similar to the Comet assay, except that a significant increase in DNA damage was observed at high doses of As^{+3} and MMA^{+3} only in thymus cells (Fig. 4.4C). This observation is consistent with our previous findings that As^{+3} induced oxidative stress in thymus cells at high concentrations (Xu et al., 2016b). These results demonstrated that bone marrow, spleen and thymus cells are more sensitive to MMA^{+3} induced

genotoxicity than As^{+3} *in vitro*, indicating that the higher sensitivities of bone marrow and thymus cells in *in vivo* exposures were likely due to the significantly increased MMA^{+3} intracellular concentrations.

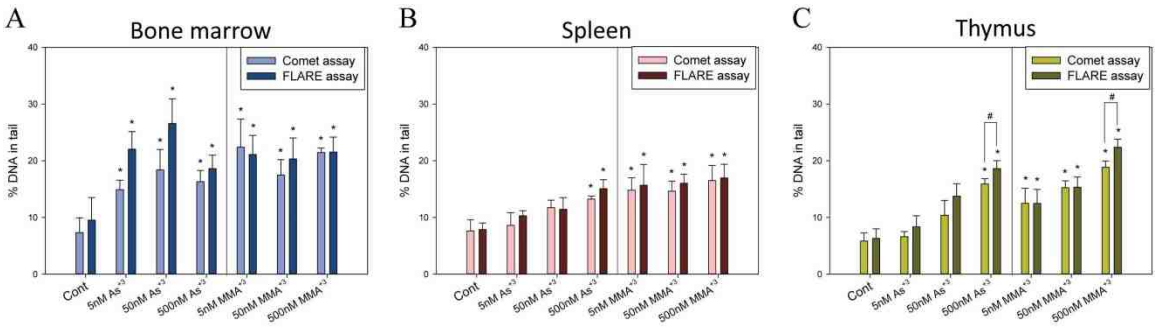

Figure 4.4. DNA damage in bone marrow, spleen and thymus cells treated with As^{+3} and MMA^{+3} *in vitro* for 4 h. Cells were isolated from three 13-week old C57BL/6J mice and pooled. Bone marrow, spleen and thymus cells were then treated with 5, 50 and 500 nM As^{+3} or MMA^{+3}. Comet assay and FLARE assay were used to analyze the DNA damage and oxidative damage induced by the treatments. A, bone marrow. B, spleen. C, thymus. *Significantly different compared to control ($p<0.05$). #Significantly different compared to the Comet assay ($p<0.05$) Results are Means ± SD.

DISCUSSION

As^{+3} is known to cause multiple and complicated biological effects. There have been many studies focusing on the toxicity of As^{+3} over the years. However, two basic questions are often ignored when we set up the biological models and expose animals or cells to As^{+3}. What is the actual level of exposure and what chemical species are responsible for immunotoxicity in various lymphoid tissues? From previous studies, we know that various inorganic and organic arsenic species have differential toxicities (Akter et al., 2005). From studies in our laboratory, we have found that cells from different immune organs and tissues have differential sensitivities to As (Ezeh et al., 2014, 2016; Li et al., 2010; Xu et al., 2016a, 2016b). Therefore, it is important to determine if lymphoid organs and tissues, such as bone marrow, spleen and thymus have differential sensitivities to As^{+3} in terms of genotoxic and non-genotoxic actions both *in vivo* and *in vitro*.

In this study, intracellular As concentrations and species were measured in lymphoid cells isolated from three immune organs following As^{+3} 30 d drinking water exposure. A correlation between increased DNA damage and increased intracellular MMA^{+3} levels were found in both bone marrow and thymus cells (Fig. 1 and Table 1). Spleen cells were not as sensitive as bone marrow and thymus cells *in vivo*, and the intracellular MMA^{+3} levels in the spleen were not as high as seen in bone marrow and thymus, which can be the reason that caused the sensitivity differences. T and B cells in the spleen are more mature than those in the bone marrow and thymus, which might be a factor that accounts for the differential intracellular As concentrations. One of our

previous studies showed that the thymus cells at the earlier stage (double negative) are more prone to As^{+3} induced toxicity than the later stage (double positive) (Xu et al., 2016a). Therefore, it is possible that more mature cells are resistant to As toxicity, due to a lower intracellular As concentration or less toxic intracellular As species. Another observation that supports this hypothesis is that bone marrow cells were sensitive to even 5 nM As^{+3} exposure *in vitro* (Fig. 4.1A). Bone marrow consists of multiple types of early progenitor cells and the very early stage of pre-T cells that migrate to the thymus. It is important to understand potential mechanisms responsible for the susceptibility of early lymphoid cells to As toxicity. Also, in the Comet assay experiments, we noticed that it is very common for bone marrow cells to have higher background DNA damage from *in vivo* exposures, which may also due to the fragility of the progenitor cells in the bone morrow.

MMA^{+3} has been shown to be more toxic than As^{+3} in lymphoid and non-lymphoid tissues. MMA^{+3} is formed *in vivo* mostly in the liver, kidneys, and lungs under the influence of the AS3MT enzyme (Chen et al., 2011). We have found little enzyme expression of AS3MT in mouse lymphoid tissue, and have found little evidence for metabolism of As^{+3} in lymphoid tissues (unpublished data). Thus we believe that the presence of MMA^{+3} in lymphoid tissues is a reflection of MMA^{+3} uptake from the blood. From Table 2, we know that although the prevalent forms of As species in the plasma are MMA^{+5}, DMA^{+3} and DMA^{+5}, MMA^{+3} concentration was also significantly increased in the high dose. On the other hand, MMA^{+3} was the most prevalent form in high dose exposed bone marrow and thymus cells. Also, there was As^{+5} in cells from all three tissues, but As^{+3} was almost undetectable in all three tissues. Therefore, we think that the

differences in bone marrow and thymus compared to spleen may result from a difference in the ability of cells either to import or export As^{+3} and MMA^{+3} or to convert MMA^{+5} to MMA^{+3}. Our current efforts are aimed at measuring these differences.

Regarding the mechanism of DNA damage produced by MMA^{+3}, it has been found that MMA^{+3} may produce stronger inhibition than As^{+3} of PARP, a zinc finger protein that is required for base excision repair, (Sun et al., 2012; Zhou et al., 2014). In our previous studies, we demonstrated a correlation between PARP activity inhibition and the increase of DNA damage in mouse thymus cells (Xu et al., 2016b). Therefore, the DNA damage increase observed in the mouse bone marrow and thymus cells following *in vivo* As^{+3} exposure appears to result from suppression of the DNA repair system.

In summary, the present study showed differential sensitivities of the cells from three important immune organs, bone marrow, spleen and thymus, to As^{+3} induced genotoxicity *in vivo*. The *in vivo* sensitivity was shown to be correlated with an increase in the trivalent methylated arsenic species, MMA^{+3}. Bone marrow cells were shown to be the most sensitive *in vitro*, which may relate to the maturity of the cell types in different tissues. These studies stress the importance of measuring lymphoid tissue exposure and performing speciation analyses for arsenic studies.

FUNDING

This work was funded by National Institute of Environmental Health Sciences at the National Institutes of Health (grant number R01 ES019968).

CHAPTER 5

Interactive Genotoxicity Induced by Environmentally Relevant Concentrations of Benzo(a)pyrene Metabolites and Arsenite in Mouse Thymus Cells

Huan Xu[*], Fredine T. Lauer[*], Ke Jian Liu[*], Laurie G. Hudson[*], and Scott W. Burchiel[* §]

*The University of New Mexico College of Pharmacy, Department of Pharmaceutical Sciences, Albuquerque, NM 87131

§To whom correspondence should be addressed. Fax: (505) 272-6749. Email: sburchiel@salud.unm.edu

Toxicological Sciences, 154(1): 153-161. DOI: 10.1093/toxsci/kfw151.

Received May 26, 2016; Revision received July 25, 2016; Accepted July 28, 2016;

Published online: August 7.

ABSTRACT

Arsenic and polycyclic aromatic hydrocarbon (PAH) exposures affect many people worldwide leading to cancer and other diseases. Arsenite (As^{+3}) and certain PAHs are known to cause genotoxicity. However, there is limited information on the interactions between As^{+3} and PAHs at environmentally relevant concentrations. The thymus is the primary immune organ for T cell development in mammals. Our previous studies showed that environmentally relevant concentrations of As^{+3} induce genotoxicity in mouse thymus cells through Poly(ADP-ribose) polymerase (PARP) inhibition. Certain PAHs, such as the metabolites of benzo(a)pyrene (BaP), are known to cause DNA damage by forming DNA adducts. In the present study, primary mouse thymus cells were examined for DNA damage following 18 hr *in vitro* treatments with 5 or 50 nM As^{+3} and 100 nM BaP, benzo[a]pyrene-7,8-dihydrodiol (BP-Diol), or benzo[a]pyrene-7,8-dihydrodiol-9,10-epoxide (BPDE). Increase of genotoxicity and apoptosis were observed following treatments with 5 nM As^{+3} + 100 nM BP-Diol and 50 nM As^{+3} + 100 nM BPDE. We attribute the increase in DNA damage to inhibition of PARP inhibition leading to decreased DNA repair. To further support this hypothesis, we found that a PARP inhibitor, 3,4-dihydro-5[4-(1-piperindinyl) butoxyl]-1(2H)-isoquinoline (DPQ), also interacted with BP-diol to produce an increase in DNA damage. Interestingly, we also found that As^{+3} and BP-diol increased CYP1A1 and CYP1B1 expression, suggesting that increased PAH metabolism may also contribute to genotoxicity. In summary, these results show that the suppression of PARP activity and induction of CYP1A1/CYP1B1 may act together to increase DNA damage produced by As^{+3} and PAHs.

INTRODUCTION

Polycyclic aromatic hydrocarbons (PAHs) are widespread organic pollutants, which naturally occur in soil, air, and following the burning of fossil fuels. PAHs are generated from combustion of wood, coal, oil and tobacco, and they are also abundant in overcooked and processed foods. The toxicity of PAHs is dependent on their structures. Benzo(a)pyrene (BaP), a Group One carcinogen listed by International Agency for Research on Cancer, has been associated with increased levels of colon cancer (Le Marchand et al., 2002), as well as genotoxicity in the lung of smokers (Denissenko et al., 1996). BaP is considered a pro-carcinogen, as metabolism and activation by CYP1A1, CYP1B1 and epoxide hydrolase are required to cause cancer (Jones et al., 1995; Shimada and Fujii-Kuriyama, 2004). BaP is first metabolized to benzo[a]pyrene-7,8-dihydrodiol (BP-Diol), which is then converted into benzo[a]pyrene-7,8-dihydrodiol-9,10-epoxide (BPDE). BPDE binds covalently to DNA forming adducts resulting in DNA damage and mutation (Kim et al., 1998; Schwarz et al., 2001). The expression of CYP1A1 and CYP1B1 is regulated by aryl hydrocarbon receptor (AhR), which has been shown to be induced by BaP (Hockley et al., 2007).

Arsenic exposure from food and drinking water sources is a world-wide public health concern. Environmental exposures of arsenic can range from several to several hundred ppb (10 ppb ≈ 130 nM) for different areas and populations (Rahman et al., 2006; Sherwood et al., 2013). The trivalent from of inorganic arsenic, arsenite (As^{+3}), has been associated with many diseases such as diabetes, skin lesions, and cancers (Argos et al., 2010; Schuhmacher-Wolz et al., 2009; Vahter, 2008). One of the primary genotoxic

mechanisms of As^{+3} is the inhibition of DNA repair (Faita et al., 2013). As^{+3} has been shown to compete with Zn^{+2} on C3H1 and C4 zinc fingers, decreasing the activity of zinc finger proteins involved in DNA repair such as Poly(ADP-ribose) polymerase (PARP) and Xeroderma Pigmentosum, Complementation Group A (XPA) (Qin et al., 2012; Zhou et al., 2011; Zhou et al., 2014). Our previous studies demonstrated a dose-dependent increase in DNA damage and PARP inhibition in mouse thymocytes (Xu et al., 2016). At environmentally relevant concentrations, DNA damage induced by As^{+3} in thymic cells appears to result from PARP inhibition at low exposure levels (e.g., 50 nM As^{+3}). Higher *in vitro* exposure levels (e.g., 500 nM As^{+3}) result in oxidative stress that is associated with more DNA damage and double strand breaks. The findings are in agreement with those obtained by other groups (Litwin et al., 2013; Qin et al., 2012). There is also evidence showing that PARP contributes to XPA repair of double strand breaks (King et al., 2012).

As^{+3} has been documented to interact with other environmental agents, such as UVR (Cooper et al., 2009; Cooper et al., 2013; Evans et al., 2004; Zhou et al., 2011). There is also evidence showing that co-exposure with As^{+3} increases BaP DNA adduct formation and mutations in mouse hepatoma Hepa-1 cells *in vitro* (Maier et al., 2002). An *in vivo* study revealed that arsenic co-exposure can increase BaP adducts formation in both lung and skin (Evans et al., 2004). However, studies have not addressed the effects of As^{+3} and PAH co-exposure on immune cells in the thymus.

Our previous studies revealed that As^{+3} interacted with PAHs to increase the suppression of progenitor pre-B cell formation in murine bone marrow at very low concentrations both *in vitro* and *in vivo* (Ezeh et al., 2014; Ezeh et al., 2015). Synergistic

immunosuppression of T-dependent antibody responses by different PAHs and As^{+3} spleen cells were also observed (Li et al., 2010). Evidences also indicated that human T cells from certain healthy individuals were suppressed by extreme low concentrations (1-100 nM) of As^{+3} *in vitro* (Buechiel et al., 2014). Thymocytes are primarily early T cells which have been shown to be very sensitive to As^{+3} induced genotoxicity, which can occur at low exposure levels not associated with oxidative stress (Xu et al., 2016). Therefore, our hypothesis is that co-exposure of low concentrations of As^{+3} and PAHs will induce genotoxicity in mouse thymus cells.

MATERIALS AND METHODS

Chemicals and Reagents

Sodium arsenite (As^{+3}, CAS 774-46-5), benzo(a)pyrene (BaP, CAS 50-32-8), benzo(e)pyrene (BeP, CAS 192-97-2), anthracene (ANTH, CAS 120-12-7), dibenz(a,c)anthracene (DAC, CAS 215-58-7), dibenz(a,h)anthracene (DAH, CAS 53-70-3), 3-methylcholanthrene (3-MC, CAS 56-49-5), benz(a)anthracene (BA, CAS 56-55-3), 7,12-dimethylbenz(a)anthracene (DMBA, CAS 57-97-6), 9,10-dimethylanthracene (DMA, CAS 781-43-1) were purchased from Sigma-Aldrich (St. Louis, MO). Dibenzo(def,p)chrysene (DBC, CAS 191-30-0) was purchased from AccuStandard (New Haven, CT). BaP-trans-7,8-dihydrodiol (BP-diol), BaP-trans-7,8-dihydrodiol-9,10-epoxide (BPDE) and DMBA-trans-3,4-dihydrodiol (DMBA-diol), 11,12-dihydroxy-11,12-dihydrodibenzo(def,p)chrysene (DBC-diol) were obtained from National Cancer Institute Chemical Repository (Midwest Research Institute, Kansas City, MO). Hanks Balanced Salt Solution (HBSS) was purchased from Lonza (Walkersville, MD). Penicillin/Streptomycin 10,000 (mg/ml)/10,000 (U/ml) and 200 mM L-Glutamine were purchased from Life Technologies (Grand Island, NY). Dulbecco's phosphate buffered saline w/o Ca^{+2} or Mg^{+2} ($DPBS^{-}$) and RPMI 1640 HEPES modified medium base, sodium azide and dimethylsulfoxide (DMSO) were purchased from Sigma-Aldrich. Fetal Bovine Serum (FBS) was purchased from HyClone Laboratories (Logan, UT). 3,4-Dihydro-5[4-(1-piperindinyl) butoxyl]-1(2H)-isoquinoline (DPQ, CAS 129075-73-6) was purchased from Santa Cruz Biotechnology (Dallas, TX). HT chemiluminescent PARP/apoptosis assay kit (Cat. No. 4685-096-K) and CometAssay® 20 well ES starter

kit (Cat. No. 4252-040-ESK) were purchased from Trevigen (Gaithersburg, MD). Pierce™ BCA protein assay kit (Cat. No. 23225) was purchased from Thermo Fisher Scientific (Waltham, MA). FITC Annexin V Apoptosis Detection Kit II (Cat. No. 556570) was purchased from BD Biosciences (San Jose, CA). RNeasy Mini Kit ™ and QIAshredder™ were purchased from Qiagen (Valencia, CA). High Capacity cDNA reverse transcription kit (Cat. No. 4368814), CYP1A1 (Mm00487218_m1)/ CYP1B1 (Mm00487229_m1) TaqMan® gene expression assays and TaqMan® universal PCR master mix (Cat. No. 4304437) and Dihydroethidium (DHE, Cat. No. D11347) were purchased from Life Technologies. CYP1A1/1B1 P450-Glo^{TM} assay (Cat. No. V8751) was purchased from Promega (Madison, WI).

Isolation of primary mouse thymus cells

8 to 10 week old C57BL/6J male mice were purchased from Jackson Laboratory (Bar Harbor, ME). All animal experiments were performed following protocols approved by the Institutional Animal Use and Care Committee at the University of New Mexico Health Sciences Center. Thymuses were harvested and transferred to the laboratory in HBSS. Cell suspensions from 3 mice were pooled, centrifuged at 200 x *g* for 10 min and resuspended in the mouse medium (RPMI 1640 plus 10% FBS, 2 mM L-glutamine, 100 mg/ml streptomycin, 100 units/ml penicillin). Cell viability was determined by acridine orange/propidium iodide (AO/PI) staining and counting using the Nexcelom Cellometer 2000.

The single cell gel electrophoresis assay (Comet assay)

Cells were treated *in vitro* and washed with DPBS^{-}, immobilized in a 1.5 ml microcentrifuge tube containing 250 µl low melting point agarose and then applied to a

Trevigen CometSlide™. Cells were lysed with Lysis Solution with 10% DMSO, and electrophoresed in NaOH buffer (pH>13) with 21 volts for 30 min. Slides were air dried, stained with Sybr Green and imaged with an Olympus IX70 inverted fluorescence microscope. 50 cells from each well of the slides were scored using CometScore (TriTek Corp., Sumerduck, VA).

PARP activity ELISA assay

After harvest, *in vitro* treated cells were lysed with Cell Extraction Buffer from the kit and the protein concentration of each lysate was quantified by BCA protein assay. 200 ng of total protein was combined with activated DNA and nicotinamide adenine dinucleotide (NAD) to form PAR, which became fixed on the bottom of histone-coated strip wells. Anti-PAR monoclonal antibody was added to the wells to target PARP and HRP conjugated secondary antibody was added to bind the primary antibody. TACS-Sapphire™ was used to generate the chemiluminescence signal. The reaction was stopped by adding 0.2 M HCl. Absorbance was read at 450 nm using SpectraMax® 340PC microplate reader (Molecular Devices).

Annexin V/Propidium Iodide staining

1 x 10^5 cells were washed twice with $DPBS^-$ and resuspended in 100 µl 1X Annexin V Binding Buffer. 5 µl of FITC Annexin V and 5 µl of Propidium Iodide staining solution were added to each sample. After 15 min incubation at room temperature in dark, 400 µl of 1X Annexin V Binding Buffer was added to each sample. BD Accuri™ C6 flow cytometer was used to analyze the samples. Thymus cells treated with 10 µM Etoposide for 4 h were used as positive control. For negative control, 5 µg of

purified recombinant Annexin V was added to thymus cells to block the FITC conjugated Annexin V binding.

DHE staining

1 mg DHE was suspended with 158 µl DMSO. 5 µl of the suspended DHE was diluted with 20 ml $DPBS^-$ to a final concentration of 5 µM. 1 x 10^6 treated thymus cells were washed twice with cold wash buffer ($DPBS^-$ +1% FBS +0.9% sodium azide). Each sample was stained using 100 µl 5 µM DHE in DPBS- with 37 °C incubation for 30 min. Cells were then washed with cold wash buffer, resuspended in 500 µl DPBS- and analyzed on BD Accuri™ C6 flow cytometer. Thymus cells treated with 100 µM H_2O_2 for 10 min at 37 °C were used as positive controls.

RNA isolation and CYP1A1/1B1 RT-qPCR

RNA isolation was conducted following the instruction manual for the RNeasy Mini Kit ™ and QIAshredder™ supplied by the manufacturer. The amount of extracted RNA was then quantified on an Agilent Nanodrop spectrophotometer. For each reverse transcriptase (RT) reaction, 60 µl containing a minimum of 1080 ng RNA was run on SimpiAmps thermal cycler (Life Technologies) using the high capacity cDNA reverse transcription kit. Samples were then diluted to ~9 ng/ µl with RNase, DNase free water and stored at -20 °C. Real time PCR (qPCR) reactions were performed with TaqMan® gene expression assays of CYP1A1 and CYP1B1 on Applied Biosystem's 7900HT system. Comparative C_T (first amplification cycle exceeding threshold) was applied for relative quantification, and GADPH gene was used as the endogenous control. The method to calculate the comparative C_T is described in detail in the manual from Life Technologies.

CYP1A1/1B1 activity assay

The CYP1A1/1B1 substrate, Luciferin-CEE was supplied in the P450-Glo^{TM} assay. Experiment was performed followed the lytic assay protocol provided by Promega. Isolated primary thymus cells were treated with As^{+3}, BP-diol/BPDE and their combinations for 18 h. Luciferin-CEE was then added to the culture, and the cells were incubated for another 3 h at 37 °C. Then 50 µl of cells were combined with equal amount of Luciferin substrate resuspended in the reconstitution buffer, transferred to a 96-well, white polystyrene plate, and incubate at RT for 20 min. Luminescence was recorded on a Tecan Infinite 200 (Männedorf, Switzerland).

Statistics

Excel 2010 and Sigma Plot 12.5 software were used for data analysis. One-way analysis of variance (ANOVA) and Dunnett's t-test were used to determine differences between groups. Three replicates were performed and analyzed for each single dose. CDI (coefficient of drug interaction) was calculated as CDI = AB / (A × B), A, B and AB are the ratios of the treatments to control. Synergistic effect was indicated with CDI > 1 (Xu et al., 2007).

RESULTS

Inhibition of PARP activity by different PAHs in primary mouse thymus cells

As a control for PARP inhibition studies in murine thymocytes, we examined the direct effects of PAH on PARP activity following *in vitro* exposures. Thymus cells harvested from male C57BL6J mice were treated with 100 nM BaP, BeP, 3-MC, DMBA, DAC, DAH, DMA, ANTH, BA, DBC, BP-diol, BPDE, DMBA-diol or DBC-diol for 18 h *in vitro*. As shown in Figure 5.1, PARP activity was inhibited by 3-MC, DMBA, DAC, DAH, DBC, BPDE, DMBA-diol and DBC-diol, while BaP, BeP, DMA, ANTH, BA and BP-diol did not cause PARP inhibition. The mechanism of differential inhibition of PARP activity by PAHs was not determined in this study. Cell recoveries and viabilities after the exposure to PAHs are listed in Table 5.1. Based on this PARP screening, it appeared that BaP, BP-diol, and BPDE were good candidates for examining interactions with As^{+3} based on their relative lack of direct PARP inhibition and their environmental relevance.

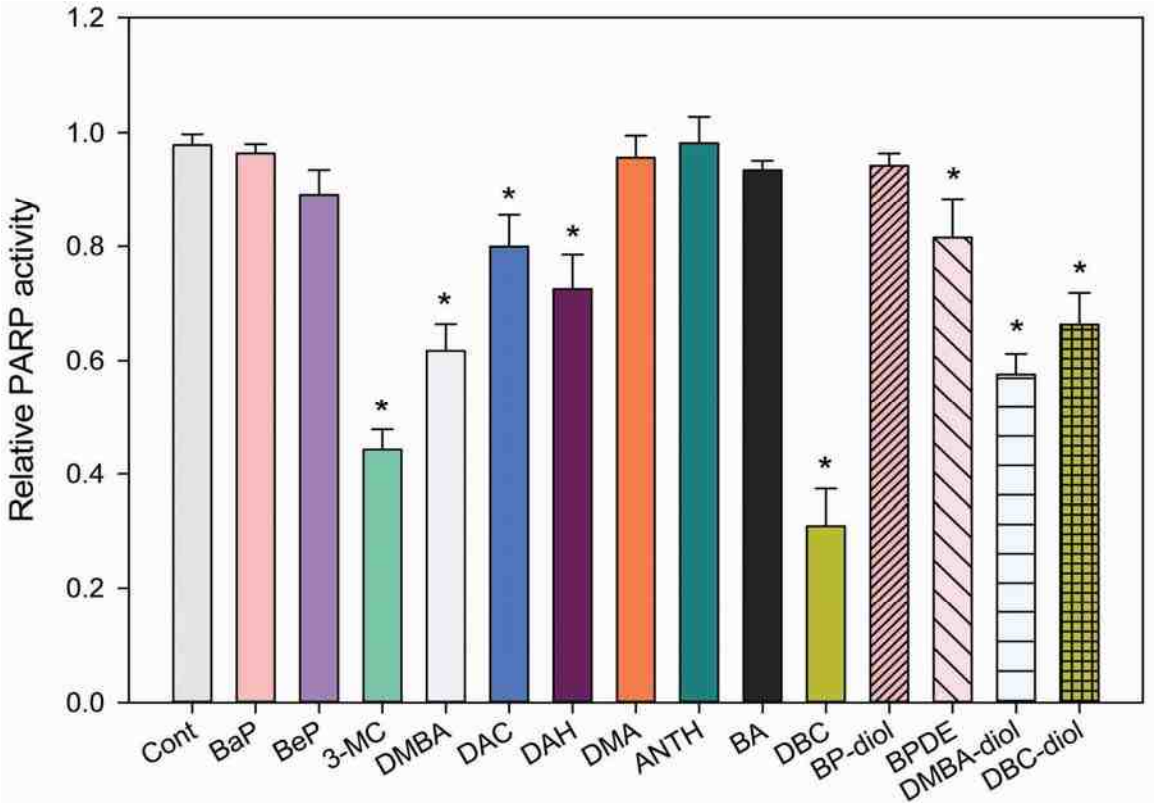

Figure 5.1. PARP activity in primary mouse thymus cells treated with PAHs *in vitro*. Primary thymus cells isolated from C57BL/6J male mice were exposed to different PAHs at 100 nM for 18 h *in vitro*. PARP activity was measured using Trevigen ELISA kits. *Significantly different compared to control ($p<0.05$). Results are Means ± SD.

Table 5.1. Cell recovery and viability of 2 x 10^6 (Viability at plating: 88.7%) of primary thymus cells following exposure to different PAHs at 100 nM *in vitro* for 18 h; Viability was measured by AO/PI staining and Cellometer[1].

Treatments (100 nM)	**Cell Counts (10^6 cells)**	**Viability (%)**
Control (no treatment)	1.84 ± 0.07	84.2 ± 1.1
BaP	1.89 ± 0.11	83.5 ± 0.8
BeP	1.81 ± 0.12	82.9 ± 1.2
3-MC	1.77 ± 0.09	81.4 ± 1.1*
DMBA	1.78 ± 0.15	80.9 ± 1.2*
DAC	1.76 ± 0.09	83.2 ± 1.3
DAH	1.75 ± 0.14	82.7 ± 1.1
DMA	1.76 ± 0.11	84.1 ± 0.9
ANTH	1.81 ± 0.03	84.5 ± 0.8
BA	1.83 ± 0.09	82.9 ± 1.1
DBC	1.55 ± 0.08*	79.9 ± 1.7*
BP-diol	1.75 ± 0.13	83.2 ± 0.9
BPDE	1.60 ± 0.05*	78.9 ± 1.2*
DMBA-diol	1.69 ± 0.08	80.1 ± 0.8*
DBC-diol	1.43 ± 0.12*	72.6 ± 1.5*

[1]Triplicate samples were analyzed for each PAH treatment. Results are Means ± SD.
*Significantly different from Cont ($p<0.5$)

Interactive genotoxicity induced by low concentrations of As^{+3} and BP-diol/BPDE

In order to examine the interactions between BaP/BP-diol/BPDE and As^{+3}, primary thymus cells were treated *in vitro* with 100 nM BaP, BP-diol or BPDE, 5 or 50 nM As^{+3} and in combinations for 18 h. A Comet assay was used to detect the DNA damage induced by different treatments. A synergistic increase in DNA damage was observed with the combined treatments of 5 nM As^{+3} + 100 nM BP-diol and 50 nM As^{+3} + 100 nM BPDE (Fig. 5.2A). A significant decrease in PARP activity was also seen with the same treatments (Fig. 5.2B). Thus, As^{+3} at very low concentrations interacts with BP-diol and BPDE leading to inhibition of PARP and to a synergistic increase in DNA damage. However, since BaP, did not cause an interactive effect with As^{+3}, the two metabolites, BP-diol and BPDE we focused on these PAHs in the subsequent studies.

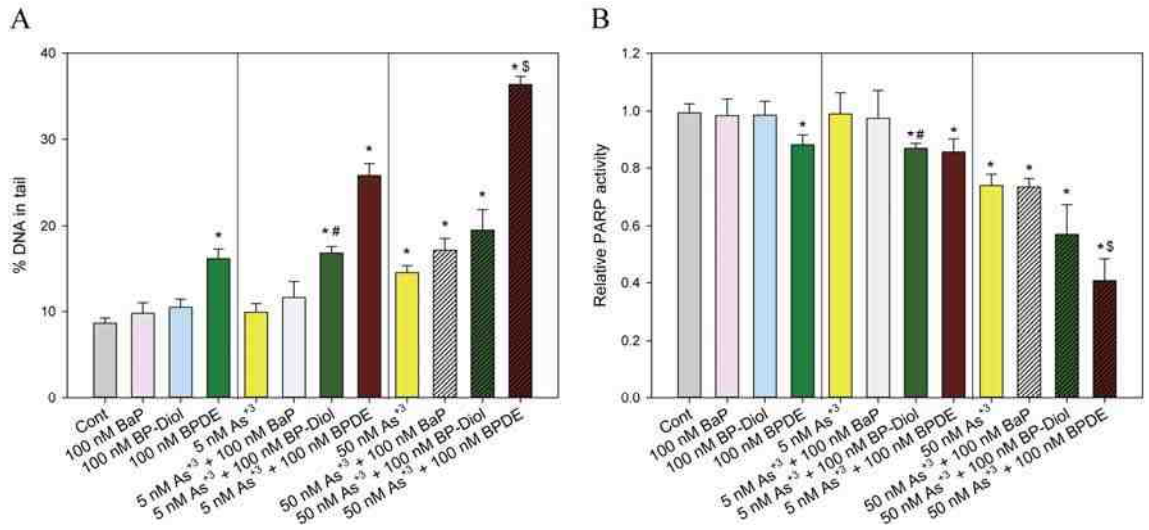

Figure 5.2. DNA damage and PARP activity in primary thymus cells treated with As^{+3}, BaP/BP-diol/BPDE and the combinations *in vitro*. Primary thymus cells isolated from C57BL/6J male mice were exposed to 5 or 50 nM As^{+3}, 100 nM BaP, BP-diol or BPDE and the combinations of As^{+3} and BaP/BP-diol/BPDE for 18 h *in vitro*. A, Comet assay images were scored by CometScore. B, PARP activity measured with Trevigen ELISA kits represented by absorbance at 450 nm. *Significantly different compared to control ($p<0.05$). # Synergistic effect compared to 5 nM As^{+3} and 100 nM BP-diol (CDI > 1). $ Synergistic effect compared to 50 nM As^{+3} and 100 nM BPDE (CDI > 1). Results are Means ± SD.

Co-exposure to As^{+3} and BP-diol/BPDE induced apoptosis in thymus cells

Annexin V staining and flow cytometry were used to see if the interactive genotoxicity induced by the combined treatments caused an increase in apoptosis. Primary thymus cells were treated with 5 or 50 nM As^{+3}, 100 nM BP-diol or BPDE, and their combinations *in vitro* for 18 h. A decrease in Annexin V-positive and PI-negative cells (e.g. viable cells), and an increase in Annexin V-positive cells (e.g. early and late apoptotic cells) was seen with treatments of 5 nM As^{+3} + 100 nM BP-diol and 50 nM As^{+3} + 100 nM BPDE (Fig. 5.3A and 5.3B). Again, an apparent effect was observed with combination treatments, as neither As^{+3} or BP-diol cause any decrease in viability when present as single agents. The increase in the percentage of apoptotic cells was correlated with the decrease of cell viability (Fig. 3A and 3C). Therefore, the co-exposure of low concentrations of As^{+3} and BaP metabolites not only induced significant genotoxicity, but also caused cell apoptosis in primary thymus cells.

Co-exposure to As^{+3} and BP-diol/BPDE did not induce superoxide production in thymus cells

In order to see if the interactive effects observed were caused by an induction of reactive oxygen species (ROS), primary thymus cells were treated with 5 or 50 nM As^{+3}, 100 nM BP-diol or BPDE, and their combinations *in vitro* for 18 h. DHE staining by flow cytometry was performed to see the superoxide levels in these treatments. As there was no significant change in superoxide production in these treatments (Fig. 5.4), the interactive effects observed in As^{+3} and BP-diol/BPDE combined treatments were not caused by superoxide production.

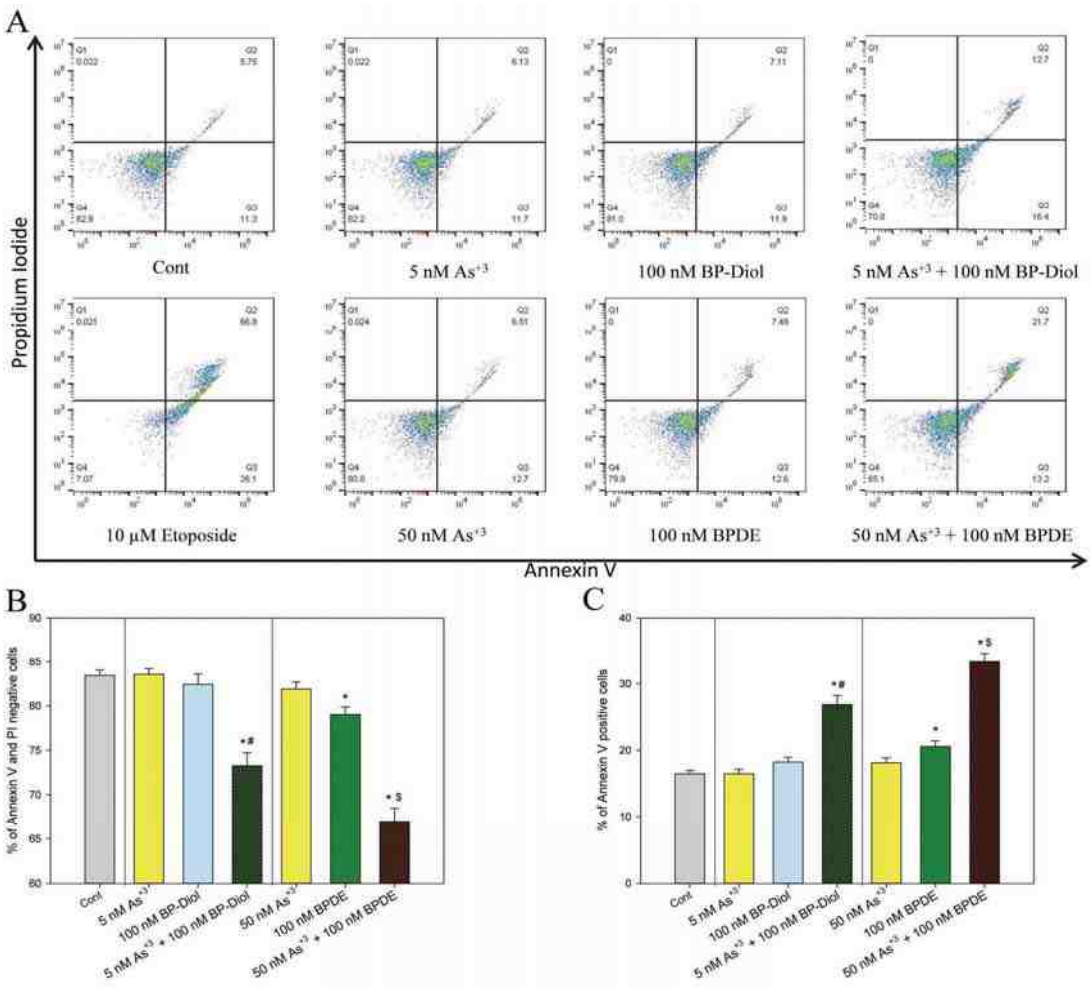

Figure 5.3. Annexin V and Propidium Iodide staining in primary thymus cells treated with As^{+3}, BP-diol/BPDE and the combinations *in vitro.* Primary thymus cells isolated from C57BL/6J male mice were exposed to 5 or 50 nM As^{+3}, 100 nM BP-diol or BPDE and the combinations of As^{+3} and BP-diol/BPDE for 18 h *in vitro*. A. flow cytometry results showing cells which are Annexin V-PI- (LL), Annexin V+PI- (LR), Annexin V-PI+ (UL), or Annexin V+PI+ (UR). B, viability (% of Annexin V-PI- cells). C. % of early and late apoptotic cells (% of Annexin V+ cells). *Significantly different compared to control ($p<0.05$). # Synergistic effect compared to 5 nM As^{+3} and 100 nM BP-diol (CDI > 1). $ Synergistic effect compared to 50 nM As^{+3} and 100 nM BPDE (CDI > 1). Results are Means ± SD.

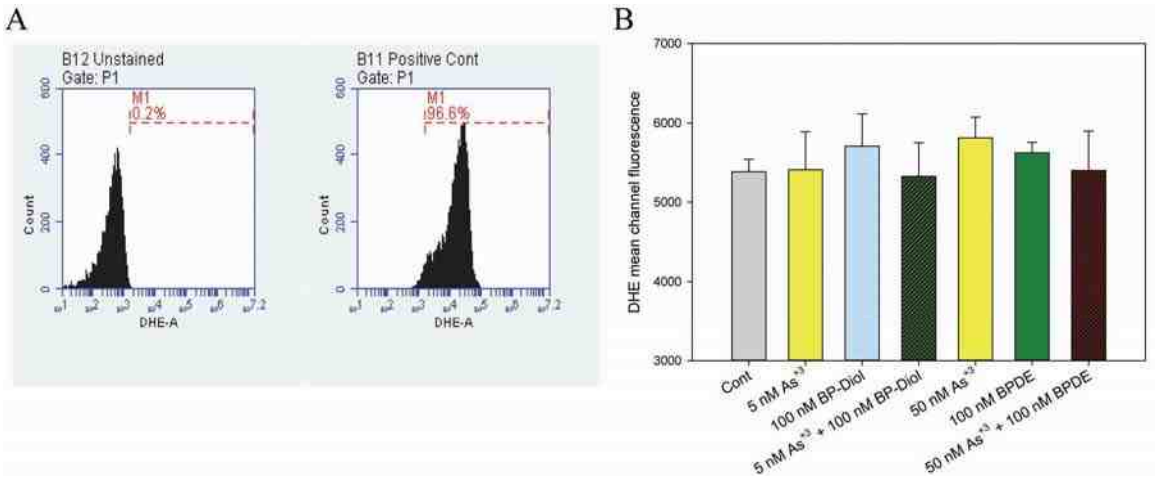

Figure 5.4. . DHE staining in primary thymus cells treated with As^{+3}, BP-diol/BPDE and the combinations *in vitro.* Primary thymus cells isolated from C57BL/6J male mice were exposed to 5 or 50 nM As^{+3}, 100 nM BP-diol or BPDE and the combinations for 18 h *in vitro*. A, flow cytometry results showing unstained cells and positive control (100 μM H_2O_2 for 10 min). B, DHE mean channel fluorescence.

Interactive effects on DNA damage were induced by As^{+3} direct PARP inhibition

To further test our hypothesis that As^{+3} induced interactive genotoxicity with BP-diol/BPDE by PARP inhibition, we utilized a potent specific PARP inhibitor, DPQ (Suto et al., 1991), to treat primary thymus cells together with BP-diol/BPDE *in vitro* for 18 h. A significant increase in DNA damage was observed in cells treated with 1 μM DPQ + 100 nM BP-diol and 1 μM DPQ + 100 nM BPDE (Fig. 5.5), indicating that PARP inhibition is associated with a synergistic increase in DNA damage produced by BP-diol/BPDE.

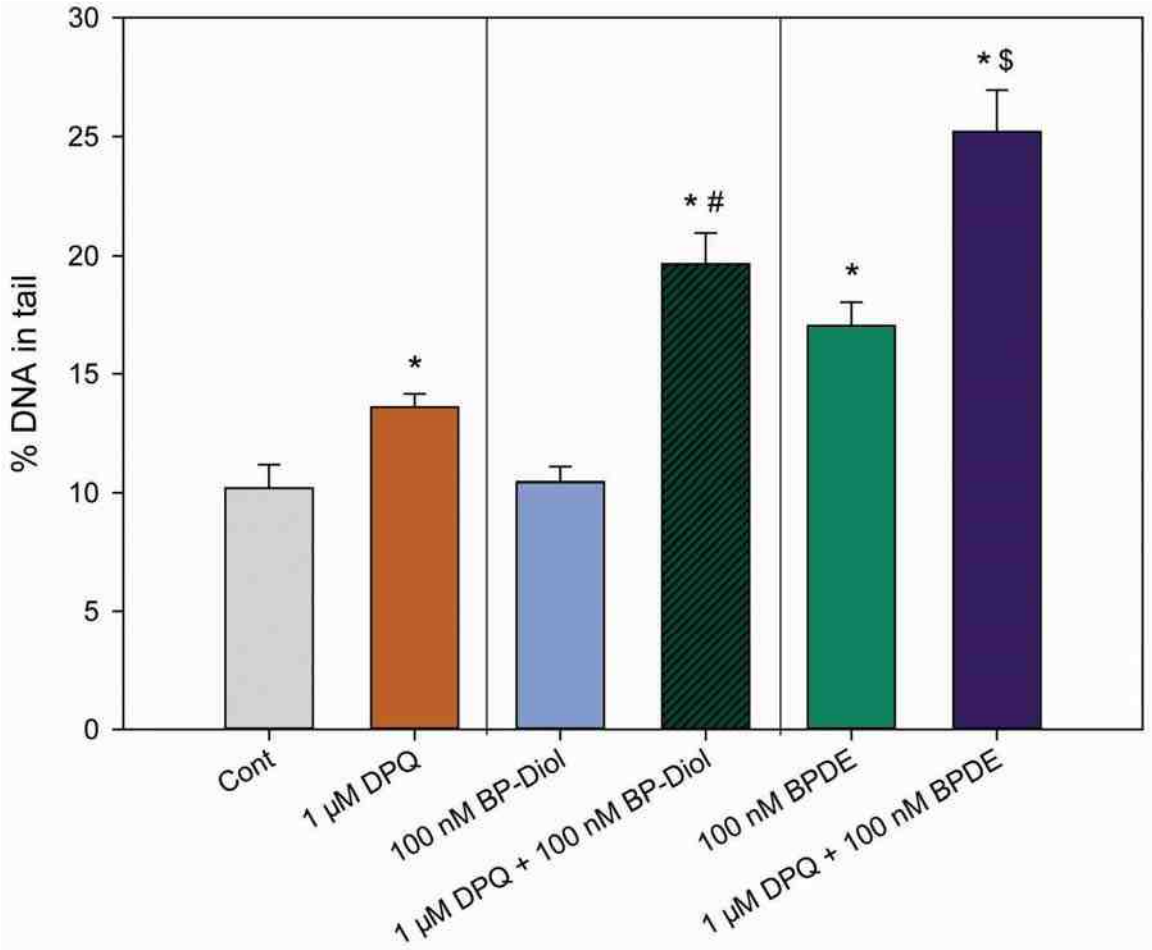

Figure 5.5. DNA damage in primary thymus cells treated with DPQ (a known PARP inhibitor), BP-diol/BPDE and the combinations *in vitro* for 18 h. Primary thymus cells isolated from C57BL/6J male mice were exposed to 1 µM DPQ, 100 nM BP-diol or BPDE and the combinations for 18 h *in vitro*. DNA damage was measured by percentage of DNA in tail using alkaline Comet assay *Significantly different compared to control ($p<0.05$). # Synergistic effect compared to 1 µM DPQ and 100 nM BP-diol (CDI > 1). $ Synergistic effect compared to 1 µM DPQ and 100 nM BPDE (CDI > 1). Results are Means ± SD.

CYP1A1 and CYP1B1 RNA expressions and activities were altered by As^{+3} and BP-diol/BPDE co-exposures

The metabolism of BaP and BP-diol is dependent on CYP1A1 and CYP1B1. In order to see if the co-exposures might affect the metabolism of BaP, primary thymus cells were treated with As^{+3}, BP-diol/BPDE and the combinations for 18 h *in vitro*. Expression of CYP1A1 and CYP1B1 was analyzed by qPCR. We found that As^{+3} increased the expression of CYP1A1 and CYP1B1 only when combined with BP-diol (Fig. 6A and 6B). Interestingly, BPDE (100 nM) decreased the expression of CYP1A1 and CYP1B1 when combined with 50 nM As^{+3} (Fig. 5.6A and 5.6B). The induction of CYP1A1 and CYP1B1 suggests that As^{+3} may also increase BPDE adduct formation by BP-diol through enzyme induction, which is also supported by a trend of increase of BPDE adduct formation measured by a chemiluminescence immunoassay in As^{+3} and BP-diol 18 h co-treatment. In order to confirm the activities of CYP1A1 and CYP1B1 were altered by these combined treatments, a luminescent CYP1A1/1B1 activity assay was performed using a prolyciferin CYP1A1/1B1 common substrate-Luciferin-CEE. Again, significant increase of CYP1A1/1B1 activity was observed in 5 nM As^{+3} and 100 nM BP-diol combined treatments, and 50 nM As^{+3} + 100 nM BPDE decreased the activity (Fig. 5.7), indicating the alteration of CYP1A1 and CYP1B1 mRNA expression did affect their activities.

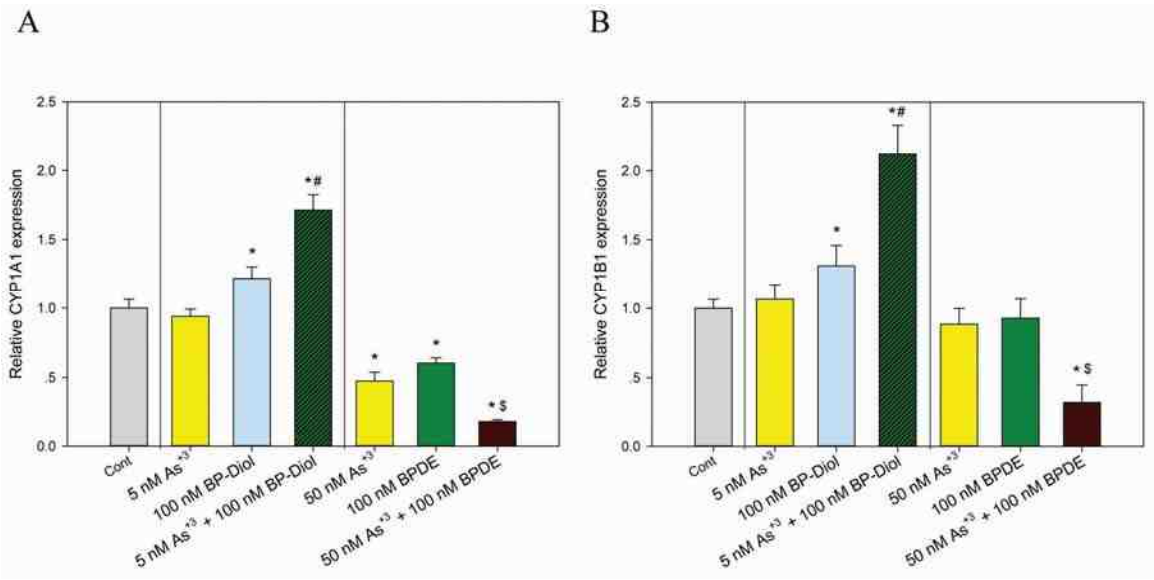

Figure 5.6. mRNA expression of CYP1A1 and CYP1B1 in primary thymus cells treated with As^{+3}, BP-diol/BPDE and the combinations *in vitro*. Primary thymus cells isolated from C57BL/6J male mice were exposed to 5 or 50 nM As^{+3}, 100 nM BP-diol or BPDE and the combinations of As^{+3} and BP-diol/BPDE for 18 h *in vitro*. Expression of CYP1A1 and CYP1B1 were examined by RT-qPCR. A, CYP1A1 expression. B, CYP1B1 expression. *Significantly different compared to control ($p<0.05$). # Synergistic effect compared to 5 nM As^{+3} and 100 nM BP-diol (CDI > 1). $ Synergistic effect compared to 50 nM As^{+3} and 100 nM BPDE (CDI > 1). Results are Means ± SD.

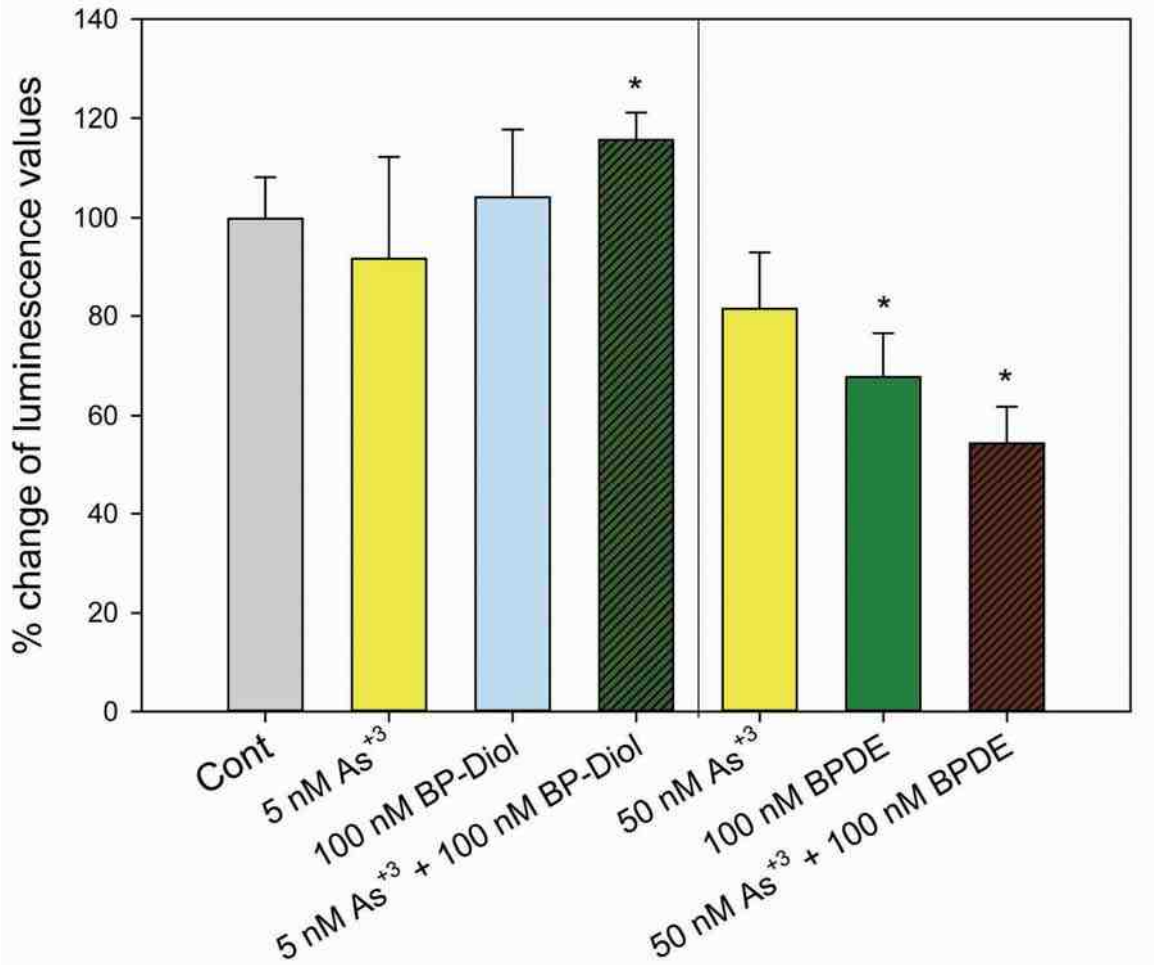

Figure 5.7. CYP1A1/1B1 activities in primary thymus cells treated with As^{+3}, BP-diol/BPDE and the combinations *in vitro*. Primary thymus cells isolated from C57BL/6J male mice were exposed to 5 or 50 nM As^{+3}, 100 nM BP-diol or BPDE and the combinations of As^{+3} and BP-diol/BPDE for 18 h *in vitro*. CYP1A1/1B1 activities were examined using a Luciferin substrate. After 3 h incubation, the Luciferin substrate was added and luminescence was measured. Data was presented as % of changes in luminescence compared to Cont. *Significantly different compared to control ($p<0.05$).

DISCUSSION

Environmental exposures to As^{+3} and PAHs such as BaP are common and are known to produce adverse health effects in millions of people throughout the world. The interactions between these chemicals and related family members have not been well studied. BaP and its metabolites are known to cause DNA damage through DNA adduct formation that induce strand breaks (Hockley et al., 2007). Our previous reports indicated that As^{+3} induces genotoxicity in mouse primary thymus cells at environmentally relevant levels through PARP inhibition associated with DNA repair which may lead to immunotoxicity (Xu et al., 2016). Since many people are co-exposed to PAHs and arsenic, it is important to understand their potential mechanism(s) of interaction.

Previous studies on the interactions between BaP and As^{+3} have shown that As^{+3} potentiates BaP toxicity (Lewińska et al., 2007; Maier et al., 2002). However, these studies were conducted at high concentrations that exceeded those expected to result from environmental exposures. Our previous studies demonstrated that DBC is a strong immunosuppressant of murine spleen cells (Lauer et al, 2015), and that As^{+3} interacts with DBC at extremely low concentrations to suppress mouse bone marrow pre-B cells (Ezeh et al., 2015). In the present study, the interactions between As^{+3} and the metabolites of BaP on genotoxicity in mouse thymus cells were analyzed within the nanomolar range of exposure, which are more representative of environmental exposures.

PARP is the initiator of base excision repair of DNA damage. Inhibition of PARP is known to cause DNA damage during cell replication (Dale Rein et al., 2015). Based on our previous findings on genotoxicity of arsenic and PAHs (Harper et al., 2015; Li et

al., 2010; Xu et al., 2016), we proposed that As^{+3} potentiates the DNA damage induced by PAHs through PARP inhibition. Our preliminary experiments revealed that certain PAHs did not interact with low concentrations of As^{+3}, which might have been due to their ability to inhibit PARP activity on their own (data not shown). Therefore, we screened different PAHs for their ability to inhibit PARP, and the results indicated that some PAHs (such as DBC, 3-MC, DMBA, and DAC) can inhibit PARP activity (Fig. 5.1). We selected the BaP family in subsequent studies based on the lack of PARP inhibition by its two metabolites (BP-diol and BPDE) and their environmental relevance. The inhibition of PARP by DBC, 3-MC, DAC and DMBA confounds the ability to see their interactive effects based on DNA damage alone. We did not investigate the mechanism(s) of inhibition of PARP by these PAHs in the present study. Further mechanistic studies need to be conducted in order to form a complete picture of the genotoxicity induced by certain PAHs and their potential interactions with As^{+3}.

CYP1A1 and CYP1B1 are essential for the metabolism of BaP and BP-diol to BPDE. Previous studies on the effect of arsenic on CYP1A1 and CYP1B1 expression have yield mixed results. Some studies showed that As^{+3} diminished CYP1A1 and CYP1B1 induction in breast cancer cells *in vitro* (Spink et al., 2002), while others revealed that As^{+3} could increase their expression by AhR induction in lung cells after *in vivo* exposure (Wu et al., 2009). In our study, we showed differential effects of As^{+3} + BP-diol and As^{+3} + BPDE (Fig. 5.6A and 5.6B). It is very interesting that As^{+3} potentiated CYP1A1 and CYP1B1 expression following the co-treatment with 100 nM BP-diol at 5 nM As^{+3}. BP-diol is known to be an agonist of the AhR (Chen et al., 2003), but the mechanism by which As^{+3} increases CYP1A1 and CYP1B1 in thymus cells is

unknown and needs to be identified in future studies. Also, we found a trend of increase in BPDE adduct formation in thymus cells treated with low concentrations of As^{+3} and BP-diol (Supplementary Fig. 1), using a highly sensitive chemiluminescence immunoassay (Divi, et al., 2002). Therefore, it is likely that low concentrations of As^{+3} induce interactive genotoxicity with BP-diol not only by inhibiting DNA repair, but also by increasing the formation of DNA adducts resulting from the conversion of BP-diol to BPDE.

The decrease in expression of CYP1A1 and CYP1B1 that occurred following co-treatments with As^{+3} and BPDE may be the result of apoptosis. We found that low concentrations of As^{+3} and BP-diol/BPDE produced apoptosis following co-treatments, which correlated with an increase in DNA damage (Fig. 5.2A and 5.3A). The concentrations of As^{+3} and BP-diol/BPDE used in our study were very low and had limited cytotoxicity on their own. However, the fact that As^{+3} and BP-diol/BPDE co-treatments induced significant apoptosis in primary thymus cells at such low concentrations is significant.

In summary, As^{+3} potentiates the DNA damage induced by the metabolites of BaP at environmentally relevant concentrations through PARP inhibition. Interactive genotoxicity and apoptosis were observed at low concentrations of As^{+3} in combination with BP-diol/BPDE. The induction of CYP1A1 and CYP1B1 expression by As^{+3} and BP-diol may play a partial role in the synergistic genotoxicity found in these studies. These findings show that As^{+3} and certain PAHs may interact with thymus cells at extremely low concentrations. These interactions should be considered in the assessment of risk associated with human exposures.

FUNDING

This work was funded by National Institute of Environmental Health Sciences by grant number R01 ES019968.

ACKNOWLEDGEMENT

We would like to thank Dr. Regina. M Santella at Columbia University Mailman School of Public Health for analyzing the BP adducts.

CHAPTER 6

Efflux Transporters Regulate Arsenite Induced Genotoxicity in Double Negative and Double Positive T Cells

Huan Xu[a], Sebastian Medina[a], Fredine T. Lauer[a], Christelle Douillet[b], Ke Jian Liu[a], Laurie G. Hudson[a], Miroslav Stýblo[b], Lauren M. Aleksunes[c], and Scott W. Burchiel[a d]

[a]The University of New Mexico College of Pharmacy, Department of Pharmaceutical Sciences, Albuquerque, NM 87131

[b]Department of Nutrition, Gillings School of Global Public Health, University of North Carolina at Chapel Hill, Chapel Hill, NC 27516

[c]Rutgers, The State University of New Jersey, Ernest Mario School of Pharmacy, Department of Pharmacology and Toxicology, Piscataway, NJ 08854

[d]To whom correspondence should be addressed. Fax: (505) 272-6749. Email: sburchiel@salud.unm.edu

ABSTRACT

Arsenite (As^{+3}) exposure is known to cause immunotoxicity in human and animal models. Our previous studies demonstrated that As^{+3} at low concentrations induced both genotoxicity and non-genotoxicity in mouse thymus cells. Developing T cells at CD4-CD8- double negative (DN) stage, the first stage after early T cells are transported from bone marrow to thymus, were found to be more sensitive to As^{+3} toxicity than the T cells at CD4+CD8+ double positive (DP) stage *in vitro*. Induction of Mdr1 (*Abcb*1) and Mrp1 (*Abcc*1), two multidrug resistance transporters and exporters of As^{+3}, was also associate with the reversal of As^{+3} induced double strand breaks and DNA damage. In order to confirm the differential sensitivities of thymic cell populations to As^{+3} *in vivo*, male C57BL/6J mice were exposed to 0, 100 and 500 ppb As^{+3} in drinking water for 30 d. A significant decrease in DN cell percentage was observed with exposure to 500 ppb As^{+3}. Low concentrations of As^{+3} were also shown to induce higher genotoxicity in sorted DN cells than DP cells *in vitro*. Calcein AM uptake and Mdr1/Mrp1 mRNA quantification results revealed that DN cells not only had limited As^{+3} exporter activity, but also lacked the ability to activate these exporters with As^{+3} treatments, resulting in a higher accumulation of intracellular As^{+3}. Knockdown study of As^{+3} exporters in the DN thymic cell line, D1 using siRNA, demonstrated that Mdr1 and Mrp1 regulate intracellular As^{+3} accumulation and genotoxicity. Taken together, the results indicate that transporter regulation is an important mechanism for differential genotoxicity induced by As^{+3} in thymocytes at different developmental stages.

INTRODUCTION

Arsenic (As) contamination of food and drinking water affects millions of people world-wide. Arsenite (As^{+3}) is a prevalent trivalent inorganic form of As in the environment. As^{+3} exposure has been associated with multiple diseases such as diabetes, cardiovascular diseases and cancers (Argos et al., 2010; Schuhmacher-Wolz et al., 2009;Vahter et al., 2008). The immunosuppression caused by As^{+3} exposure in humans and animal models has been reported by multiple groups (Gonsebatt et al., 1994; Soto-Pena et al., 2006; Biswas, et al., 2008; Kozul et al., 2009). Many studies have demonstrated that As^{+3} has detrimental effects on different types of immune cells (Ezeh et al., 2015; 2016; Sakurai et al., 2006). The thymus is the primary immune organ for the development of T cells, which are key in both humoral and the cell-mediated immunity. During development in thymus, T cells undergo changes in surface marker expression that allow us to recognize distinct subsets: double negative (CD4-CD8-, DN), double positive (CD4+CD8+, DP) and single positive (CD4+ or CD8+, SP) (Germain, 2002). Epidemiological studies have indicated that children exposed to low levels of As^{+3} *in utero* have impaired thymic function and reduced numbers and types of peripheral T cells (Ahmed et al., 2012).Thymic atrophy and cell cycle arrest have also been observed in mice exposed to As^{+3} *in viv*o (Nohara et al., 2008; Schulz et al., 2002). These studies highlight the necessity for gaining an understanding of the mechanisms of As^{+3} induced toxicities in the thymus.

Our previous studies have demonstrated that As^{+3} at environmentally relevant concentrations can induce DNA damage in mouse thymus cells through the inhibition of poly ADP ribose polymerase (PARP) activity as well as the generation of oxidative stress (Xu et al., 2016d). PARP has a DNA binding domain that contains two zinc (Zn) fingers. As^{+3} is known to cause functional impairment of PARP by replacing the Zn on the Zn fingers (Qin et al., 2012; Sun et al., 2014; Zhou et al., 2011, 2014). Studies have indicated that the dual actions of As^{+3} also include the induction of oxidative stress at higher concentrations (Ding et al., 2009; Qin et al., 2008), which was confirmed in our mouse thymic cell model *in vitro* at a 500 nM As^{+3} concentration (Xu et al., 2016d). Previous studies in our laboratory have also demonstrated that immune cells are extremely sensitive to As^{+3} treatments (Burchiel et al., 2014; Ezeh et al., 2014; Li et al., 2010; Xu et al., 2016b). We have also described the differential sensitivities of mouse peripheral lymphoid organs and tissues to As^{+3} (Xu et al., 2016c). Therefore, understanding the mechanism of the differential sensitivity of different types of immune cells is important for evaluating As^{+3} induced immunotoxicity.

As^{+3} enters cells via the aquaglyceroporins (AQP3, AQP7, AQP9, AQP10), the glucose permeases (GLUT1, GLUT2, GLUT5), and the organic anion transporting polypeptides (OATP1B1, OATP2B1) (Maciaszczyk-Dziubinska et al., 2012). Multidrug resistance protein, Mdr1 (ABCB1, P-glycoprotein 1), and multidrug resistance-associated proteins, Mrp1 (ABCC1) and Mrp2 (ABCC2), are the known exporters of As^{+3} in eukaryotic cells. Many studies have indicated that the over-expression of Mdr1, Mrp1 and Mrp2 is responsible for As^{+3} resistance in certain type of cells (Liu et al., 2001; Liu et al., 2002). In our previous studies, we demonstrated that up-regulation of Mdr1 and

Mrp1 in a thymic T cell line, D1, decreased oxidative DNA damage (Xu et al., 2016d). Therefore, these ATP binding cassette subfamily transporters may be the key factors that regulate the toxicity induced by As^{+3}.

Our previous studies demonstrated that DN cells are more prone to As^{+3} induced toxicity than DP cells *in vitro* (Xu et al., 2016a). In the present study, the genotoxicity induced of As^{+3} in DN and DP cells was analyzed and compared. We also examined differences in the expression of As^{+3} exporters between DN and DP cells and studied the roles of these exporters in the regulation of As^{+3} induced genotoxicity in thymus cells.

MATERIALS AND METHODS

Chemicals and reagents

Sodium arsenite (CAS 774-46-5, Cat. No. S7400, Purity > 90%), Dulbecco's phosphate buffered saline w/o Ca^{+2} or Mg^{+2} ($DPBS^{-}$), RPMI 1640 HEPES modified medium , dimethylsulfoxide (DMSO, Cat. No. D2650) and β-Mecaptoethanol (2-ME, Cat. No. M3148) were purchased from Sigma-Aldrich (St. Louis, MO). Hanks Balanced Salt Solution (HBSS) was purchased from Lonza (Walkersville, MD). Fetal Bovine Serum (FBS) was purchased from Atlanta Biologicals (Flowery Branch, GA). CometAssay® 20 well ES starter kit (Cat. No. 4252-040-ESK) was purchased from Trevigen (Gaithersburg, MD). RNeasy Mini Kit™ and QIAshredder™ were purchased from Qiagen (Valencia, CA). Penicillin/Streptomycin 10,000 (U/ml and 10,000 (μg/mL)), 200 mM L-Glutamine, Dihydroethidium (DHE, Cat. No. D11347), high capacity cDNA reverse transcription kit (Cat. No. 4368814), Gapdh (Mm99999915_g1), Mdr1a (Mm00440761_m1), Mdr1b (Mm00440736_m1), Mrp1 (Mm00456156_m1), Mrp2 (Mm00496899_m1), Nrf2 (Mm00477784_m1), Hmox1 (Mm00516005_m1) TaqMan® gene expression assays and TaqMan® universal PCR master mix (Cat. No. 4304437) were purchased from Life Technologies (Grand Island, NY). Recombinant murine IL-7 (Cat. No. 217-17) was purchased from Peprotech (Rocky Hill, NJ). Mdr1 (Cat. No. sc-35891), Mrp1 (Cat. No. sc-35961), scrambled negative control (Cat. No. sc-37007) and FITC-conjugated positive control (Cat. No. sc-36869) siRNAs were purchased from Santa Cruz Biotechnology (Dallas, TX). Accell siRNA delivery media (Cat. No. B-005000-500) was purchased from Dharmacon (Lafayette, CO). FITC rat anti-

mouse CD8a (Cat. No.553031), PE rat anti-mouse CD8 (Cat. No.553033), PE rat anti-mouse CD4 (Cat. No. 553730) and APC rat anti-mouse CD4 (Cat. No.553051) antibodies were purchased from BD Biosciences (San Jose, CA). EasySep™ PE positive selection kit (Cat. No. 18557) was purchased from STEMCELL Technologies (Cambridge, MA). Cellometer staining solution, acridine orange/propidium iodide (AO/PI) staining (Cat. No. CS2-0106-5ML) was purchased from Nexcelom Bioscience (Manchester, UK). Calcein acetoxymethyl ester (Calcein AM, Cat. No.14948), Verapamil (Cat. No. 14288), and MK-571 (Cat. No. 10029) were purchased from Cayman Chemical (Ann Arbor, MI).

Animal exposures and primary mouse thymus cells isolation

C57BL/6J male mice were purchased from Jackson Laboratory (Bar Harbor, ME) at 8-10 weeks age. Experiments or treatments were performed after at least one week of acclimation in our animal facility. All animal experiments were performed following the protocols approved by the Institutional Animal Use and Care Committee at the University of New Mexico Health Sciences Center. For *in vivo* experiments, 2-3 mice (5 per group) were housed per cage and exposed to As^{+3} at 0 (control), 100 or 500 ppb via drinking water for 30 d. Mice were fed with 2020X Teklad global soy protein-free extruded rodent diet (Envigo, Indianapolis, IN) throughout the experiment. As^{+3} doses were prepared fresh weekly by weighing each water bag and determining the appropriate amount of As^{+3} stock to add to each bag. Water bags were weighed after each weekly collection and the change in weight was used to estimate the amount of water consumed by mice in each cage. Concentrations of As^{+3} in drinking water bags were verified using Mass Spectrometry by Dr. Abdul-Mehdi S. Ali at Department of Earth and Planetary Sciences, University of New Mexico. Mice were euthanized after 30 d exposure or on the day of *in*

vitro experiment. Thymuses were harvested and transferred to the laboratory on ice in HBSS on ice. Single cell suspensions of spleen and thymus cells were prepared by homogenizing the organ between the frosted ends of two sterilized microscope slides into a dish containing 5 mLof cold mouse medium (RPMI 1640 with 10% FBS, 2 mM L-glutamine, 100 units/mL penicillin and 100 µg/mL streptomycin). For *in vitro* experiments, cell suspensions from 3 mice were pooled. Cells were then centrifuged at 200 x *g* for 10 min and resuspended in fresh mouse medium. Cell numbers and viabilities were determined by AO/PI staining and counting using the Nexcelom Cellometer 2000.

CD4, CD8 and DHE staining

DHE was resuspended with 158 µl DMSO and diluted to a final concentration of 5 µM with $DPBS^-$. 1 x 10^6 cells were washed with $DPBS^-$, resuspended in 100 µl of 5 µM DHE solution and stained with 0.5 µg of APC-conjugated anti-CD4 and FITC-conjugated anti-CD8 antibodies for 30 min in a 37 °C incubator. Cells were washed twice with $DPBS^-$ before analysis on an AccuriC6 Flow Analyzer (BD Bioscences).

DN cell enrichment and cell sorting

In order to yield enough DN cells for our experiments, an aliquot of the isolated thymus cells were concentrated to 1 x 10^8 cells/mL in mouse medium and stained with 2 µg/mL PE-conjugated anti-CD4 and PE-conjugated anti-CD8 antibodies for 15 min at RT. 100 µl of PE selection cocktail was then added to 1 mL of cell suspension. After 15 min RT incubation, 50 µl of magnetic nanoparticles was added to the cell suspension and mixed by pipetting followed by a 10 min incubation at RT. Then cell volumes were brought up to 2.5 mL by adding $DPBS^-$ containing 2% FBS and 1 mM EDTA. Tubes

were then placed into the magnet for 5 min and cells that remained in suspension (DN cells) were collected into a fresh tube. Enriched DN cells and the remaining total thymus cells were stained with 2 μg/mL FITC-conjugated anti-CD8 and APC-conjugated anti-CD8 in mouse medium and DN and DP cells were sorted on an iCyt SY3200 cell sorter (Sony, San Jose, CA) at 15,000 events/s to achieve >99% purity. The enrichment step with magnetic nanoparticles increased the efficiency of getting DN cells by approximately twenty times.

The single cell gel electrophoresis assay (Comet assay)

Cells were washed with $DPBS^-$ and resuspended at 1 x 10^6 cells/mL in $DPBS^-$. 30 μl of cells were placed into a 1.5 mL microcentrifuge tube containing 250 μl low melting point agarose at 37 °C and then each sample was applied to a one well of a 20-well CometSlide™ (Trevigen). After the agarose was solidified, cells were lysed overnight with Lysis Solution + 10% DMSOl The following day the slide was electrophoresed in ice cold alkaline buffer with 1 mM EDTA (pH>13) at 21 volts for 30 min. Slides were dried, stained with Sybr Gold and imaged with an Olympus IX70 inverted fluorescence microscope. 50 cells from each well of the slides were scored using CometScore (TriTek Corp., Sumerduck, VA).

Oxidation state specific Hydride Generation- Cryotrapping- Inductively Coupled Plasma- Mass Spectrometry

The analysis of As species by HG-CT-ICP-MS was performed as previously described (Currier et al., 2014; Matoušek et al., 2013). Briefly, cell pellets were lysed in ice-cold deionized water. The trivalent species were measured in an aliquot of cell lysate directly. Another aliquot was treated with 2% cysteine and analyzed for total inorganic

As (As^{+3} and As^{+5}), total methyl-As (MMA^{+3} and MMA^{+5}), and total DMAs (DMA^{+3} and DMA^{+5}). Cysteine-treated pentavalent As standards were used for calibration as previously described (Hernández-Zavala et al., 2008). The LODs for As species analyzed by HG-CT-ICP-MS ranged from 0.04 pg As for methylated arsenicals to 2.0 pg As for inorganic arsenicals. All values were expressed as pg of As in an arsenic species.

RNA isolation and qPCR

RNA isolation was performed on mouse thymus cells following the manual of the RNeasy Mini Kit ™ and QIAshredder™ from the manufacturer. An Agilent Nanodrop spectrophotometer (Santa Clara, CA) was used to quantify the concentrations of extracted RNA in each sample. 60 µl mixed solution containing a minimum of 1080 ng RNA was reverse transcribed (RT reaction) on SimpiAmps thermal cycler (Life Technologies) using the high capacity cDNA reverse transcription kit. Samples were then diluted to ~6 ng/ µl with RNase, DNase free water and stored at -20 °C. Real time PCR (qPCR) reactions were performed in 10 µl per reaction in a 384-well plate with TaqMan® gene expression assays of GAPDH, Mdr1a, Mdr1b, Mrp1, Mrp2, Nrf2 and Hmox1 probes on a Applied Biosystems ViiA™ 7 Real-Time PCR System (Life Technologies). Comparative C_T (first amplification cycle exceeding threshold) was applied for quantification, and GADPH was used as the endogenous control. The method to calculate the comparative C_T is described in detail in the manual from Life Technologies.

Calcein AM uptakessay

The calcein AM assay was performed according to the uptake assay procedures previously described (Bircsak et al., 2013; Olson et al., 2001; Udasin et al., 2016). Briefly, calcein AM was added into 1 x 10^6 mouse thymus cells in 1 mL of 37 °C pre-

warmed mouse medium to a final concentration of 50 nM. Samples were incubated at 37 °C in the dark for 30 min with or without 20 μM Verapamil (Mdr1 inhibitor) or 50 μM MK-571 (Mrps inhibitor). For cell subset differentiation, cells were then washed and resuspended in 100 μl cold $DPBS^-$, stained with 0.5 μg of APC-conjugated anti-CD4 and PE-conjugated anti-CD8 antibody for 30 min on ice in the dark. After two washes with cold DPBS-, cells were analyzed on an AccuriC6 Flow Analyzer (BD Bioscences).

Mdr1, Mrp1 siRNA knockdown in D1 cells

The D1 cell line was a gift from Dr. Scott K. Durum (Center for Cancer Research, NIH, Frederick, MD). The D1 cell line is a CD4-CD8-, IL-7 dependent early T cell line established from p53 knockout mouse thymocytes (Kim et al., 2003). As previously described, cells were maintained in mouse medium with 55 μM 2-ME and 50 ng/mL IL-7 and sub-cultured every three days (Xu et al., 2016a). For siRNA knockdown experiments, D1 cells were resuspended in siRNA delivery medium (Accell siRNA delivery media + 2% FBS + 50 ng/mL IL-7) at 2 x 10^5 cells/mL with mouse Mrp1, mouse Mdr1, scrambled or FITC-labeled scrambled control siRNA at 20 nM concentration and incubated in 37 °C, 5% CO_2 humidified incubator for 52 h as previously described (Ruppert et al., 2012). Cells were then re-plated into a 6 well plate in mouse medium with 55 μM 2-ME and 50 ng/mL IL-7, treated with As^{+3} at 50 and 500 nM concentrations for 18 h.

Statistics

Excel 2010 and Sigma Plot 12.5 software were used for data analysis. One-way analysis of variance (ANOVA) followed by a Dunnett's Method (multiple comparisons versus control group) were used to determine differences between control and treatment

groups. For the *in vivo* As^{+3} experiments, 5 animals (n=5) were assigned to each group. Three independent experiments were conducted and comparable results were acquired. For the *in vitro* experiments, three replicates were performed and analyzed for each dose.

RESULTS

Selective toxicity in DN cells population after *in vivo* As^{+3} exposure

Previous studies in our lab demonstrated As^{+3} treatments selectively decreased DN cell percentage *in vitro* (Xu et al., 2016a). In order to see whether DN cells are more sensitive to As^{+3} *in vivo*, 9-week old male C57BL/6J mice were exposed to 0, 100 and 500 ppb As^{+3} for 30 d via drinking water. Thymus cells were isolated and stained with CD4 and CD8 cell surface markers and analyzed on a flow cytometer. A significant decrease in DN cell percentage was observed at 500 ppb (Fig. 6.1A). There was no change in DP cell percentage (Fig. 6.1B). We also calculated the total cell number of each population using the total thymus cell recovery from each individual mouse to determine if the absolute cell numbers in the DN and DP populations were affected. Although significant decreases in total cell numbers were observed in both DN and DP cells (Fig. 6.1C and 6.1D), the decrease in DN cells was higher than in DP cells. These results indicated that As^{+3} exposure *in vivo* selectively reduced DN cell percentage, which resulted in an overall decrease of the cell numbers at later stage.

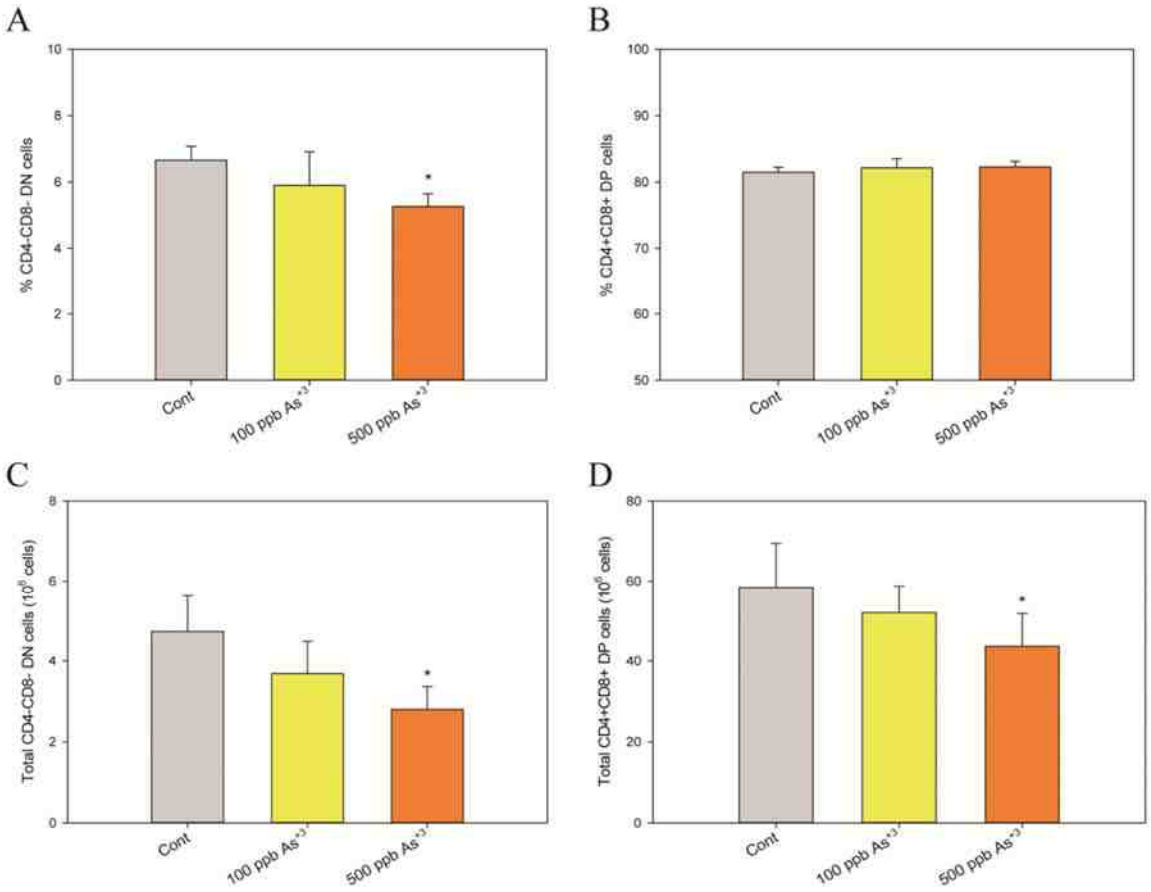

Figure 6.1. DN and DP percentage of cells and cell numbers from 30 d As^{+3} drinking water-exposed mice. 9-week old male C57BL/6J mice were exposed to 0, 100 and 500 ppb As^{+3} through drinking water for 30 d. Thymus cells were isolated, stained with CD4 and CD8 surface markers, and analyzed on a flow cytometer. A, % of DN cells in thymus cells. B, % of DP cells in thymus cells. C, total DN cell numbers (% of DN cells x total cell recovery). D, total DP cell numbers (% of DP cells x total cell recovery). * Significantly different compared to control ($p<0.05$, $n=5$). Results are Means ± SD.

DN cells were more sensitive to As^{+3} induced genotoxicity and oxidative stress than DP cells *in vitro*

The selective reduction of DN cell percentage was observed both *in vitro* and *in vivo*. In order to see if As^{+3} induces higher genotoxicity in DN cells than DP cells, primary thymus cells from four12-week old male C57BL/6J mice were isolated, pooled and sorted into the DN and DP cell populations (Fig. 6.2A). DN, DP and un-sorted thymus cells were treated with 0 (control), 50 and 500 nM As^{+3} for 18 h *in vitro*. Cell viability was examined using AO/PI staining, and DNA damage was analyzed by Comet assay. A significant decrease in cell viability was only observed at 500 nM As^{+3} treatment for DN cells (Fig. 6.2B). A dose-dependent increase of DNA damage was observed in DN cells starting at 50 nM (Fig. 6.2C), indicating that DN cells are more prone to As^{+3} induced DNA damage. Oxidative stress in sorted DN and DP cells was measured by DHE staining on a flow cytometer and Hmox1 mRNA expression by qPCR. Dose-dependent increases in both DHE fluorescence and Hmox1 expression were observed in DN cells after 18 h *in vitro* treatments with As^{+3}(Fig 6.3A and 6.3B), which was more significant than in DP cells. The expression of Nrf2, the oxidative stress regulator, was also analyzed by qPCR. Up-regulation of Nrf2 was observed in both DN and DP cells only at 500 nM (Fig. 6.3C).

Previous studies in our lab indicated that higher genotoxicity was associated with greater intracellular As (Xu et al., 2016c). Therefore, we used HG- CT- ICP- MS system to determine the intracellular As^{+3} accumulation in DN and DP cells after *in vitro* treatments. More intracellular As^{+3} was observed in DN cells than DP cells with 18 h

treatments of 50 and 500 nM As^{+3} (Fig. 6.4), suggesting that the selective genotoxicity in DN cells may be the result of higher intracellular As^{+3} accumulation.

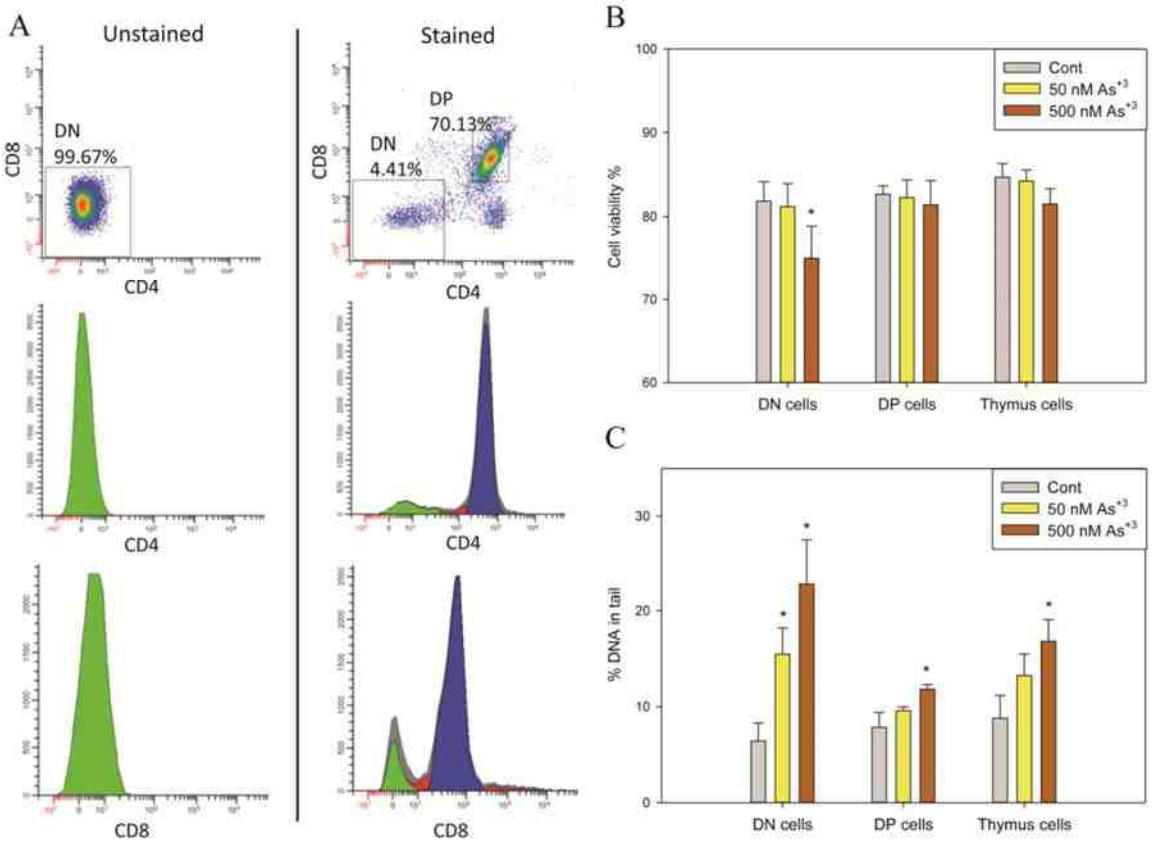

Figure 6.2. Viability and DNA damage in DN and DP cells after 18 h *in vitro* treatments with As^{+3}. Thymus cells were isolated from three 12-14 week old male C57BL/6J mice and pooled. Cells were enriched with STEMCELL EasySep™ PE positive selection kit, stained with CD4 and CD8 surface markers and sorted into DN and DP cell populations. Sorted cells were treated with 50 and 500 nM As^{+3} for 18 h *in vitro*. A, thymus cells were sorted into DN and DP cells. B, cell viability were measured by AO/PI staining. C, DNA damage was measured by alkaline Comet assay. * Significantly different compared to control ($p<0.05$). Results are Means ± SD.

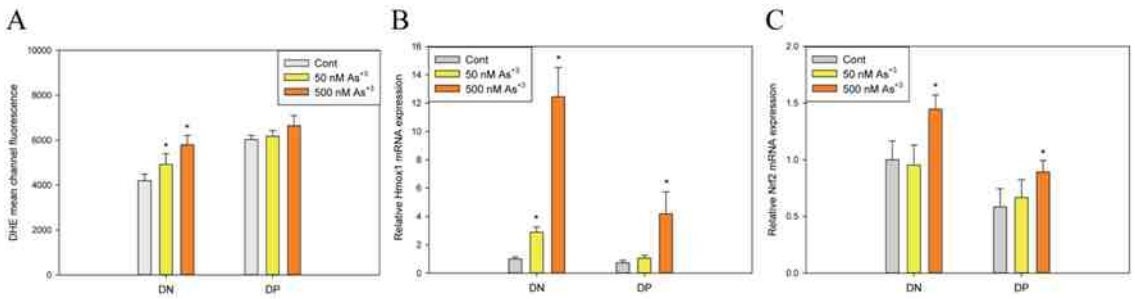

Figure 6.3. Oxidative stress in DN and DP cells treated with As^{+3} for 18 h *in vitro*. Thymus cells were isolated from three 12-14 week old male C57BL/6J mice, pooled, sorted into DN and DP populations and treated with 50 or 500 nM of As^{+3} for 18 h. A, superoxide production was measured by DHE mean channel fluorescence. B, Hmox1 mRNA expression was measured by qPCR. C, Nrf mRNA expression was measured by qPCR. * Significantly different compared to control ($p<0.05$). Results are Means ± SD.

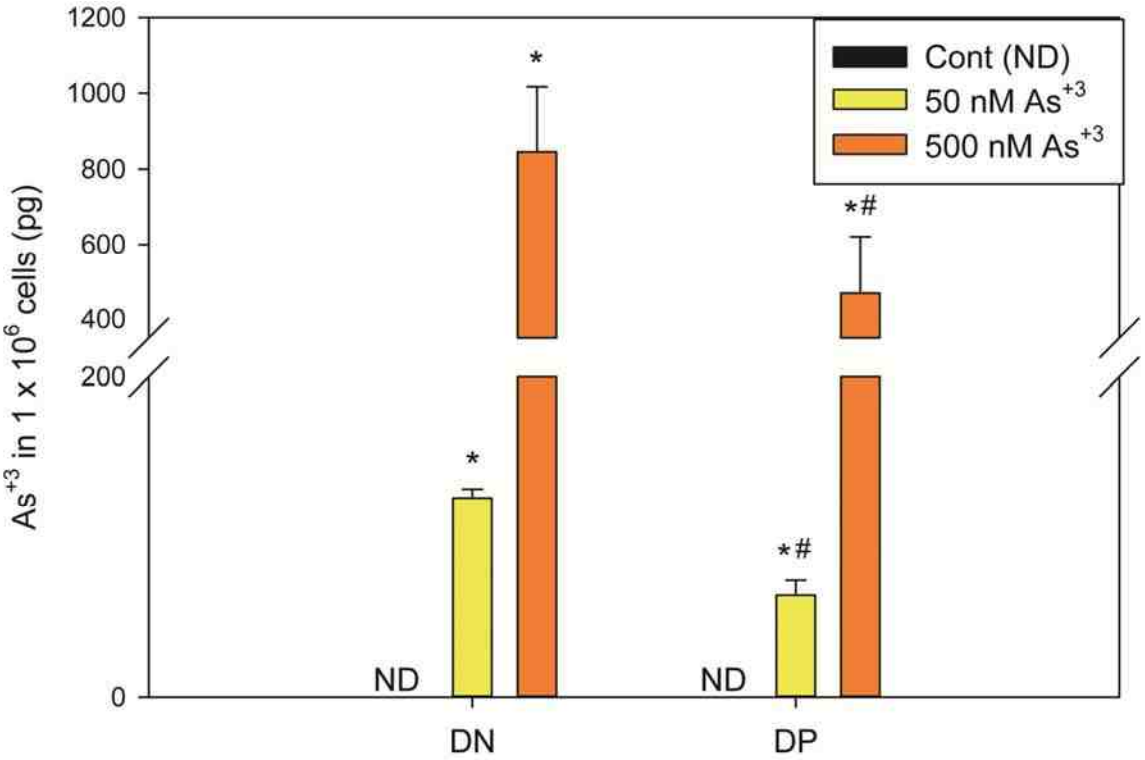

Figure 6.4. Intracellular As^{+3} concentrations in DN and DP cells treated with As^{+3} *in vitro* for 18 h. Thymus cells were isolated from three 12-14 week old male C57BL/6J mice, pooled, sorted into DN and DP populations and treated with 50 or 500 nM of As^{+3} for 18 h. Intracellular As^{+3} accumulation was measured by HG-CT-ICP-MS. ND, not detected. * Significantly different compared to control ($p<0.05$). # Significantly different compared to the relative dose in DN cells ($p<0.05$). Results are Means ± SD.

As^{+3} exporter mRNA expressions and activities in DN and DP cells after *in vitro* As^{+3} treatments

Mdr1 and Mrp1 are the exporters of As^{+3} in eukaryotic cells. Previous findings in our lab suggested that the up-regulation of Mdr1 and Mrp1 in mouse thymus cells treated with 500 nM As^{+3} decreased the oxidative stress and double strand breaks (Xu et al., 2016d). To examine whether the DN and DP cells have differential Mdr1 and Mrp1 expressions, sorted DN and DP cells were treated with 0, 50, and 500 nM As^{+3} for 18 h *in vitro*. Mdr1 (a and b) and Mrp1 expressions were analyzed by qPCR. Significant increase of Mrp1 expression was observed in DP cells starting from 50 nM (Fig. 6.5C). Although there was no significant increase in both Mdr1a and Mdr1b expression in DP cells, a slight decrease in both Mdr1a and Mdr1b expression was observed in DN cells at 500 nM (Fig. 6.5A and 6.5B). We also performed qPCR analysis on Mrp2 and did not see any amplification, indicating that Mrp2 is not expressed in early T cells (data not shown). These results suggested that DN and DP cells express different levels of the two As^{+3} exporters, especially with the treatments of As^{+3}.

The Calcein AM assay has been used to measure Mdr1 and Mrp1 activities (Evseenko et al., 2006; Oslon et al., 2001). We used the Calcein AM uptake assay to compare exporter activities in DN and DP cells and optimized the staining concentration to make it compatible with the surface marker staining. The Calcein mean channel fluorescence was higher in DN cells than in DP cells with or without As^{+3} treatment, suggesting that DN cells have lower exporter activities in general (Fig. 6.6). Treatment with 500 nM As^{+3} for 18 h significantly increased calcein fluorescence in DN cells and decreased calcein fluorescence in DP cells (Fig. 6.6B), indicating the differential patterns

of exporter activation in DN and DP cells with As^{+3} treatments. Overall, these results supported our hypothesis that Mdr1 and Mrp1 expressions and activations are different in DN and DP cells, which may be the reason for differential sensitivities to As^{+3} induced genotoxicity in the DN and DP cells.

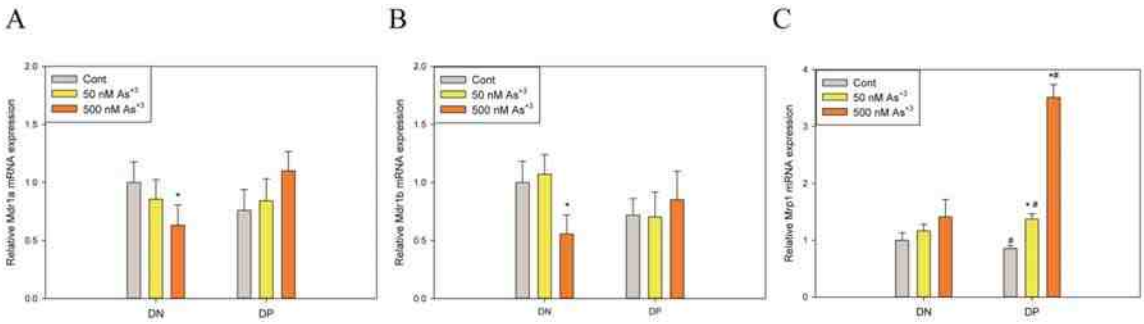

Figure 6.5. Mdr1a, Mdr1b and Mrp1 mRNA expression in DN and DP cells treated with As^{+3} *in vitro* for 18 h. Thymus cells were isolated from three 12-14 week old male C57BL/6J mice, pooled, sorted into DN and DP populations and treated with 50 or 500 nM of As^{+3} for 18 h. A, Mdr1a mRNA expression was measured by qPCR. B, Mdr1b mRNA expression was measured by qPCR. C. Mrp1 mRNA expression was measured by qPCR. *Significantly different compared to control ($p<0.05$). # Significantly different compared to the relative dose in DN cells ($p<0.05$). Results are Means ± SD.

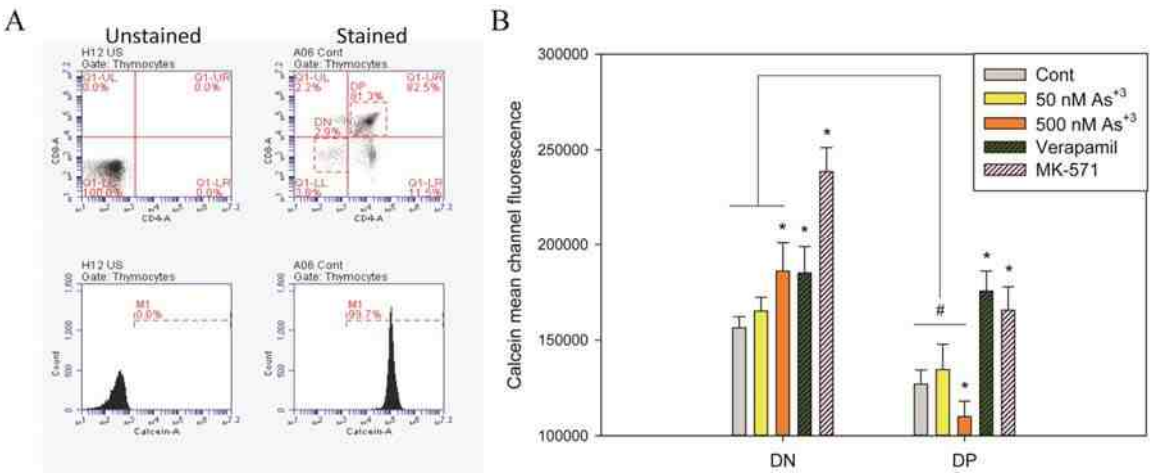

Figure 6.6. Calcein AM uptake in DN and DP cells treated with As^{+3} *in vitro* for 18 h. Thymus cells were isolated from three 12-14 week old male C57BL/6J mice, pooled, and treated 500 nM As^{+3}. Calcein AM uptake assay was used to measure the activity of exporters in DN and DP cells separated by CD4 and CD8 surface marker staining. A, Histogram of unstained and calcein stained cells. B, Calcein mean channel fluorescence in DN and DP cells after As^{+3} treatments. *Significantly different compared to control ($p<0.05$). # Significantly different compared to the relative dose in DN cells ($p<0.05$). Results are Means ± SD.

Knockdown of Mdr1 and Mrp1 increased As^{+3} induced genotoxicity *in vitro*

A mouse thymic DN T cell line, D1, was utilized to confirm whether the decreases in Mdr1 or Mrp1 expression affect the genotoxicity. D1 cells were cultured in siRNA delivery medium with Mdr1 or Mrp1 siRNA and the successful delivery of siRNA was confirmed (Fig. 6.7A). Significant increases calcein fluorescence was observed with both Mdr1 and Mrp1 siRNA knockdown (Fig 6.7B), indicating a suppression of exporter functions. Cells were also treated with As^{+3} for 18 h *in vitro*. Significant increase of intracellular As^{+3} was observed in both knockdowns (Fig. 6.7C), and there was no methylated forms of As in these cells. Interestingly, Mrp1 knockdown increased the intracellular As^{+3} accumulation more significantly than Mdr1 knockdown. These results suggested that the successful delivery of the siRNAs decreased the activities of exporters and lead to increased intracellular As^{+3} accumulation in D1 cells.

The siRNA knockdown of Mdr1 and Mrp1 at mRNA levels was analyzed by qPCR. A significant decrease in Mdr1 and Mrp1 mRNA expression was observed with Mdr1 and Mrp1 siRNA, and Mrp1 siRNA achieved a higher percentage of knockdown than Mdr1 siRNA (Fig. 6.8A, 6.8B and 6.8C). The knockdowns also confirmed the activation of both genes by As^{+3} treatments. Interestingly, a slight increase in Mrp1 expression was observed with the knockdown of Mdr1 (Fig. 6.8A and 6.8B). Hmox1 was also analyzed by qPCR in the siRNA knockdown samples and Mrp1 showed a much higher increase in Hmox1 expression than Mdr1 with As^{+3} treatments. These results were in agreement with the increase of intracellular As^{+3} levels after the siRNA knockdown (Fig. 6.7C).

The effects of the Mdr1 and Mrp1 knockdowns in D1 cells on viability and DNA damage induced by As^{+3} were also examined. Decrease in cell viabilities and increase in DNA damage were observed in Mdr1 and Mrp1 knockdowns (Fig. 6.9). Mrp1 siRNA knockdown had stronger effects on viability and DNA damage than Mdr1 siRNA knockdown, which correlated with the intracellular As^{+3} accumulation (Fig. 6.7C). Collectively, these results indicate that differences in Mdr1 and Mrp1 expression and activity could result in differential cellular sensitivities to As^{+3} induced genotoxicity.

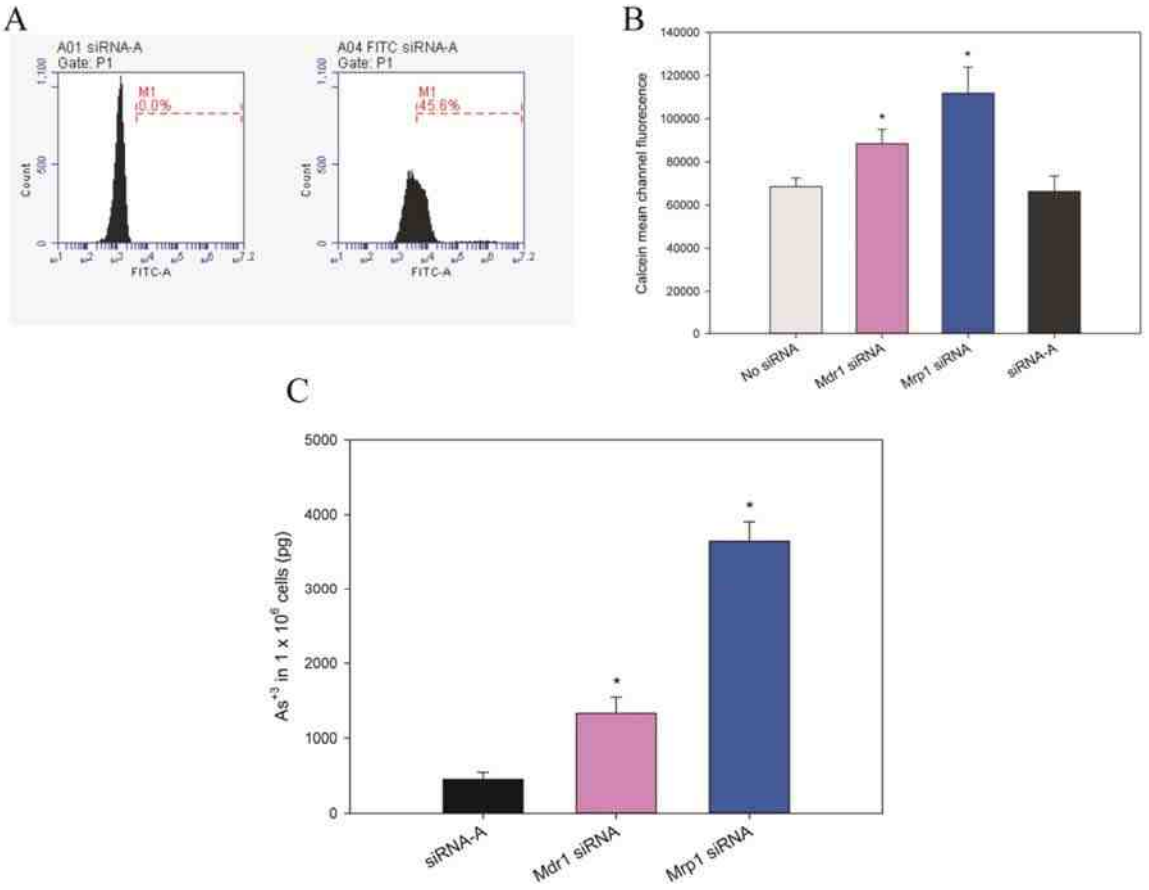

Figure 6.7. Mdr1 and Mrp1 siRNA knockdowns in D1 cells. D1 cells were cultured in Dharmacon Accell siRNA delivery system with Mdr1 and Mrp1 siRNAs for 52 h and treated with As^{+3} for 18 h. siRNA-A was a scrambled siRNA as a control for delivery. A, flow cytometry result to compare FITC fluorescence of siRNA-A with/without FITC label after 52 h of culture in delivery medium. B, calcein fluorescence in D1 cells transfected with Mdr1, Mrp1 siRNAs and siRNA-A. C, As^{+3} accumulation in D1 cells transfected with Mdr1, Mrp1 siRNAs and siRNA-A. *Significantly different compared to no siRNA or siRNA-A ($p<0.05$). Results are Means ± SD.

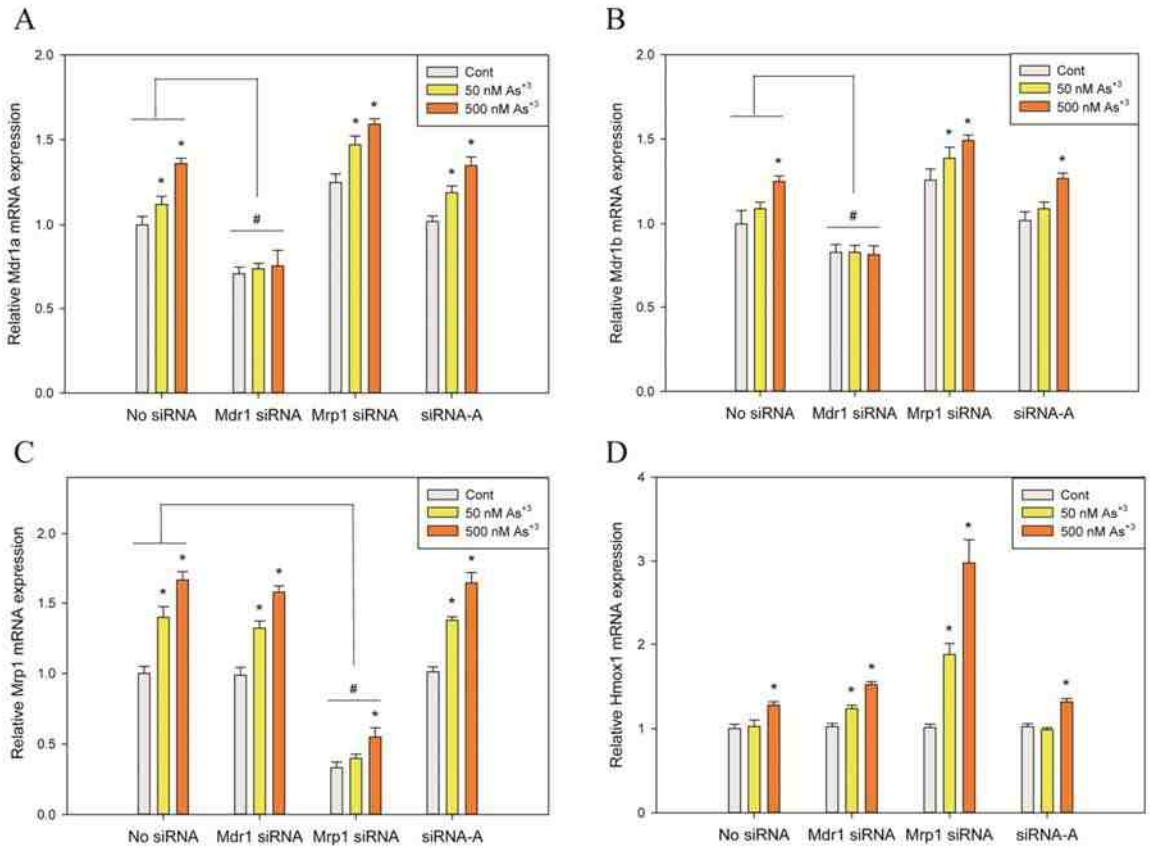

Figure 6.8. Mdr1a, Mdr1b, Mrp1 and Hmox1 mRNA expression in D1 cells transfected with Mdr1 and Mrp1 siRNA and treated with As^{+3} *in vitro* for 18 h. D1 cells were transfected with Mdr1, Mrp1 siRNAs or siRNA-A. Transfected cells were then treated with As^{+3} for 18 h and mRNA expressions were measured by qPCR. A, Mdr1a mRNA expression. B, Mdr1b mRNA expression. C, Mrp1 mRNA expression. D, Hmox1 mRNA expression. *Significantly different compared to Control ($p<0.05$), # Significantly different compared to the relative dose in no siRNA ($p<0.05$). Results are Means ± SD.

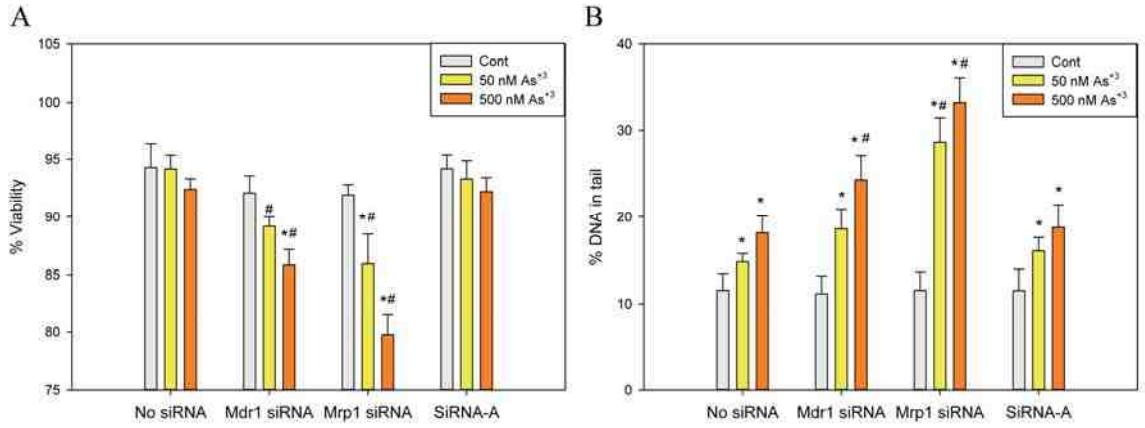

Figure 6.9. Viability and DNA damage in D1 cells after 18 h *in vitro* treatment with As^{+3} in Mdr1 and Mrp1 knockdowns. D1 cells were transfected with Mdr1, Mrp1 siRNAs or siRNA-A. Transfected cells were then treated with As^{+3} for 18 h. A, cell viability were measured by AO/PI staining. B, DNA damage was measured by alkaline Comet assay. *Significantly different compared to Control ($p<0.05$). # Significantly different compared to the relative dose in no siRNA ($p<0.05$). Results are Means ± SD.

DISCUSSION

As^{+3} is known to cause detrimental effects on multiple types of cells and systems (Argos et al., 2010; Biswas et al., 2008; Gonsebatt et al., 1994; Cooper et al., 2009; 2013; Soto-Peña et al., 2006). Our previous results demonstrated that As^{+3} induced both genotoxicity and non-genotoxicity in mouse thymus cells (Xu et al., 2016a; 2016d). Although immune cells in general have high sensitivities to As^{+3}, the early T cells at DN stage were shown to be selectively targeted by low concentrations of As^{+3} *in vitro* (Xu et al., 2016a). In this study, we confirmed that the selective decrease of DN cells also occurred in mice exposed to As^{+3} via drinking water. The percentage of the DN cells, but not the DP cells, was decreased in 500 ppb As^{+3} exposed mice (Fig. 6.1A and 6.1B). The absolute DN and DP cell numbers were also decreased in 500 ppb As^{+3} exposed mice (Fig 6.1C and 6.1D), indicating that the As^{+3} effects on cells at early stage resulted in a decrease in later stage cell numbers. The study suggested that the reduction of thymus cell number in 500 ppb As^{+3} exposed mice was the result of the selective toxicity on early DN cells.

Mdr1, Mrp1 and Mrp2 are important As^{+3} efflux proteins in eukaryotic cells. While Mrp2 is mainly expressed by hepatocytes, Mdr1 and Mrp1 are known to be expressed in human immune cells (Jedlitschky et al., 2006; van der Kolk et al., 2001). Our previous study demonstrated the induction of Mdr1 and Mrp1, which correlated with the decreases of As^{+3}, induced oxidative stress and double strand breaks in thymus cells (Xu et al., 2016d). Therefore, we measured Mdr1 and Mrp1 mRNA expression and activity to see if the differential sensitivities of DN and DP cells to As^{+3} induced toxicity

were due to As^{+3} export. Our results demonstrate that the exporter activity in DN cells was lower than in DP cells (Fig. 6.6B). Also, Mdr1 and Mrp1 mRNAs were not significantly induced in DN cells after 18 h 50 and 500 nM As^{+3} *in vitro* treatments in contrast to the DP cells. These results suggested that the high As^{+3} genotoxicity in DN cells was due to increased exposure resulting from limited exporter induction.

In order to confirm that the high sensitivity of DN cells to As^{+3} was due to As^{+3} export, we measured the intracellular As^{+3} in sorted DN and DP cells treated with As^{+3} *in vitro*. The accumulation of intracellular As^{+3} levels was significantly higher in DN cells than in DP cells at 18 h (Fig. 6.4), which may be the result of limited exporter activity. Since we already confirmed from *in vivo* studies that intracellular As accumulation was responsible for differential genotoxicity in cells from multiple immune organs (Xu et al., 2016c), the higher As^{+3} accumulation in DN cells observed in this study provided an explanation for why DN cells are more sensitive to As^{+3} induced toxicity than DP cells. DN cells are also highly IL-7 dependent cells. Our previous findings indicated that As^{+3} can suppress the IL-7 signaling pathway which cause cell cycle arrest (Xu et al., 2016a). Therefore, the selective decrease in DN cell population after As^{+3} exposure may be the result of a combination effect of both genotoxicity and non-genotoxicity.

Mdr1 and Mrp1, also known as Abcb1 and Abcc1, are two ATP-dependent multi-drug resistant proteins. As^{+3} is often used in the form of arsenic trioxide (ATO) to treat different types of malignant diseases such as leukemia and cancers. Many studies have demonstrated that certain malignant cells with high expressions of Mdr1 and Mrp1 were resistant to ATO therapy (Seo et al., 2007; Sertel et al., 2012). In this study, we

performed siRNA knockdown for both Mdr1 and Mrp1 in a mouse DN -T cell line to confirm the association between Mdr1/Mrp1 expression and the genotoxicity. The knockdown of Mdr1 and Mrp1 not only increased the DNA damage induced by As^{+3} in D1 cells, but also decreased the cell viability after 18 h As^{+3} treatment (Fig. 6.9). These results study show that the inhibition on these exporters specifically may enhance the As^{+3} toxicity in certain type of cells. The effect of Mrp1 knockdown was much greater than Mdr1 knockdown. Since Mrp1 export GSH-conjugated As^{+3}, and Mdr1 export unconjugated As^{+3}, it is possible that most of the intracellular As^{+3} are GSH-bound and need to be transported by Mrp1.

In summary, the study confirmed that As^{+3} selectively target DN thymus cells. The greater sensitivity of DN cells compared to DP cells was a result of more intracellular As^{+3} accumulation and therefore exposure. The expressions and induction of two major As^{+3} exporters after As^{+3} treatments, Mdr1 and Mrp1, were found to be responsible for the differential intracellular As^{+3} and genotoxicities. This is the first study that clearly demonstrated a relationship between intracellular As^{+3} level and As^{+3} exporter activities and expressions, which suggested an explanation of how As^{+3} exporters regulate the As^{+3} induced toxicity in thymus cells at different stages.

FUNDING

This work was funded by National Institute of Environmental Health Sciences grant number R01 ES019968. This work was also supported by National Institutes of Health Grant DK056350 to the UNC-Chapel Hill Nutrition Obesity Research Center.

CHAPTER 7

GENERAL DISCUSSION AND SIGNIFICANCE

CHAPTER 7

GENERAL DISCUSSION AND SIGNIFICANCE

GENERAL DISCUSSION

Many studies revealed that arsenic induces immunotoxicity (Ahmed et al., 2014; Biswas et al., 2008; Gonsebatt et al., 1994; Nadeau et al., 2014; Soto-Pen˜ a et al., 2006; Vahter, 2008). However, few studies have ever addressed the toxicity induced by arsenic in thymus cells from a mechanistic perspective. Early T cells in thymus are developing from early DN stage to CD4 or CD8 SP cells. Most of the cells will die through apoptosis during the positive and negative selections (Klein et al., 2014). Studies have indicated that suppression of the early T cells could result in detrimental effects on immune functions (Ohm et al., 2003; Seinen and Penninks, 1979). Since arsenic has been demonstrated to alter immune functions and peripheral T cells (Dangleben et al.,2013), it is possible that the suppressive effects of arsenic are due to its toxicity on the early thymic T cells. This comprehensive study on arsenic induced toxicity in early thymic T cells not only revealed the mechanism of how arsenic affects a certain type of early immune progenitor cells, but also indicated a possible mechanism of arsenic induced immunotoxicity in the body.

Many studies have focused on the immunotoxicity of arsenic at high concentrations, which may not be representative of real environmental exposures. Epidemiology studies have indicated that people consuming contaminated drinking water

are usually exposed to arsenic up to several hundred ppb (Chowdhury et al., 2000). Therefore, 500 ppb was selected as the high dose for the study in the *in vivo* experiments in this project. The conversion of ppb doses of As^{+3} to nanomolar concentrations is 10 ppb ≈ 130 nM. The high dose in our *in vitro* treatments was 500 nM, which is in the same range of intracellular arsenic amounts in the thymus cells after the 30 d high dose (500 ppb) *in vivo* exposure (Table 4.2). Therefore, the amounts of arsenic used in both the *in vivo* and *in vitro* experiments in this study are close reflections of real environmental conditions. The results from our studies are more environmentally relevant than most of the other studies on arsenic immunotoxicity.

Previous studies have indicated that arsenic affects multiple systems (Argos et al., 2010; Schuhmacher-Wolz et al., 2009; Vahter, 2008). In this study, the toxicity of arsenic to early thymic T cells at environmentally relevant concentrations was assessed from both genotoxic and non-genotoxic (cell signaling) aspects. Both pathways were confirmed by experiments to be involved in the suppressive effects of arsenic to early thymic T cells. In the genotoxicity study, As^{+3} exposures *in vivo* and in *vitro* caused increase of DNA damage by the inhibition PARP1, the initiator of BER, at low concentrations (Xu et al., 2016c). Oxidative stress was observed with the higher concentrations of As^{+3} in thymus cells (Xu et al., 2016d). The dual-action model of As^{+3} genotoxicity was confirmed in thymus cells at lower concentrations compared to the previous studies (Qin et al., 2008). The suppressive effects of As^{+3} and MMA^{+3} on IL-7 signaling were observed in DN T cells, which resulted in the decrease of cell cycle gene expression (Xu et al., 2016a). The study results were similar to our previous studies in the early pre-B cells (Ezeh et al., 2016). Taken together, these results indicated that arsenic induced toxicity in early

thymus cells is a complicated phenomenon, which involves its actions on different pathways.

Most toxicology studies are designed to focus on just one chemical. However, it is not uncommon that people are exposed to multiple toxicants at the same time in environmental conditions. Previous reports indicated that the co-exposures of arsenic with other chemicals enhanced the toxicity and carcinogenesis (Burns et al., 2008; Cooper et al., 2014; Maier et al., 2002). BaP is a ubiquitous contaminant that can be found in wood and cigarette smoke, over-processed food and contaminated water sources, the exposure of which is known to be related to the chimney sweeps' carcinoma, a squamous cell carcinoma of the skin of the scrotum (Crawford, 1988). Previous studies have demonstrated that the interaction between BaP and arsenic could enhance the cytotoxicity and formation of adducts (Evans et al., 2004; Maier et al., 2002). The *in vitro* co-treatment experiment of BP-diol and As^{+3} indicated that the environmentally relevant low dose exposures could increase the toxicity of BP-diol and As^{+3} and induce apoptosis in mouse thymus cells (Fig 5.3). The mechanism of these interactive effects involved both accelerated metabolism of BP-diol to BPDE from the increased expression of CYP1A1 and CYP1B1, and the inhibition of DNA damage repair by As^{+3}.

Cells from different tissues were shown to have differential sensitivity to arsenic (Burchiel et al., 2014; Chen et al., 2016; Rangwala et al., 2012). However, the mechanism of the differential sensitivity is still not clear. Many studies on arsenic trioxide (ATO) resistant tumor cells demonstrated that the overexpression of two As^{+3} exporters, Mdr1 and Mrp1, are responsible for the resistance of ATO treatment (Liu et al., 2001; Liu et al., 2002). This study confirmed that the difference in Mdr1 and Mrp1

expression correlated with alterations in intracellular As^{+3} levels in the thymus cells at DN and DP stages. The sensitivity to As^{+3} in other types of cell may also be related to the expression of these exporters.

In summary, this project is the first comprehensive study of the toxicity of arsenic at environmentally relevant concentrations in early T cells in thymus that addressed both genotoxicity and non-genotoxicity. The mechanism of the interactions between As^{+3} and the metabolites of BaP on the genotoxicity to thymus cells was also revealed. The differential sensitivity of thymic T cells at DN and DP stages to As^{+3} was also mechanistically studied (Fig 7.1). The results will provided information for the evaluation and prediction of arsenic induced toxicity in thymus cells from environmental exposures.

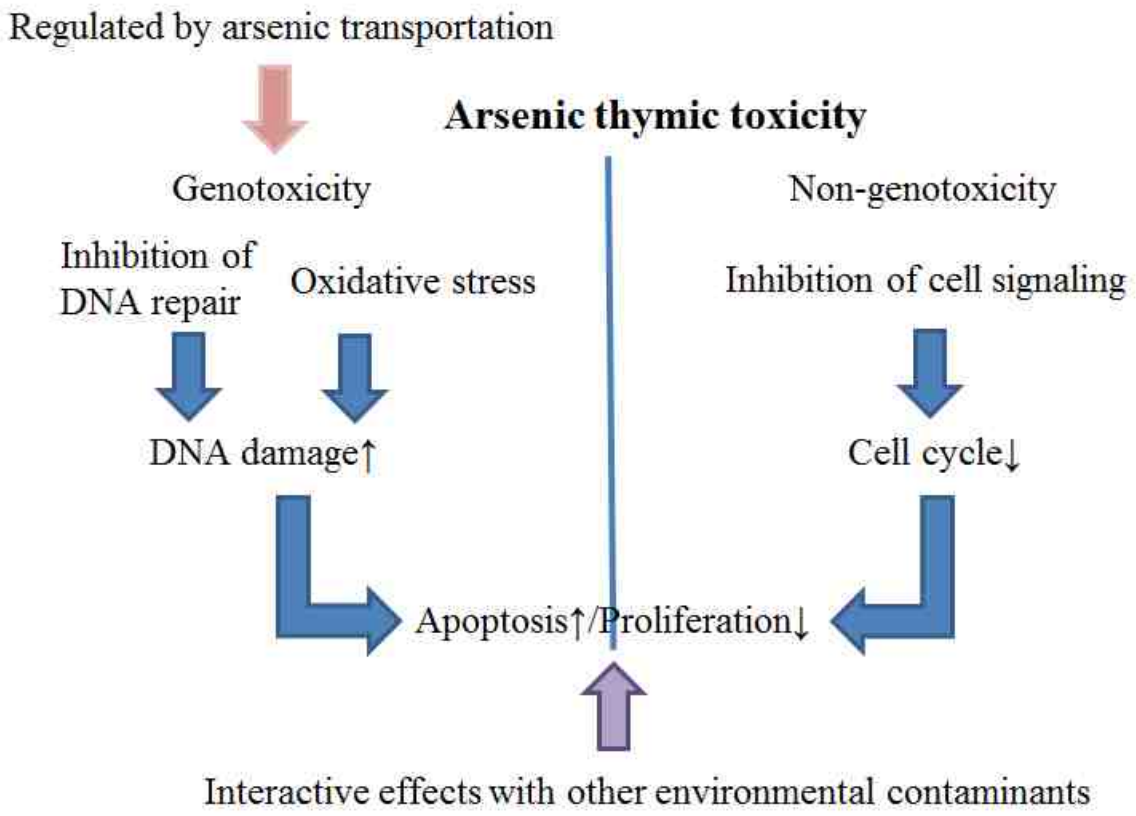

Figure 7.1. Mechanisms of environmentally relevant concentrations of arsenic induced thymic toxicity. Arsenic induces genotoxicity through the inhibition of DNA repair (lower concentrations) and oxidative stress (higher concentrations). Inhibition of cell signaling by arsenic decreases the expression of certain cell cycle gene(s). The suppressive effects of arsenic on the thymus cells can interact with other environmental contaminants. The genotoxicity induced by arsenic was shown to be regulated by arsenic transportation.

SUMMARY OF AIM 1 FINDINGS AND THEIR SIGNIFICANCE

Primary thymus cells isolated from 10-14 wks old male C57BL/6J mice and the D1 cells were used to assess the genotoxicity induced by As^{+3} at 5-500 nM concentrations *in vitro*. The dose range were chosen based on our preliminary studies on low dose As^{+3} toxicity in immune cells and previous studies of immunosuppressions of As^{+3} that mimicked environmental exposures (Ezeh et al., 2014; Kozul et al., 2008).

Observations in this study indicated for the first time that As^{+3} increased the DNA damage in isolated primary thymus cells and the D1 cells after *in vitro* treatment of 50 nM As^{+3} for 4 and 18 h (Fig 2.1 and 2.2). Inhibition of PARP activity was confirmed to contribute to the increase of DNA damage (Fig 2.2). Oxidative stress was observed only at 500 nM As^{+3} concentration in D1 cells at 4 h time point, which was reversed at the 18 h later time point (Fig 2.3). Expressions of two As^{+3} exporters, Mdr1 and Mrp1, were found to be associated with the oxidative stress and DNA damage increase. These results confirmed the previously developed dual-action model of As^{+3} toxicity that inhibition of DNA repair was related to genotoxicity at lower concentrations, and oxidative stress was only involved at high concentrations (Qin et al., 2008; Zhou et al., 2011). However, the thymus cells seemed to be more sensitive to As^{+3} induced genotoxicity than keratinocytes, raising the question about the mechanism of the high sensitivity of thymus cells. The mechanism of this high sensitivity of the early thymus cells was discussed and evaluated in Aim 3.

Following the observation that DN T cells in the thymus were selectively targeted by As^{+3} exposures (Fig 3.4A), IL-7 signaling pathway, the crucial cytokine signaling for

DN cell survival and proliferation, was also studied. *In vitro* experiments revealed that the STAT5 and JAKs phosphorylation was inhibited by As^{+3} and MMA^{+3}, which was similar to our previous findings in the IL-7 dependent pre-B cells (Ezeh et al., 2016). The suppression of the IL-7 signaling pathway resulted in the decreased expression of cyclin D1, an important cell cycle gene (Fig 3.4D). These results indicated another pathway of arsenic induced suppression of the early thymic T cells, and provided the evidence of the higher sensitivity of DN cells than DP cells.

Another significant observation in this study is the arsenic distribution and speciation in three immune organs, bone marrow, spleen and thymus, after *in vivo* As^{+3} exposures. Bone marrow was found to be more sensitive to As^{+3} than spleen and thymus, and spleen was the least sensitive among the three (Fig 4.1). After the in vivo As^{+3} exposures, thymus cells contained the highest amount of intracellular arsenic (Table 4.2). The DNA damage increase was proportional to the As^{+3} dose increase in both the bone marrow and thymus cells. MMA^{+3} was confirmed to be the most abundant arsenical species in bone marrow and thymus cells (Table 4.2), indicating that the increased DNA damage observed in the bone marrow and thymus at 500 ppb As^{+3} dose was caused by MMA^{+3}. These findings revealed that the differential sensitivity to arsenic in different cells may be due to the intracellular arsenic levels and species. The study also confirmed, for the first time, that MMA^{+3} was important for the arsenic induced toxicity *in vivo*.

In summary, these results from the study in Aim 1 confirmed the hypothesis that As^{+3} could induce both genotoxicity and non-genotoxicity in mouse thymus cells. This was the first comprehensive study on the arsenic induced toxicity in the early developing

T cells in the thymus, and compared the differential sensitivities of the cells from three important immune organs to arsenic.

SUMMARY OF AIM 2 FINDINGS AND THEIR SIGNIFICANCE

Previous studies in our laboratory demonstrated that arsenic interacted with DMBA and DBC at low concentrations to suppress immune cell functions (Ezeh et al., 2015; Li et al., 2010). The present study was designed to reveal the mechanism of the interactive effects between arsenic and PAHs. Several PAHs and their metabolites were evaluated for their ability to inhibit PARP activation (Fig 5.1), and BaP and its metabolites were selected as the model to study the interactive effects with As^{+3} at environmentally relevant concentrations. Synergistic increase of DNA damage and PARP inhibition were observed in As^{+3} + BP-diol treatments at low concentrations, with a significant increase of cell apoptosis (Fig 5.2 and 5.3). As^{+3} and BP-diol co-treatment was also found to up-regulate the expression of CYP1A1 and CYP1B1, two important enzymes for the metabolism of BP-diol to BPDE (Fig 5.6).

These results clearly showed for the first time that BP-diol, an intermediate metabolite of BaP, interacted with As^{+3} synergistically to increase the genotoxicity to the primary thymus cells. The possible mechanism of the interactive effects was also revealed from this study. BP-diol was metabolized into BPDE and formed DNA adducts to increase DNA damage. As^{+3} inhibited PARP, the zinc finger DNA repair protein, so that the DNA damage could not be properly repaired. The co-treatment of As^{+3} and BP-diol significantly increased the expression of CYP1A1 and CYP1B1, which accelerated the generation of BPDE. The results confirmed our hypothesis in Aim 2, and provided a possible mechanism of arsenic and PAHs interactions at environmentally relevant concentrations.

SUMMARY OF AIM 3 FINDINGS AND THEIR SIGNIFICANCE

Findings in Aim 1 and Aim 2 demonstrated that environmentally relevant concentrations of arsenic could induce significant toxicity in mouse thymus cells. The DN cells in thymus, the earliest subset of thymocytes, were found to be the most sensitive among the DN, DP, CD4SP and CD8SP subsets. Besides the suppressive effects of arsenic on the critical cytokine signaling pathway that is required for the development of early progenitor cells, the bone marrow and thymus were also found to be more sensitive than the spleen to As^{+3} and MMA^{+3} induced genotoxicity (Fig 4.1). The hypothesis that the differential sensitivity was caused by the differences in arsenic transportation and intracellular accumulation was evaluated in Aim 3.

DN and DP cell populations were separated by cell sorting, and As^{+3} induced genotoxicity in DN was found to be more significant than in DP cells (Fig 6.2). More intracellular As^{+3} accumulation in DN cells than DP cells was confirmed by HG-CT-ICP-MS analysis (Fig 6.4). The lack of the expressions of two major As^{+3} exporters, Mdr1 and Mrp1, were found to be associated with the high sensitivity of DN cells to As^{+3}. Knockdown experiments in D1 cells confirmed that Mdr1 and Mrp1 expressions were related to As^{+3} accumulation and toxicity (Fig 6.9). These results demonstrated for the first time that lack of As^{+3} exporter expression could result in higher As^{+3} toxicity in certain types of cells. The study confirmed the hypothesis that arsenic transportation affected its toxicity, and provided a mechanism related to differential sensitivity to As^{+3} in different types of cells.

OVERALL IMPACT OF THESE STUDIES AND POTENTIAL AREAS FOR NEW STUDIES

This is the first comprehensive study on the toxicity induced by environmentally relevant concentrations of arsenic on thymocytes. The study revealed both the genotoxic and non-genotoxic effects of arsenic at low concentrations on the early thymic T cells. The early T cells in thymus were found to be very sensitive to arsenic exposures. Numerous studies have showed the strong relationship between arsenic exposure and T cell immunosuppression in human and animal models. The toxicity induced by arsenic on the early T cells may be the reason of the immunosuppression of the matured T cells.

The differential sensitivity to arsenic toxicity of different types of cells was noticed before by many other studies. However, few studies have ever related the sensitivity to the distribution of arsenic *in vivo*. In this study, the differential sensitivities to arsenic in cells from bone marrow, spleen and thymus were compared and evaluated. The intracellular arsenic amounts in the cells from the three immune organs from As^{+3} exposed mice were also analyzed. A proportional increase of DNA damage to the increase of intracellular arsenic amounts was observed in cells from the bone marrow and thymus, the two organs that were sensitive to environmentally relevant concentrations of arsenic induced toxicity. Also, MMA^{+3} was confirmed to be the most prevalent form of arsenic in the bone marrow and thymus cells, which provided supporting evidence for our previous studies on the toxicity of MMA^{+3} in bone marrow pre-B cells (Ezeh et al., 2014). More MMA^{+3} studies at the *in vivo*-relevant doses should be conducted *in vitro* to examine the mechanism of MMA^{+3} induced toxicity in thymus cells in the future.

The interactive genotoxicity of As^{+3} and BaP was reported before (Maier et al., 2002). In this study, interactive genotoxicity of As^{+3} and BP-diol, the metabolite of BaP, was observed in mouse thymus cells at lower concentrations. The mechanism of the interactive genotoxicity was also revealed in detail. Since it is common to expose to multiple contaminants at the same time in real environmental conditions, the study on the low dose interactive effects between arsenic and BaP on the early thymic T cells provided an example of how different environmental agents could interact with each other to enhance the toxicity.

While more and more population-based studies, such as the Emory Health and Exposome Research Center: Understanding Lifetime Exposures (HERCULES) project, the Human Early-Life Exposome (HELIX) project in Europe, and the Health and the Environment-wide Associations based on Large population Surveys (HEALS) project founded by the European Union, are focusing on the interactive effects of multiple environmental pollutants to the human body, most of the mechanistic studies in environmental toxicology are still being conducted with a single chemical. The complexity of the biological reactions induced by one chemical is a big limitation to the study of interactive toxicity. However, our study confirmed that such kind study could be conducted in certain mechanistically well-characterized chemicals based on carefully-designed experiments and explicit hypothesis. It is predictable that more and more studies focusing on the interactive effects of multiple chemicals will be conducted in the future.

The study also demonstrated for the first time that the toxicity of As^{+3} was dependent on the transportation of As^{+3}. Previous studies showed that certain malignant cells with up-regulation of Mdr1 and Mrp1 were resistant to arsenic treatments (Liu et al.,

2001; Liu et al., 2002). However, the key evidence for the relationship between the Mdr1 and Mrp1 over-expression and more arsenic efflux was not showed in these studies. The present study revealed that high sensitivity of DN cells were due to the accumulation of As^{+3} in the cells, which was related to the expression and up-regulation of the two As^{+3} exporters, Mdr1 and Mrp1. Knockdown of Mdr1 and Mrp1 in the D1 cells also confirmed that the expressions of Mdr1 and Mrp1 were important for the exportation of As^{+3}. These results indicated a mechanism that could be responsible for differential sensitivity of different types of cells to arsenic induced toxicity.

The Aim 1 part of this project confirmed the previously described mechanisms of arsenic induced genotoxicity and non-genotoxicity in primary thymus cells. It also demonstrated that the high sensitivity of thymus cells to arsenic induced toxicity was due to the high intracellular accumulation of arsenic. The results from the Aim 1 provided supporting evidence and ideas for the Aim 2 and Aim 3 part. The Aim 2 part of this project revealed the mechanism of how the metabolites of BaP could interact with arsenic synergistically to enhance the genotoxicity. The interactive effect was observed from the *in vitro* treatment of BP-Diol and As^{+3} at extremely low concentrations. The activation of the key enzymes for the metabolism of BP-Diol may also happen in *in vivo* conditions and enhances the genotoxicity in human body in the real environmental exposures. The mechanism also explained the previously described observations that the co-exposure of arsenic and BaP significantly increased the BaP adducts in rats (Evans et al., 2004). The Aim 3 part of the study was based on the observations from Aim 1, and provided a mechanism of how cells at different stages of their development may have differential sensitivity to arsenic induced toxicity. Previous observations indicated that certain types

of cancers are resistant to As^{+3} treatments (Seo et al., 2007; Sertel et al., 2012). Since the DN cells are more prone to As^{+3} induced apoptosis due to the limited activation of As^{+3} exporters, the As^{+3} resistance of these tumor cells may be the result of high exporter expression. The results from Aim 3 part also provided the idea that quantification of the real amount of exposure is very important in the future studies of arsenic toxicity.

Since arsenic exposure is a world-wide public health issue, this first comprehensive study on arsenic induced toxicity in thymus cells will contribute to the understanding of the whole picture of how the exposure can induce immunosuppression in human body. The study on the mechanism of the toxicity and suppressive effects induced by arsenic on the early developing T cells may potentially benefit the populations in the arsenic contaminated areas to prevent the dysfunction of the immune system and many other types of diseases associated with arsenic exposure.

The experimental models of the project were based on the thymus cells from C57BL/6J mice. The doses and treatment concentrations applied in the studies were selected based on environmental conditions. However, just like many other controlled exposure studies in laboratory using inbred animal models, the real environmental exposures in humans may have different effects. There are some population-based studies conducted in *in utero* exposed kids as mentioned in Chapter 1, but more evidence from epidemiology studies in adults is also required to compare the experimental results and clinical findings. Therefore, future studies with human samples from exposed individuals should be also performed to provide evidence for safety evaluation and assessment.

Based on the results of the study, the following questions should be addressed in the follow-up studies:

- What is the genotoxicity induced by MMA^{+3} in thymocytes? – Based on the findings in Aim 1 that the most prevalent arsenic species in thymus cells after in vivo As^{+3} exposure was MMA^{+3}, the genotoxicity of MMA^{+3} should be conducted in vitro to connect the in vivo and in vitro findings.
    - Possible study: DNA damage and PARP activity in thymus cells after MMA^{+3} exposures.
    - Possible study: Oxidative stress and DSBs in thymus cells after MMA^{+3} exposures at different time points.
- Is there selective toxicity in DN1 to DN4 subsets? – DN cells can be differentiated into DN1 to DN4 subsets. Previous study indicated that cadmium altered the DN1 and DN2 populations after *in vivo* exposures (Holásková et al., 2012). Arsenic may also selectively target certain subsets in DN cells.
    - Possible study: Flow cytometry study using CD25, CD44 or CD127R cell surface markers to evaluate the changes in DN1 to DN4 cell populations after *in vivo* and *in vitro* exposures to As^{+3}.
- What are the effects of As^{+3} and BP-diol interactions *in vivo*? Are there more PAHs that interact with arsenic? – In Aim 2, we demonstrated that As^{+3} interacted with BP-diol *in vitro* to increase the DNA damage and apoptosis in thymus cells. Whether the similar interactions can happen in vivo should be studied. The interactions between As^{+3} and other PAHs could also be addressed in future studies.
    - Possible study: Co-exposure of low dose As^{+3} and BP-Diol in C57BL/6J mice; Cell recovery, DNA damage and PARP activity studies in thymus cells.

- Possible study: Co-treatments of As^{+3} and other PAHs in vitro; DNA damage, PARP activity, apoptosis studies.

- What are the effects of arsenic exposure on the immune cell populations and functions in humans? – The study was conducted in inbred mouse models. More evidence should be provided by population-based studies in humans for a better understanding of the effects in real environmental conditions.
  - Possible study: Flow cytometry study on human PBMC samples from arsenic exposed individuals using immune cell surface markers, including the specific markers for T cells, such as CD3, CD4 and CD8.
  - Possible study: Flow cytometry study on human PBMC samples using IL-7R marker for early and memory T cells.
  - Possible study: mitogenesis assay using Concanavalin A to study the proliferation of T cells from arsenic exposed individuals.
- Is there an interactive effect between arsenic and other heavy metals in the environment, such as uranium? – It is very common that other heavy metals, such as cadmium, lead or uranium, present together with arsenic in contaminated drinking water sources. Therefore, the potential interactions between these heavy metals should be examined.
  - Possible study: DNA damage and PARP activity in thymus cells after As^{+3}/MMA^{+3} and uranium combined exposures at environmentally relevant doses.
  - Possible study: Oxidative stress and DSBs in thymus cells after As^{+3}/MMA^{+3} and uranium combined exposures at different time points.

LIST OF ABREVIATIONS

2-ME	2-mercaptoethanol
3-MC	3-methylcholanthrene
AAALAC	Association for Assessment and Accreditation of Laboratory Animal Care
Ab	Antibody
ABCB	ATP binding cassette subfamily B member
ABCC	ATP binding cassette subfamily C member
AhR	Ayl hydrocarbon receptor
ANOVA	Analysis of variance
ANTH	Anthracene
AO/PI	Acridine Orange/Propidium Iodide
APC	Accessory photosynthesis Pigment of the Cyanobacteria
APC	Antigen presenting cell
AQP	Aquaglyceroporin
As	Arsenic
As^{+3}	Arsenite
As^{+5}	Arsenate
AS3MT	Arsenite methyltransferase
BA	Benz(a)anthracene
BaP	Benzo(a)pyrene
BCA	Bicinchoninic acid
BeP	Benzo(e)pyrene

BM	Bone Marrow
BP-diol	Benzo(a)pyrene-7,8-dihydrodiol
BPDE	Benzo(a)pyrene-7,8-dihydrodiol-9,10-epoxide
Caspase	Cysteinyl aspartate-specific proteases
CD	Cluster of differentiation
CYP	Cytochrome P450
CYP1A1	Cytochrome P450 1A1
CYP1B1	Cytochrome P450 1B1
cDNA	copy Deoxyribonucleic acid
DAC	Dibenz(a,c)anthracene
DAH	Dibenz(a,h)anthracene
DBC	Dibenzo[def,p]chrysene
DC	Dendritic Cell
DHE	Dihydroethidium
DMA	9,10-Dimethylanthracene
DMA^{+3}	Dimethylarsonous acid
DMA^{+5}	Dimethylarsinic acid
DMBA	7, 12-Dimethylbenz[a]anthracene
DMBA-diol	Dimethylbenz[a]anthracene-trans-3,4-dihydrodiol
DN	Double Negative
DP	Double Positive
DPBS	Dulbecco's Phosphate Buffered Saline
$DPBS^{-}$	Dulbecco's Phosphate Buffered Saline without calcium and magnesium

DSBs	Double strand breaks
EDTA	Ethylenediamine teraacetate acid
FBS	Fetal bovine serum
FITC	Fluorescein Isothiocyanate
FL	Fluorescence channel
FSC	Forward Scatter
GAPDH	Glyceraldehyde-3-Phosphate Dehydrogenase
HBSS	Hanks Balanced Salt Solution
HPBMC	Human Peripheral Blood Mononuclear Cell
HSC	Hematopoietic Stem Cell
HRP	Horse Radish Peroxidase
IARC	International Agency for Research on Cancer
IAUCC	Institutional Animal Care and Use Committee
Ig	Immunoglobulin
IgG	Immunoglobulin G
IFN-γ	Interferon gamma
IL	Interleukin
IL-7	Interleukin-7
IL-7R	Interleukin-7 receptor
JAK	Janus Kinase
kD	kilo Dalton
mAb	monoclonal antibody
Mdr	Multidrug resistance protein

Mrp	Multidrug resistance-associated protein
µl	microliter
MMA^{+3}	Monomethylarsonous acid
MMA^{+5}	Monomethylarsinic acid
mRNA	messenger Ribonucleic acid
NK	Natural Killer cell
ng	nanogram
NIH	National Institutes of Health
PAGE	Polyacrylamide gel electrophoresis
PAHs	Polycyclic Aromatic Hydrocarbons
PARP	Poly (ADP-ribose) polymerase
PAX5	Paired Box-containing transcription factor 5
PCR	Polymerase Chain Reaction
PE	Phycoerythrin
PE-Cy7	Phycoerythrin-Cyanine7
PI	Propidium Iodide
ppb	parts per billion
ppm	parts per million
pSTAT5	phosphorylated STAT5
pJAK1	phosphorylated JAK 1
qPCR	quantitative Polymerase Chain Reaction
RPMI	Roswell Park Memorial Institute
RIPA	Radioimmunoprecipitation assay

RNS	Reactive nitrogen species
ROS	Reactive oxygen species
SDS	Sodium dodecyl sulfate
STAT	Signal Tranducer and Activator of Transcription
TCDD	2,3,7,8-terachlorodibenzo-*p*-dioxin
TDAR	T-Dependent Antibody Responses
UV	Ultraviolet light
UVR	Ultraviolet light radiation
Zn	Zinc

REFERENCES

Ahmed, S., Ahsan, K. B., Kippler, M., Mily, A., Wagatsuma, Y., Hoque, A. M., Ngom, P. T., El Arifeen, S., Raqib, R., Vahter, M. (2012). In utero arsenic exposure is associated with impaired thymic function in newborns possibly via oxidative stress and apoptosis. *Toxicol. Sci.* **129(2),** 305-314.

Ahmed, S., Moore, S. E., Kippler, M., Gardner, R., Hawlader, M. D., Wagatsuma, Y., Raqib, R., Vahter, M. (2014). Arsenic exposure and cell-mediated immunity in pre-school children in rural Bangladesh. *Toxicol. Sci.* **141(1),** 166-175.

Al-Forkan, M., Islam, S., Akter, R., Shameen Alam, S., Khaleda, L., Rahman, Z., Salma Chowdhury, D. U. (2015). A Sub-Chronic Exposure Study of Arsenic on Hematological Parameters, Liver Enzyme Activities, Histological Studies and Accumulation Pattern of Arsenic in Organs of Wistar Albino Rats. *J. Cytol. Histol.* **S5,** 06.

Akter, K. F., Owens, G., Davey, D. E., Naidu, R. (2005). Arsenic speciation and toxicity in biological systems. *Rev. Environ. Contam. Toxicol.* **184,** 97-149.

Amariglio, N., Lev, A., Simon, A., Rosenthal, E., Spirer, Z., Efrati, O., Broides, A., Rechavi, G., Somech, R. (2010). Molecular assessment of thymus capabilities in the evaluation of T-cell immunodeficiency. *Pediatr. Res.* **67(2),** 211-216.

Aposhian, H. V., Aposhian, M. M. (2006). Arsenic toxicology: five questions. *Chem. Res. Toxicol.* **19(1),** 1-15.

Aposhian, H. V., Gurzau, E. S., Le, X. C., Guazau, A., Healy, S. M., Lu, X., Ma, M., Yip, L., Zakharyan, R. A., Maiorino, R. M., Dart, R.C., Tircus, M. G., Gonzalez-Ramirez, D., Morgan, D. L., Avram, D., and Aposhian, M. M. (2000). Occurrence of monomethylarsonous acid in urine of humans exposed to inorganic arsenic. *Chem. Res. Toxicol.* **13,** 693-697.

Argos, M., Kalra, T., Rathouz, P. J., Chen, Y., Pierce, B., Parvez, F., Islam, T., Ahmed, A., Rakibuz-Zaman, M., Hasan, R., Sarwar, G., Slavkovich, V., van Geen, A., Graziano, J., Ahsan, H. (2010). Arsenic exposure from drinking water, and all-cause and chronic-disease mortalities in Bangladesh (HEALS): a prospective cohort study. *Lancet.* **376(9737),** 252-258.

Asao, H., Okuyama, C., Kumaki, S., Ishii, N., Tsuchiya, S., Foster, D., Sugamura, K. (2001). Cutting edge: the common gamma-chain is an indispensable subunit of the IL-21 receptor complex. *J. Immunol.* **167 (1),** 1–5.

Bauer, M., Goldstein, M., Christmann, M., Becker, H., Heylmann, D., Kaina, B. (2011). Human monocytes are severely impaired in base and DNA double-strand break repair that renders them vulnerable to oxidative stress. *Proc. Natl. Acad. Sci. USA.* **108(52),** 21105-21110.

Beck, C., Robert, I., Reina-San-Martin, B., Schreiber, V., Dantzer, F. (2014). Poly(ADP-ribose) polymerases in double-strand break repair: focus on PARP1, PARP2 and PARP3. *Exp. Cell Res.* **329(1),** 18-25.

Benramdane, L., Accominotti, M., Fanton, L., Malicier, D., Vallon, J. J. (1999). Arsenic Speciation in Human Organs following Fatal Arsenic Trioxide Poisoning—A Case Report. *Clin. Chem.* **45(2),** 301-306.

Bircsak, K. M., Gibson, C. J., Robey, R. W., Aleksunes, L. M. (2013). Assessment of drug transporter function using fluorescent cell imaging. *Curr. Protoc. Toxicol.* **57,** Unit 23.6.

Biswas, R., Ghosh, P., Banerjee, N., Das, J. K., Sau, T., Banerjee, A., Roy, S., Ganguly, S., Chatterjee, M., Mukherjee, A., Giri, A. K. (2008). Analysis of T-cell proliferation and cytokine secretion in the individuals exposed to arsenic. *Hum. Exp. Toxicol.* **27(5),** 381-386.

Boudil A, Matei IR, Shih HY, Bogdanoski G, Yuan JS, Chang SG, Montpellier B, Kowalski PE, Voisin V, Bashir S, Bader GD, Krangel MS, Guidos CJ. (2015). IL-7 coordinates proliferation, differentiation and Tcra recombination during thymocyte β-selection. *Nat. Immunol.* **16**, 397-405.

Burchiel, S. W., Lauer, F. T., Beswick, E. J., Gandolfi, A. J., Parvez, F., Liu, K. J., Hudson, L. G. (2014). Differential susceptibility of human peripheral blood T cells to suppression by environmental levels of sodium arsenite and monomethylarsonous acid. *PLoS One*. **9(10),** e109192.

Burns, F. J., Rossman, T., Vega, K., Uddin, A., Vogt, S., Lai, B., Reeder, R. J. (2008). Mechanism of selenium-induced inhibition of arsenic-enhanced UVR carcinogenesis in mice. *Environ. Health Perspect.* **116(6),** 703-708.

Calatayud, M., Barrios, J. A., Vélez, D., Devesa, V. (2012). In vitro study of transporters involved in intestinal absorption of inorganic arsenic. *Chem. Res. Toxicol.* **25,** 446–453.

Carlson, E. A., Li, Y., Zelikoff, J. T. (2004). Suppressive effects of benzo[a]pyrene upon fish immune function: evolutionarily conserved cellular mechanisms of immunotoxicity. *Mar. Environ. Res.* **58(2-5),** 731-734.

Carrozza, M. J., Stefanick, D. F., Horton, J. K., Kedar, P. S., Wilson, S. H. (2009). PARP inhibition during alkylation-induced genotoxic stress signals a cell cycle checkpoint response mediated by ATM. *DNA Repair*. **8(11),** 1264-1272.

Cepeda, V., Fuertes, M. A., Castilla, J., Alonso, C., Quevedo, C., Soto, M., Pérez, J. M. (2006). *Recent Pat. Anticancer Drug Discov.* **1(1),** 39-53.

Chen, B., Arnold, L. L., Cohen, S. M., Thomas, D. J., Le, X. C. (2011). Mouse arsenic (+3 oxidation state) methyltransferase genotype affects metabolism and tissue dosimetry of arsenicals after arsenite administration in drinking water. *Toxicol Sci.* **124**, 320-326.

Chen, J., Cheng, J., Yi, J., Xie, B., Lin, L., Liu, Z., Zhao, H., Wang, B., Ai, Z., Yang, Y., Wei, H. (2016). Differential expression and response to arsenic stress of MRPs and ASAN1 determine sensitivity of classical multidrug-resistant leukemia cells to arsenic trioxide. *Leuk. Res.* **50,** 116-122.

Chen S, Nguyen N, Tamura K, Karin M, Tukey RH. (2003). The role of the Ah receptor and p38 in benzo[a]pyrene-7,8-dihydrodiol and benzo[a]pyrene-7,8-dihydrodiol-9,10-epoxide-induced apoptosis. J Biol Chem. **278**, 19526-19533.

Chen, Y., Graziano, J. H., Parvez, F., Liu, M., Slavkovich, V., Kalra, T., Argos, M., Islam, T., Ahmed, A., Rakibuz-Zaman, M., Hasan, R., Sarwar, G., Levy, D., van Geen, A., and Ahsan, H. (2011). Arsenic exposure from drinking water and mortality from cardiovascular disease in Bangladesh: prospective cohort study. *BMJ*. **342,** d2431.

Cheng, H. Y., Li, P., David, M., Smithgall, T. E., Feng, L., Lieberman, M. W. (2004). Arsenic inhibition of the JAK-STAT pathway. *Oncogene.* **(20),** 3603-12.

Chowdhury, U. K., Biswas, B. K., Chowdhury, T. R., Samanta, G., Mandal, B. K., Basu, G. C., Chanda, C. R., Lodh, D., Saha, K. C., Mukherjee, S. K., Roy, S., Kabir, S., Quamruzzaman, Q., Chakraborti, D. (2000). Groundwater arsenic contamination in Bangladesh and West Bengal, India. *Environ. Health Perspect.* **108(5),** 393-397.

Choudhury, S., Gupta, P., Ghosh, S., Mukherjee, S., Chakraborty, P., Chatterji, U., Chattopadhyay, S. (2016). Arsenic-induced dose-dependent modulation of the NF-κB/IL-6 axis in thymocytes triggers differential immune responses. *Toxicology.* **357-358,** 85-96.

Collins, A. R. (2004). The comet assay for DNA damage and repair: principles, applications, and limitations. *Mol. Biotechnol.* **26(3),** 249-261.

Cooper, K. L., Liu, K. J., Hudson, L. G. (2009). Enhanced ROS production and redox signaling with combined arsenite and UVA exposures: contributions of NADPH oxidase. *Free Radi. Biol. Med.* **47,** 381-388.

Cooper, K. L., King, B. S., Sandoval, M. M., Liu, K. J., Hudson, L. G. (2013). Reduction of arsenite-enhanced ultraviolet radiation-induced DNA damage by supplemental zinc. *Toxicol. Appl. Pharmacol.* **269(2),** 81-88.

Cooper, K. L., Yager, J. W., Hudson, L. G. (2014). Melanocytes and keratinocytes have distinct and shared responses to ultraviolet radiation and arsenic. *Toxicol. Lett.* **224(3)**, 407-415.

Crawford, W. A. (1988). On air pollution, environmental tobacco smoke, radon, and lung cancer. *JAPCA.* **38(11),** 1386-1391.

Currier, J. M., Ishida, M. C., González-Horta, C., Sánchez-Ramírez, B., Ballinas-Casarrubias, L., Gutiérrez-Torres, D. S., Cerón, R. H., Morales, D. V., Terrazas, F. A., Del Razo, L. M., García-Vargas, G. G., Saunders, R. J., Drobná, Z., Fry, R. C., Matoušek, T., Buse, J. B., Mendez, M. A., Loomis, D., Stýblo, M. (2014). Associations between arsenic species in exfoliated urothelial cells and prevalence of diabetes among residents of Chihuahua, Mexico. *Environ. Health Perspect.* **122(10),** 1088-1094.

Dale Rein, I., Solberg Landsverk, K., Micci, F., Patzke, S., Stokke, T. (2015). Replication-induced DNA damage after PARP inhibition causes G2 delay, and cell line-dependent apoptosis, necrosis and multinucleation. *Cell Cycle*. **14(20),** 3248-3260.

Dangleben, N. L., Skibola, C. F., Smith, M. T. (2013). Arsenic immunotoxicity: a review. *Environ. Health.* **12(1),** 73.

de Groot, R. P., Raaijmakers, J. A., Lammers, J. W., Koenderman, L. (2000). STAT5-Dependent CyclinD1 and Bcl-xL expression in Bcr-Abl-transformed cells. *Mol. Cell. Biol. Res. Commun.* **3(5),** 299-305.

De Jong, W. H., Kroese, E. D., Vos, J. G., Van Loveren, H. (1999). Detection of immunotoxicity of benzo[a]pyrene in a subacute toxicity study after oral exposure in rats. *Toxicol. Sci.* **50(2),** 214-220.

Denissenko, M. F., Paom, A., Tang, M., Pfeifer, G. P. (1996). Preferential formation of benzo[a]pyrene adducts at lung cancer mutational hotspots in P53. *Science.* **274(5286),** 430-432.

Ding, W., Liu, W., Cooper, K. L., Qin, X. J., de Souza Bergo, P. L., Hudson, L. G., Liu, K. J. (2009). Inhibition of poly(ADP-ribose) polymerase-1 by arsenite interferes with repair of oxidative DNA damage. *J. Biol. Chem.* **284(11),** 6809-6817.

DiTusa, S. F., Fontenot, E. B., Wallace, R. W., Silvers, M. A., Steele, T. N., Elnagar, A. H., Dearman, K. M., Smith, A. P. (2016). A member of the Phosphate transporter 1 (Pht1) family from the arsenic-hyperaccumulating fern Pteris vittata is a high-affinity arsenate transporter. *New Phytol.* **209(2),** 762-72.

Divi, R. L., Beland, F. A., Fu, P.P., Von Tungeln, L. S., Schoket, B., Camara, J. E., Ghei, M., Rothman, N., Sinha, R., Poirier, M. C. (2002). Highly sensitive chemiluminescence immunoassay for benzo[a]pyrene-DNA adducts: validation by comparison with other methods, and use in human biomonitoring. *Carcinogenesis.* **23(12),** 2043-2049.

Douillet, C., Huang, M. C., Saunders, R. J., Dover, E. N., Zhang, C., Stýblo, M. (2016). Knockout of arsenic (+3 oxidation state) methyltransferase is associated with adverse metabolic phenotype in mice: the role of sex and arsenic exposure. *Arch. Toxicol.* Epub ahead of print.

Drobna, Z., Styblo, M., Thomas, D. J. (2009). An Overview of Arsenic Metabolism and Toxicity. *Curr. Protoc. Toxicol.* **42(431),** 4.31.1-4.31.6.

Drobná, Z., Walton, F. S., Paul, D. S., Xing, W., Thomas, D. J., Stýblo, M. (2010). Metabolism of arsenic in human liver: the role of membrane transporters. *Arch. Toxicol.* **84,** 3–16.

Dutta, K., Prasad, P., Sinha, D. (2015). Chronic low level arsenic exposure evokes inflammatory responses and DNA damage. *Int. J. Hyg. Environ. Health.* **218(6),** 564-74.

Evans, C. D., LaDow, K., Schumann, B. L., Savage, R. E. Jr., Caruso, J., Vonderheide, A., Succop, P., Talaska, G. (2004). Effect of arsenic on benzo[a]pyrene DNA adduct levels in mouse skin and lung. *Carcinogenesis.* **25(4),** 493-497.

Evseenko, D. A., Paxton, J. W., Keelan, J. A. (2006). ABC drug transporter expression and functional activity in trophoblast-like cell lines and differentiating primary trophoblast. *Am. J. Physiol. Regul. Integr. Comp. Physiol.* **290(5),** R1357-1365.

Ezeh, P. C., Lauer, F. T., Liu, K. J., Hudson, L. G., Burchiel, S. W. (2015). Arsenite Interacts with Dibenzo[def,p]chrysene (DBC) at Low Levels to Suppress Bone Marrow Lymphoid Progenitors in Mice. *Biol. Trace. Elem. Res.* **166(1),** 82-88.

Ezeh, P. C., Lauer, F. T., MacKenzie, D., McClain, S., Liu, K. J., Hudson, L. G., Gandolfi, A. J., Burchiel, S. W. (2014). Arsenite selectively inhibits mouse bone marrow lymphoid progenitor cell development *in vivo* and *in vitro* and suppresses humoral immunity *in vivo*. *PLoS One.* **9(4),** e93920.

Ezeh, P. C., Xu, H., Lauer, F. T., Liu, K. J., Hudson, L. G., Burchiel, S. W. (2016). Monomethylarsonous acid (MMA+3) Inhibits IL-7 Signaling in Mouse Pre-B Cells. *Toxicol. Sci.* **149(2),** 289-299.

Faita, F., Cori, L., Bianchi, F., Andreassi, M. G. (2013). Arsenic-Induced Genotoxicity and Genetic Susceptibility to Arsenic-Related Pathologies. *Int. J. Environ. Res. Public Health.* **10(4),** 1527-1546.

Germain, R. N. (2002). T-cell development and the CD4-CD8 lineage decision. *Nat. Rev. Immunol.* **2(5),** 309-322.

Ginsberg, G. L., Atherholt, T. B., Butler, G. H. (1989). Benzo[a]pyrene-induced immunotoxicity: comparison to DNA adduct formation in vivo, in cultured splenocytes, and in microsomal systems. *J. Toxicol. Environ.* Health. **28(2),** 205-220.

Gonsebatt, M. E., Vega, L., Montero, R., Garcia-Vargas, G., Del Razo, L. M., Albores, A., Cebrian, M. E., Ostrosky-Wegman, P. (1994). Lymphocyte replicating ability in individuals exposed to arsenic via drinking water. *Mutat. Res.* **313,** 293-299.

Gusman G. S., Oliveira, J. A., Farnese, F. S., Cambraia, J. (2013). Arsenate and arsenite: the toxic effects on photosynthesis and growth of lettuce plants. *Acta Physiologiae Plantarum.* **35(4),** 1201–1209.

Haan, C., Rolvering, C., Raulf, F., Kapp, M., Drückes, P., Thoma, G., Behrmann, I., Zerwes, H. G. (2011). Jak1 has a dominant role over Jak3 in signal transduction through γc-containing cytokine receptors. *Chem. Biol.* **18(3),** 314-323.

Harper, T. A. Jr., Morré, J., Lauer, F. T., McQuistan, T. J., Hummel, J. M., Burchiel, S. W., Williams, D. E. (2015). Analysis of dibenzo[def,p]chrysene-deoxyadenosine adducts in wild-type and cytochrome P450 1b1 knockout mice using stable-isotope dilution UHPLC-MS/MS. *Mutat. Res. Genet. Toxicol. Environ. Mutagen.* **782,** 51-56.

Hayashi, T., Hideshima, T., Akiyama, M., Richardson, P., Schlossman, R. L., Chauhan, D., Munshi, N. C., Waxman, S., Anderson, K.C. (2002). Arsenic trioxide inhibits growth of human multiple myeloma cells in the bone marrow microenvironment. *Mol. Cancer. Ther.* **1(10),** 851-860.

Hernández-Castro, B., Doníz-Padilla, L. M., Salgado-Bustamante, M., Rocha, D., Ortiz-Pérez, M. D., Jiménez-Capdeville, M. E., Portales-Pérez, D. P., Quintanar-Stephano, A., González-Amaro, R. (2009). Effect of arsenic on regulatory T cells. *J. Clin. Immunol.* **29(4),** 461-469.

Hernández-Zavala, A., Matoušek, T., Drobná, Z., Paul, D. S., Walton, F., Adair, B. M., Jiří, D., Thomas, D. J., Stýblo, M. (2008). Speciation analysis of arsenic in biological matrices by automated hydride generation-cryotrapping-atomic absorption spectrometry with multiple microflame quartz tube atomizer (multiatomizer). *J. Anal. At. Spectrom.* **23,** 342-351.

Hockley, S. L., Arlt, V. M., Brewer, D., Te Poele, R., Workman, P., Giddings, I., Phillips, D. H. (2007). AHR- and DNA-damage-mediated gene expression responses induced by benzo(a)pyrene in human cell lines. *Chem. Res. Toxicol.* **20(12),** 1797-1810.

Holásková, I., Elliott, M., Hanson, M. L., Schafer, R., Barnett, J. B. (2012). Prenatal cadmium exposure produces persistent changes to thymus and spleen cell phenotypic repertoire as well as the acquired immune response. *Toxicol. Appl. Pharmacol.* **265(2),** 181-9.

Hughes, M. F., Edwards, B. C., Herbin-Davis, K. M., Saunders, J., Styblo, M., Thomas, D. J. (2010). *Toxicol. Appl. Pharmacol.* **249(3),** 217-223.

Jedlitschky, G., Hoffmann, U., Kroemer, H. K. (2006). Structure and function of the MRP2 (ABCC2) protein and its role in drug disposition. *Expert Opin. Drug. Metab. Toxicol.* **2(3),** 351-366.

Jeong, J. H., Jo, A., Park, P., Lee, H., Lee, H. O. (2015). Brca2 deficiency leads to T cell loss and immune dysfunction. *Mol. Cells.* **38(3),** 251-258.

Jiang, X., McDermott, J. R., Ajees, A. A., Rosen, B. P., Liu, Z. (2010). Trivalent arsenicals and glucose use different translocation pathways in mammalian GLUT1. *Metallomics.* **2,** 211–219.

Jiang, Y. J., Lu, B., Kim, P., Elias, P. M., Feingold, K. R. (2006). Regulation of ABCA1 expression in human keratinocytes and murine epidermis. *J. Lipid Res.* **47(10),** 2248-2258.

Jones, J. P., Shou, M., Korzekwa, K. R. (1995). Stereospecific activation of the procarcinogen benzo[a]pyrene: a probe for the active sites of the cytochrome P450 superfamily. *Biochemistry.* **34(21),** 6956-6961.

Josyula, A. B., Poplin, G. S., Kurzius-Spencer, M., McClellen, H. E., Kopplin, M. J., Stürup, S., Clark Lantz, R., Burgess, J. L. (2006). Environmental arsenic exposure and sputum metalloproteinase concentrations. *Environ. Res.* **102(3),** 283-290.

Jubin, T., Kadam, A., Jariwala, M., Bhatt, S., Sutariya, S., Gani, A. R., Gautam, S., Begum, R. (2016). The PARP family: insights into functional aspects of poly (ADP-ribose) polymerase-1 in cell growth and survival. *Cell Prolif.* **49(4),** 421-437.

Kaina, B. (2003). DNA damage-triggered apoptosis: critical role of DNA repair, double-strand breaks, cell proliferation and signaling. *Biochem. Pharmacol.* **66(8),** 1547-1554.

Kala, S. V., Neely, M. W., Kala, G., Prater, C. I., Atwood, D. W., Rice, J. S., Lieberman, M. W. (2000). The MRP2/cMOAT transporter and arsenic-glutathione complex formation are required for biliary excretion of arsenic. *J. Biol. Chem.* **275(43),** 33404-33408.

Kchour, G, Rezaee, R., Farid, R., Ghantous, A., Rafatpanah, H., Tarhini, M., Kooshyar, M. M., El Hajj, H., Berry, F., Mortada, M., Nasser, R., Shirdel, A., Dassouki, Z., Ezzedine, M., Rahimi, H., Ghavamzadeh, A., de Thé, H., Hermine, O., Mahmoudi, M., Bazarbachi, A. (2013). The combination of arsenic, interferon-alpha, and zidovudine restores an "immunocompetent-like" cytokine expression profile in patients with adult T-cell leukemia lymphoma. *Retrovirology.* **10,** 91.

Kim, J. H., Stansbury, K. H., Walker, N. J., Trush, M. A., Strickland, P. T., Sutter, T. R. (1998). Metabolism of benzo[a]pyrene and benzo[a]pyrene-7,8-diol by human cytochrome P450 1B1. *Carcinogenesis.* **19(10),** 1847-1853.

Kim, K., Khaled, A. R., Reynolds, D., Young, H. A., Lee, C. K., Durum, S. K. (2003). Characterization of an interleukin-7-dependent thymic cell line derived from a p53−/− mouse. *J. Immunol. Methods.* **274,** 177-184.

King, B. S., Cooper, K. L., Liu, K.J., Hudson, L. G. (2012). Poly(ADP-ribose) contributes to an association between poly(ADP-ribose) polymerase-1 and xeroderma pigmentosum complementation group A in nucleotide excision repair. *J. Biol. Chem.* **287(47),** 39824-39833.

Klein, L., Kyewski, B., Allen, P. M., Hogquist, K. A. (2014). Positive and negative selection of the T cell repertoire: what thymocytes see (and don't see). *Nat. Rev. Immunol.* **14(6),** 377-391.

Kozul, C. D., Ely, K. H., Enelow, R. I., Hamilton, J. W. (2009). Low-dose arsenic compromises the immune response to influenza A infection in vivo. *Environ. Health. Perspect.* **117(9),** 1441-1447.

Kumar, A., Malhotra, A., Nair, P., Garg, M., Dhawan, D. K. (2010). Protective role of zinc in ameliorating arsenic-induced oxidative stress and histological changes in rat liver. *J. Environ. Pathol. Toxicol. Oncol.* **29(2),** 91-100.

Lauer FT, Walker MK, Burchiel SW. (2013). Dibenzo[def,p]chrysene (DBC) suppresses antibody formation in spleen cells following oral exposures of mice. *J Toxicol. Environ. Health A*. **76(1),** 16-24.

Le Marchand, L., Hankin, J. H., Pierce, L. M., Sinha, R., Nerurkar, P. V., Franke, A. A., Wilkens, L. R., Kolonel, L. N., Donlon, T., Seifried, A., Custer, L. J., Lum-Jones, A., Chang ,W. (2002). Well-done red meat, metabolic phenotypes and colorectal cancer in Hawaii. *Mutat. Res.* **506-507,** 205-214.

Leslie, E. M., Haimeur, A., Waalkes, M. P. (2004). Arsenic transport by the human multidrug resistance protein 1 (MRP1/ABCC1). Evidence that a tri-glutathione conjugate is required. *J. Biol. Chem.* **279(31),** 32700-32708.

Leung, J., Pang, A., Yuen, W. H., Kwong, Y. L., Tse, E. W. (2007) Relationship of expression of aquaglyceroporin 9 with arsenic uptake and sensitivity in leukemia cells. *Blood.* **109,** 740–746.

Lewińska, D., Arkusz, J., Stańczyk, M., Palus, J., Dziubałtowska, E., Stepnik, M. (2007). Comparison of the effects of arsenic and cadmium on benzo(a)pyrene-induced micronuclei in mouse bone-marrow. *Mutat. Res.* **632(1-2),** 37-43.

Li, D., Morimoto, K., Takeshita, T., Lu, Y. (2001). Arsenic induces DNA damage via reactive oxygen species in human cells. *Environ. Health. Prev. Med.* **6(1),** 27-32.

Li, Q., Lauer, F. T., Liu, K. J., Hudson, L. G., Burchiel, S. W. (2010). Low-dose synergistic immunosuppression of T-dependent antibody responses by polycyclic aromatic

hydrocarbons and arsenic in C57BL/6J murine spleen cells. *Toxicol. Appl. Pharmacol.* **245,** 344–351.

Lieber, M. R. (2010). The mechanism of double-strand DNA break repair by the nonhomologous DNA end-joining pathway. *Annu. Rev. Biochem.* **79,** 181-211.

Linowes, B. A., Ligons, D. L., Nam, A. S., Hong, C., Keller, H. R., Tai, X., Luckey, M. A., Park, J. H. (2013). Pim1 permits generation and survival of CD4+ T cells in the absence of γc cytokine receptor signaling. *Eur. J. Immunol.* **43(9),** 2283-2294.

Litwin, I., Bocer, T., Dziadkowiec, D., Wysocki, R. (2013). Oxidative stress and replication-independent DNA breakage induced by arsenic in Saccharomyces cerevisiae. *PLoS Genet.* **9(7),** e1003640.

Liu, J., Chen, H., Miller, D. S., Saavedra, J. E., Keefer, L. K., Johnson, D. R., Klaassen, C. D., Waalkes, M. P. (2001). Overexpression of glutathione S-transferase II and multidrug resistance transport proteins is associated with acquired tolerance to inorganic arsenic. *Mol. Pharmacol.* **60(2),** 302-309.

Liu, J., Liu, Y., Powell, D. A., Waalkes, M. P., Klaassen, C. D. (2002). Multidrug-resistance mdr1a/1b double knockout mice are more sensitive than wild type mice to acute arsenic toxicity, with higher arsenic accumulation in tissues. *Toxicology.* **170(1-2),** 55-62.

Liu, Z., Carbrey, J. M., Agre P., Rosen, B. P. (2004). Arsenic trioxide uptake by human and rat aquaglyceroporins. Biochem. Biophys. *Res. Commun.* **316,** 1178–1185.

Liu, Z., Styblo, M., Rosen, B. P. (2006). Methylarsonous acid transport by aquaglyceroporins. *Environ. Health Perspect. 114,* 527–531.

Los, M., Mozoluk, M., Ferrari, D., Stepczynska, A., Stroh, C., Renz, A., Herceg, Z., Wang, Z. Q., Schulze-Osthoff, K. (2002). Activation and caspase-mediated inhibition of PARP: a molecular switch between fibroblast necrosis and apoptosis in death receptor signaling. *Mol. Biol. Cell.* **13(3),** 978-988.

Maier, A., Schumann, B. L., Chang, X., Talaska, G., Puga, A. (2002). Arsenic co-exposure potentiates benzo[a]pyrene genotoxicity. *Mutat. Res.* **517(1-2),** 101-111.

Maciaszczyk-Dziubinska, E., Wawrzycka, D., Wysocki, R. (2012). Arsenic and antimony transporters in eukaryotes. *Int. J. Mol. Sci.* **13(3),** 3527-3548.

Mah, L. J., El-Osta, A., Karagiannis, T. C. (2010). GammaH2AX: a sensitive molecular marker of DNA damage and repair. *Leukemia.* **24(4),** 679-686.

Matoušek, T., Currier, J. M., Trojánková, N., Saunders, R. J., Ishida, M. C., González-Horta, C., Musil, S., Mester, Z., Stýblo, M., Dědina, J. (2013). Selective hydride generation-cryotrapping- ICP-MS for arsenic speciation analysis at picogram levels: analysis of river

and sea water reference materials and human bladder epithelial cells. *J. Anal. At. Spectrom.* **28(9),** 1456-1465.

Matsumura, I., Kitamura, T., Wakao, H., Tanaka, H., Hashimoto, K., Albanese, C., Downward, J., Pestell, R. G., Kanakura, Y. (1999). Transcriptional regulation of the cyclin D1 promoter by STAT5: its involvement in cytokine-dependent growth of hematopoietic cells. *EMBO J.* **18(5),** 1367-1377.

Morzadec, C., Bouezzedine, F., Macoch, M., Fardel, O., Vernhet, L. (2012). Inorganic arsenic impairs proliferation and cytokine expression in human primary T lymphocytes. *Toxicology.* **300(1-2),** 46-56.

Nadeau, K. C., Li, Z., Farzan, S., Koestler, D., Robbins, D., Fei, D. L., Malipatlolla, M., Maecker, H., Enelow, R., Korrick, S., Karagas, M. R. (2014). In utero arsenic exposure and fetal immune repertoire in a US pregnancy cohort. *Clin. Immunol.* **155(2),** 188-197.

Namen, A. E., Lupton, S., Hjerrild, K., Wignall, J., Mochizuki, D. Y, Schmierer, A., Mosley, B., March, C. J., Urdal, D., Gillis, S. (1988). Stimulation of B-cell progenitors by cloned murine interleukin-7. *Nature.* **333(6173),** 571–573.

Navas-Acien, A., Sharrett, A. R., Silbergeld, E. K., Schwartz, B. S., Nachman, K. E., Burke, T. A., and Guallar, E. (2005). Arsenic exposure and cardiovascular disease: a systematic review of the epidemiologic evidence. *Am. J. Epidemiol.* **162,** 1037-1049.

Noguchi, M., Nakamura, Y., Russell, S. M., Ziegler, S. F., Tsang, M., Cao, X., Leonard, W. J. (1993). Interleukin-2 receptor gamma chain: a functional component of the interleukin-7 receptor. *Science.* **262 (5141),** 1877–1880.

Nohara, K., Ao, K., Miyamoto, Y., Suzuki, T., Imaizumi, S., Tateishi, Y., Omura, S., Tohyama, C., Kobayashi, T. (2008). Arsenite-induced thymus atrophy is mediated by cell cycle arrest: a characteristic downregulation of E2F-related genes revealed by a microarray approach. *Toxicol. Sci.* **101(2),** 226-238.

Nosaka, T., Kawashima, T., Misawa, K., Ikuta, K., Mui, A. L., Kitamura, T. (1999). STAT5 as a molecular regulator of proliferation, differentiation and apoptosis in hematopoietic cells. *EMBO. J.* **18(17),** 4754-4765.

Nunes-Alves, C., Nobrega, C., Behar, S. M., Correia-Neves, M. (2013). Tolerance has its limits: how the thymus copes with infection. *Trends Immunol.* **34(10),** 502-510.

Ohm, J. E., Gabrilovich, D. I., Sempowski, G. D., Kisseleva, E., Parman, K. S., Nadaf, S., Carbone, D. P. (2003). VEGF inhibits T-cell development and may contribute to tumor-induced immune suppression. *Blood.* **101(12),** 4878-4886.

Orihuela, R., Kojima, C., Tokar, E. J., Person, R. J., Xu, Y., Qu, W., Waalkes, M. P. (2013). Oxidative DNA damage after acute exposure to arsenite and monomethylarsonous acid in biomethylation-deficient human cells. *Toxicol. Mech. Methods.* **23(6),** 389-395.

Olson, D. P., Taylor, B. J., Ivy, S. P. (2001). Detection of MRP functional activity: calcein AM but not BCECF AM as a Multidrug Resistance-related Protein (MRP1) substrate. *Cytometry.* **46(2),** 105-113.

Palmer, D. B. (2014). The effect of age on thymic function. *Front. Immunol.* **4,** 316.

Paul, D. S., Harmon, A. W., Devesa, V., Thomas, D. J., Stýblo, M. (2007). Molecular mechanisms of the diabetogenic effects of arsenic: inhibition of insulin signaling by arsenite and methylarsonous acid. *Environ. Health. Perspect.* **115(5),** 734-742.

Patra, P. H., Bandyopadhyay, S., Bandyopadhyay, M. C., Mandal, T. K. (2013). Immunotoxic and genotoxic potential of arsenic and its chemical species in goats. *Toxicol. Int.* **20(1),** 6-10.

Petrick, J. S., Ayala-Fierro, F., Cullen, W. R., Carter, D. E., Vasken Aposhian, H. (2000). Monomethylarsonous acid (MMA(III)) is more toxic than arsenite in Chang human hepatocytes. *Toxicol. Appl. Pharmacol.* **163(2),** 203-207.

Qian, Y., Castranova, V., Shi, X. (2003). New perspectives in arsenic-induced cell signal transduction. *J. Inorg. Biochem.* **96(2-3),** 271-278.

Qin, X. J., Hudson, L. G., Liu, W., Ding, W., Cooper, K. L., Liu, K. J. (2008). Dual actions involved in arsenite-induced oxidative DNA damage. *Chem. Res. Toxicol.* **21(9),** 1806-1813.

Qin, X. J., Liu, W., Li, Y. N., Sun, X., Hai, C. X., Hudson, L. G., Liu, K. J. (2012). Poly(ADP-ribose) polymerase-1 inhibition by arsenite promotes the survival of cells with unrepaired DNA lesions induced by UV exposure. *Toxicol. Sci.* **127(1),** 120-129.

Rahman, M., Vahter, M., Wahed, M. A., Sohel, N., Yunus, M., Streatfield, P. K., El Arifeen, S., Bhuiya, A., Zaman, K., Chowdhury, A. M., Ekström, E. C., Persson, L. A. (2006). Prevalence of arsenic exposure and skin lesions. A population based survey in Matlab, *Bangladesh. J. Epidemiol. Community Health.* **60(3),** 242-248.

Rangwala, F., Williams, K. P., Smith, G. R., Thomas, Z., Allensworth, J. L., Lyerly, H. K., Diehl, A. M., Morse, M. A., Devi, G. R. (2012). Differential effects of arsenic trioxide on chemosensitization in human hepatic tumor and stellate cell lines. *BMC Cancer.* **12,** 402.

Raqib, R., Ahmed, S., Sultana, R., Wagatsuma, Y., Mondal, D., Hoque, A. M., Nermell, B., Yunus, M., Roy, S., Persson, L. A., Arifeen, S. E., Moore, S., Vahter, M. (2009). Effects of in utero arsenic exposure on child immunity and morbidity in rural Bangladesh. *Toxicol. Lett.* **185(3),** 197-202.

Rodríguez-Fragoso, L., Melendez, K., Hudson, L. G., Lauer, F. T., Burchiel, S. W. (2009). EGF-receptor phosphorylation and downstream signaling are activated by benzo[a]pyrene 3,6-

quinone and benzo[a]pyrene 1,6-quinone in human mammary epithelial cells. *Toxicol. Appl. Pharmacol.* **235(3),** 321-328.

Ruppert, S. M., Chehtane, M., Zhang, G., Hu, H., Li, X., Khaled, A. R. (2012). JunD/AP-1-mediated gene expression promotes lymphocyte growth dependent on interleukin-7 signal transduction. *PLoS One.* **7(2),** e32262.

Russell, S. M., Keegan, A. D., Harada, N., Nakamura, Y., Noguchi, M., Leland, P., Friedmann, M. C., Miyajima, A., Puri, R. K., Paul, W. E. (1993). Interleukin-2 receptor gamma chain: a functional component of the interleukin-4 receptor. *Science.* **262 (5141),** 1880–1883.

Sakurai, T., Kojima, C., Ochiai, M., Ohta, T., Fujiwara, K. (2004). Evaluation of in vivo acute immunotoxicity of a major organic arsenic compound arsenobetaine in seafood. *Int. Immunopharmacol.* **4(2),** 179-184.

Sakurai, T., Ohta, T., Tomita, N., Kojima, C., Hariya, Y., Mizukami, A., Fujiwara, K. (2006). Evaluation of immunotoxic and immunodisruptive effects of inorganic arsenite on human monocytes/macrophages. *Int. Immunopharmacol.* **6(2),** 304-315.

Schellenberger, M. T., Grova, N., Willième, S., Farinelle, S., Prodhomme, E. J., Muller, C. P. (2009). Modulation of benzo[a]pyrene induced immunotoxicity in mice actively

immunized with a B[a]P-diphtheria toxoid conjugate. *Toxicol. Appl. Pharmacol.* **240(1),** 37-45.

Schuhmacher-Wolz, U., Dieter, H. H., Klein, D., Schneider, K. (2009). Oral exposure to inorganic arsenic: evaluation of its carcinogenic and non-carcinogenic effects. *Crit. Rev. Toxicol.* **39,** 271-298.

Schulz, H., Nagymajtényi, L., Institoris, L., Papp, A., Siroki, O. (2002). A study on behavioral, neurotoxicological, and immunotoxicological effects of subchronic arsenic treatment in rats. *J. Toxicol. Environ. Health A.* **65(16),** 1181-1193.

Schwarz, D., Kisselev, P., Cascorbi, I., Schunck, W. H., Roots, I. (2001). Differential metabolism of benzo[a]pyrene and benzo[a]pyrene-7,8-dihydrodiol by human CYP1A1 variants. *Carcinogenesis.* **22(3),** 453-459.

Seinen, W., Penninks, A. (1979). Immune suppression as a consequence of a selective cytotoxic activity of certain organometallic compounds on thymus and thymus-dependent lymphocytes. *Ann. N Y Acad. Sci.* **320,** 499-517.

Seo, T., Urasaki, Y., Ueda, T. (2007). Establishment of an arsenic trioxide-resistant human leukemia cell line that shows multidrug resistance. *Int. J. Hematol.* **85(1),** 26-31.

Sertel, S., Tome, M., Briehl, M. M., Bauer, J., Hock, K., Plinkert, P. K., Efferth, T. (2012). Factors determining sensitivity and resistance of tumor cells to arsenic trioxide. *PLoS One.* **7(5),** e35584.

Sherwood, C. L., Lantz, R. C., Boitano, S. (2013). Chronic arsenic exposure in nanomolar concentrations compromises wound response and intercellular signaling in airway epithelial cells. *Toxicol. Sci.* **132(1),** 222-234.

Shen, S., Li, X. F., Cullen, W. R., Weinfeld, M., Le, X. C. (2013). Arsenic binding to proteins. *Chem. Rev.* **113(10),** 7769-92.

Shi, H., Hudson, L. G., Liu, K. J. (2004). Oxidative stress and apoptosis in metal ion-induced carcinogenesis. *Free Radic. Biol. Med.* **37(5),** 582-593.

Shimada, T., Fujii-Kuriyama, Y. (2004). Metabolic activation of polycyclic aromatic hydrocarbons to carcinogens by cytochromes P450 1A1 and 1B1. *Cancer Sci.* **95(1),** 1-6.

Smith, C. C, O'Donovan, M. R., Martin, E. A. (2006). hOGG1 recognizes oxidative damage using the comet assay with greater specificity than FPG or ENDOIII. *Mutagenesis.* **21(3),** 185-190.

Soto-Peña, G. A., Luna, A. L., Acosta-Saavedra, L., Conde, P., López-Carrillo, L., Cebrián, M. E., Bastida, M., Calderón-Aranda, E. S., Vega, L. (2006). Assessment of lymphocyte

subpopulations and cytokine secretion in children exposed to arsenic. *FASEB. J.* **20(6),** 779-781.

Spink, D. C., Katz, B. H., Hussain, M. M., Spink, B. C., Wu, S. J., Liu, N., Pause, R., Kaminsky, L. S. (2002). Induction of CYP1A1 and CYP1B1 in T-47D human breast cancer cells by benzo[a]pyrene is diminished by arsenite. *Drug Metab. Dispos.* **30(3),** 262-269.

Styblo, M., Yamauchi, H., Thomas, D. J. (1995). Comparative in vitro methylation of trivalent and pentavalent arsenicals. *Toxicol. Appl. Pharmacol.* **135(2),** 172-178.

Sun, H. J., Rathinasabapathi, B., Wu, B., Luo, J., Pu, L. P., Ma, L. Q. (2014). Arsenic and selenium toxicity and their interactive effects in humans. *Environ. Int.* 69, 148-158.

Sun, X., Zhou, X., Du, L., Liu, W., Liu, Y., Hudson, L. G., Liu, K. J. (2014). Arsenite binding-induced zinc loss from PARP-1 is equivalent to zinc deficiency in reducing PARP-1 activity, leading to inhibition of DNA repair. Toxicol Appl Pharmacol. **274(2),** 313-318.

Suto, M. J., Turner, W. R., Arundel-Suto, C. M., Werbel, L. M., Sebolt-Leopold, J. S. (1991). Dihydroisoquinolinones: the design and synthesis of a new series of potent inhibitors of poly(ADP-ribose) polymerase. *Anticancer Drug Des.* **6(2),** 107-117.

Swenberg, J. A., Lu, K., Moeller, B. C., Gao, L., Upton, P. B., Nakamura, J., Starr, T. B. (2011). Endogenous versus exogenous DNA adducts: their role in carcinogenesis, epidemiology, and risk assessment. *Toxicol. Sci.* **120 Suppl. 1,** S130-145.

Takeshita, T., Asao, H., Ohtani, K., Ishii, N., Kumaki, S., Tanaka, N., Munakata, H., Nakamura, M., Sugamura, K. (1992). Cloning of the gamma chain of the human IL-2 receptor. *Science.* **257 (5068),** 379–382.

Udasin, R. G., Wen, X., Bircsak, K. M., Aleksunes, L. M., Shakarjian, M. P., Kong, A. N., Heck, D. E., Laskin, D. L., Laskin, J. D. (2016). Nrf2 Regulates the Sensitivity of Mouse Keratinocytes to Nitrogen Mustard via Multidrug Resistance-Associated Protein 1 (Mrp1). *Toxicol. Sci.* 149(1), 202-212.

Underhill, F. P. (1914). The Distribution Of Arsenic In A Human Body. *J. Biol. Chem.* **286(26),** 22855-22863. **19,** 513-515.

Vahter, M. (2008) Health effects of early life exposure to arsenic. Basic *Clin. Pharmacol. Toxicol.* **102,** 204–211.

Vahter, M., Concha, G. (2001). Role of metabolism in arsenic toxicity. *Pharmacol. Toxicol.* **89(1),** 1-5.

van der Kolk, D. M., de Vries, E. G., Noordhoek, L., van den Berg, E., van der Pol, M. A., Müller, M., Vellenga, E. (2001). Activity and expression of the multidrug resistance proteins P-glycoprotein, MRP1, MRP2, MRP3 and MRP5 in de novo and relapsed acute myeloid leukemia. *Leukemia.* **15(10),** 1544-1553.

Vile, G. F., Basu-Modak, S., Waltner, C., Tyrrell, R. M. (1994). Heme oxygenase 1 mediates an adaptive response to oxidative stress in human skin fibroblasts. *Proc. Natl. Acad. Sci. USA.* **91,** 2607-2610.

Virág, L. (2005). Poly(ADP-ribosyl)ation in asthma and other lung diseases. *Pharmacol. Res.* **52(1),** 83-92.

Wiseman, H., and Halliwell, B. (1996). Damage to DNA by reactive oxygen and nitrogen species: role in inflammatory disease and progression to cancer. *Biochem. J.* **313,** 17–29.

Wu, J. P., Chang, L. W., Yao, H. T., Chang, H., Tsai, H. T., Tsai, M. H., Yeh, T. K., Lin, P. (2009). Involvement of oxidative stress and activation of aryl hydrocarbon receptor in elevation of CYP1A1 expression and activity in lung cells and tissues by arsenic: an in vitro and in vivo study. *Toxicol. Sci.* **107(2),** 385-393.

Xu, H., Lauer, F. T., Liu, K. J., Hudson, L. G., Burchiel, S. W. (2016). Environmentally relevant concentrations of arsenite and monomethylarsonous acid inhibit IL-7/STAT5 cytokine

signaling pathways in mouse CD3+CD4-CD8- double negative thymus cells. *Toxicol. Lett.* **247,** 62-68.

Xu, H., Lauer, F. T., Liu, K. J., Hudson, L. G., Burchiel, S. W. (2016). Interactive Genotoxicity Induced by Environmentally Relevant Concentrations of Benzo(a)pyrene Metabolites and Arsenite in Mouse Thymus Cells. *Toxicol. Sci.* **154(1),** 153-161.

Xu, H., McClain, S., Medina, S., Lauer, F. T., Liu, K. J., Hudson, L. G., Stýblo, M., Burchiel, S. W. (2016). Differential Sensitivities of Bone Marrow, Spleen and Thymus to Genotoxicity Induced By Environmentally Relevant Concentrations of Arsenite. *Toxicol. Lett.* **262,** 55-61.

Xu, H., Zhou, X., Wen, X., Lauer, F. T., Liu, K. J., Hudson, L. G., Aleksunes, L. M., Burchiel, S. W. (2016). Environmentally-Relevant Concentrations of Arsenite Induce Dose-Dependent Differential Genotoxicity Through Poly(ADP-ribose) Polymerase (PARP) Inhibition and Oxidative Stress in Mouse Thymus Cells. *Toxicol. Sci.* **149(1),** 31-41.

Xu, S. P., Sun, G. P., Shen, Y. X., Peng, W. R., Wang, H., Wei, W. (2007). Synergistic effect of combining paeonol and cisplatin on apoptotic induction of human hepatoma cell lines. *Acta. Pharmacol. Sin.* **28(6),** 869-878.

Xue, P., Hou, Y., Zhang, Q., Woods, C. G., Yarborough, K., Liu, H., Sun, G., Andersen, M. E., Pi, J. (2011). Prolonged inorganic arsenite exposure suppresses insulin-stimulated AKT

S473 phosphorylation and glucose uptake in 3T3-L1 adipocytes: involvement of the adaptive antioxidant response. *Biochem. Biophys. Res. Commun.* **407(2),** 360-365.

Yelamos, J., Farres, J., Llacuna, L., Ampurdanes, C., Martin-Caballero, J. (2011).PARP-1 and PARP-2: New players in tumour development. *Am. J. Cancer Res.* **1(3),** 328-346.

Zhang, P., Nakatsukasa, H., Tu, E., Kasagi, S., Cui, K., Ishikawa, M., Konkel, J. E., Maruyama, T., Wei, G., Abbatiello, B., Wang, Z. Q., Zhao, K., Chen, W. (2013). PARP-1 regulates expression of TGF-β receptors in T cells. *Blood.* **122,** 2224-2232.

Zhang, Z., Wang, X., Cheng, S., Sun, L., Son, Y. O., Yao, H., Li, W., Budhraja, A., Li, L., Shelton, B. J., Tucker, T., Arnold, S. M., Shi, X. (2011). Reactive oxygen species mediate arsenic induced cell transformation and tumorigenesis through Wnt/β-catenin pathway in human colorectal adenocarcinoma DLD1 cells. *Toxicol. Appl. Pharmacol.* **256,** 114-121.

Zharkov, D. O. (2008). Base excision DNA repair. *Cell. Mol. Life Sci.* **65(10),** 1544-1565.

Zhou, X., Sun, X., Mobarak, C., Gandolfi, A. J., Burchiel, S. W., Hudson, L. G., Liu, K. J. (2014). Differential Binding of Monomethylarsonous Acid Compared to Arsenite and Arsenic Trioxide with Zinc Finger Peptides and Proteins. *Chem. Res. Toxicol.* **27,** 690−698.

Zhou, X., Sun, X., Cooper, K. L., Wang, F., Liu, K. J., Hudson, L. G. (2011). Arsenite Interacts Selectively with Zinc Finger Proteins Containing C3H1 or C4 Motifs. *J. Biol. Chem.* **286(26),** 22855-22863.